



THE HONG KONG  
POLYTECHNIC UNIVERSITY

香港理工大學

Pao Yue-kong Library

包玉剛圖書館

---

## Copyright Undertaking

This thesis is protected by copyright, with all rights reserved.

**By reading and using the thesis, the reader understands and agrees to the following terms:**

1. The reader will abide by the rules and legal ordinances governing copyright regarding the use of the thesis.
2. The reader will use the thesis for the purpose of research or private study only and not for distribution or further reproduction or any other purpose.
3. The reader agrees to indemnify and hold the University harmless from and against any loss, damage, cost, liability or expenses arising from copyright infringement or unauthorized usage.

### IMPORTANT

If you have reasons to believe that any materials in this thesis are deemed not suitable to be distributed in this form, or a copyright owner having difficulty with the material being included in our database, please contact [lbsys@polyu.edu.hk](mailto:lbsys@polyu.edu.hk) providing details. The Library will look into your claim and consider taking remedial action upon receipt of the written requests.

**POLYGONUM CUSPIDATUM (HU ZHANG), A TRADITIONAL  
CHINESE MEDICINE, AMELIORATES HIGH-FAT DIET-  
INDUCED FATTY LIVER IN RATS AND FREE FATTY ACID-  
INDUCED HEPATIC STEATOSIS IN LO2 CELLS**

**ZHANG HUAN**

**Ph.D**

**The Hong Kong Polytechnic University**

**2018**

**The Hong Kong Polytechnic University**  
**Department of Applied Biology and Chemical Technology**

***Polygonum cuspidatum* (Hu Zhang), a Traditional Chinese Medicine,  
ameliorates High-Fat Diet-Induced Fatty Liver in rats and Free Fatty  
Acid-Induced Hepatic Steatosis in LO2 cells**

**Zhang Huan**

**A Thesis Submitted in Partial Fulfillment of the Requirements for the  
Degree of Doctor of Philosophy**

**February 2017**

## **CERTIFICATE OF ORIGINALITY**

I hereby declare that this thesis is my own work and that, to the best of my knowledge and belief, it reproduces no material previously published or written, nor material that has been accepted for the award of any other degree or diploma, except where due acknowledgement has been made in the text.

---

**Zhang Huan**

## **Abstract**

Non-alcoholic fatty liver disease (NAFLD) is a burgeoning health problem worldwide and includes a spectrum of disease from simple steatosis to inflammatory nonalcoholic steatohepatitis (NASH), fibrosis, and cirrhosis. One fourth of the NAFLD patients progress from simple steatosis to NASH and have fibrosis in 3 years. Due to the changes in the modern diet and people's lifestyle, NAFLD has become one of the leading causes of chronic liver diseases. Moreover, NAFLD is an emerging risk factor for both cardiometabolic and hepatic mortality.

Though the pathogenesis of NAFLD is not entirely understood, it is believed that lipid accumulation arises from an imbalance between lipid acquisition (i.e., fatty acid uptake and *de novo* lipogenesis) and removal (i.e., mitochondrial fatty acid oxidation and export as a component of very-low-density lipoprotein particles) in liver is one of the major causes.

Currently, only limited treatments for NAFLD are available. Lifestyle interventions such as dietary change, weight loss and increase physical activity are strongly

recommended for improving the outcome of patients with NAFLD. However, it is hard to maintain the lifestyle change. International pharmaceutical companies put huge resources to develop drugs targeting different stages of NAFLD. Although a few pharmaceutical agents are effective, long term usage of these agents might cause many adverse effects. For example, vitamin E might increase the risk of prostate cancer or stroke and pioglitazone might cause bladder cancer. As a result, alternative therapeutic strategies are therefore warranted. Traditional Chinese medicine (TCM) might be the answer for the alternative treatment for NAFLD based on two main reasons. First, NAFLD is caused by multi-factors, the multiple-targeted TCM could regulate the dysfunction of multiple targets concurrently. Second, using TCM to prevent and treat NAFLD has received increasing attention due to its effectiveness and acceptable prices. Therefore, the patients with NAFLD can tolerate the long term treatment. In the TCM's view, NAFLD is not recognized as a particular disease. Instead, the symptoms of NAFLD including obesity, right rib hypochondriac pain, discomfort, jaundice and fatigue have been classified as "Feiqi" and "liver swelling". According to the book "Chinese medicine diagnosis" published in 1997, such symptoms have been named as

liver swelling. Phlegm and blood stasis is considered as the main pathogenesis. It was mainly divided into five types: phlegm and blood stasis, liver and spleen deficiency, intrinsic damp heat, qi stagnation and blood stasis, liver and kidney deficiency.

*Polygonum cuspidatum* sieb. et Zucc. (HZ, Hu Zhang in Chinese) is a perennial herb with both medicinal and food dual value, native to eastern Asia such as China, Japan and Korea, whose young stems are edible as a spring vegetable with a flavor similar to lemon or rhubarb. The root of HZ has been used for conditions of the heart and blood vessels including atherosclerosis and hyperlipemia and for digestion problems including constipation, liver disease (hepatitis), and gallstones.

Literature review showed that four traditional Chinese herbal formulae, Qushi Huayu Decoction, Danning Tablet, Huganning tablet, QuYuhuatan tong luo Decotion were studied as the treatment for NAFLD. Interestingly, all these four herbal formulae contained HZ, indicating that their effect on treating NAFLD may be due to the present of HZ. In addition, the channel tropism of HZ is liver, which is consistent with the main site of fatty liver. HZ can alleviate blood stasis and damp heat, which is consistent with pathogenesis and treatment of fatty liver. Based on previous findings, a potential role

of HZ in the treatment of NAFLD is of considerable interest.

Previous studies have revealed that there are three possible pathologies which might induce lipid accumulation in liver, they are oxidative stress, impaired lipophagy and bile acids synthesis. Based on the preliminary results, we further hypothesized that HZ might possess lipid reduction effects by regulating these factors concurrently.

There are three major objectives of my project: (1) to investigate the lipid reduction effects of HZ and characterize the molecular mechanisms of lipid reduction of HZ in free fatty acid (FFA)-induced steatotic cells using human liver cell line (LO2) cells *in vitro*; (2) to evaluate the lipid reduction effects of HZ in HFD-induced steatosis in rats *in vivo*; (3) to investigate the possible mechanistic pathways of HZ on lipid reduction by using molecular and metabolomics approaches.

Recent studies have revealed that impaired autophagy, indeed, may be a fundamental mechanism of some lipid metabolism disorders such as NAFLD, obesity and other metabolic syndrome. Lipophagy may therefore represent a potential therapeutic target for the treatment of NAFLD.

HZ could decrease the lipid content in FFA-induced steatosis model in LO2 cells. The lipid-lowering effect maybe related to the restoration of the down-regulated phosphorylation of adenosine 5'-monophosphate activated protein kinase (p-AMPK), peroxisome proliferator activated receptor  $\alpha$  (PPAR $\alpha$ ), low density lipoprotein receptor (LDLR), and phosphorylation of acetyl-CoA carboxylase (p-ACC) protein expressions. HZ induced autophagy to promote lipid clearance. The current study reported (for the first time) that treatment of HZ could be able to upregulate LDLR and p-ACC expressions in the absent of autophagy, suggesting that HZ reduced lipid accumulation partially by regulating autophagy induction. However, treatment of HZ was found to be not able to upregulate PPAR $\alpha$  expression in the absent of autophagy, suggesting that HZ upregulated PPAR $\alpha$  expression by regulating autophagy induction.

Further investigation was performed on the anti-NAFLD effects of HZ *in vivo*. Our *in vivo* study demonstrated that in response to HZ supplementation, both hepatic triglyceride (TG) and total cholesterol (TC) accumulation, lipid content were significantly reduced. HZ attenuated oxidative stress by elevating antioxidant enzyme such as catalase (CAT) and inhibiting malondialdehyde (MDA) levels in the liver. The

restoration of the down-regulated p-AMPK, PPAR $\alpha$ , LDLR, and p-ACC protein expressions induced by HFD were achieved in animals treated with either simvastatin or HZ. A cytosolic form of LC3 (LC3-I) is conjugated to form LC3-PE conjugate (LC3-II), is regarded as the most reliable marker protein for autophagy. HZ induced LC3-II expression, which indicated HZ may promote lipid clearance in the fatty liver by enhancing lipophagy.

It is well established that bile acids' synthesis has profound effect on facilitating cholesterol removal from the body. In the present work, combination of ultra-performance liquid chromatography-quadrupole time-of-flight mass spectrometry (UPLC-QTOF-MS) was used to examine the metabolite changes in the serum samples from rats to investigate the therapeutic effect of HZ on HFD-induced steatosis rats. Using untargeted mass spectrometry-based metabolomic platforms, multivariate statistics revealed that HFD significantly perturbed bile acids. HZ supplement to HFD rats resulted in significant increases in three primary bile acids [chenodeoxycholate (CDCA), glycochenodeoxycholate (GCDCA) and glycocholate (GCA)] and two secondary bile acids [deoxycholate (DCA) and glycodeoxycholate (GDCA)].

Decreased utilization of cholesterol [bile acid synthesis due to cholesterol 7 $\alpha$ -hydroxylase (CYP7A1) and sterol 27-hydroxylase (CYP27A1)] could contribute to the accumulation of free cholesterol in NAFLD. Regarding the mechanism of bile acid disturbance, up-regulated CYP7A1 may affect the bile acid synthetic pathway and lead to lower cholesterol content in the body. HZ significantly promoted CYP7A1 activity, indicating that HZ could accelerate the transformation of cholesterol into bile acids in the liver. Another factor that might contribute to the cholesterol lowering effect of HZ is through inhibiting dietary cholesterol absorption in the small intestine with the aids of binding effects of HZ and conjugated bile acids. Our result showed that HZ increased three conjugated bile acids (GCA, GDCA and GCDCA). These conjugated bile acids lowered the solubility of cholesterol, resulting in lowering the reabsorption of cholesterol from intestine to the hepatocytes.

In conclusion, our studies have shown that HZ reduced the lipid accumulation *in vitro* and *in vivo* mainly by regulating the imbalance between lipid acquisition and removal, especially through lipophagy and bile acids synthesis to remove lipid from the body. In addition, we demonstrated that the lipid reduction effects of HZ were achieved by

regulating multiple targets, including the suppression of oxidative stress, activation of lipophagy and enhancement of bile acid synthesis. Taken all the results together, this project indicated that HZ might be a novel drug target for the prevention and treatment of NAFLD.

## Publications

1. **Zhang, H.**, Zhou, X., Wong, M. H. Y., Man, K. Y., Pin, W. K., Yeung, J. H. K., Kwan, Y. W., Leung, G. P. H., Ho, P. M., Lee, S. M. Y., Chan, C. O., Mok, D. K. W., Yu, P. H. F., and Chan, S. W. (2017) Sichuan pepper attenuates H<sub>2</sub>O<sub>2</sub>-induced apoptosis via antioxidant activity and up-regulating heme oxygenase-1 gene expression in primary rat hepatocytes. *Journal of Food Biochemistry* e12403
2. **Zhang, H.**, Wu, M. Y., Guo, D. J., Wan, C. W., and Chan, S. W. (2017) Gui-ling-gao inhibits Concanavalin A-induced inflammation by suppressing the expressions of iNOS and proinflammatory cytokines in mice isolated splenocytes. *Journal of Food Biochemistry* e12367, 1-7
3. Sham, T. T., Li, M. H., Chan, C. O., **Zhang, H.**, Chan, S. W., and Mok, D. K. W. (2017) Cholesterol-lowering effects of piceatannol, a stilbene from wine, using untargeted metabolomics. *Journal of Functional Foods* 28, 127-137
4. Gao, X., Li, C., Tang, Y. L., **Zhang, H.**, and Chan, S. W. (2016) Effect of *Hedyotis diffusa* water extract on protecting human hepatocyte cells (LO2) from H<sub>2</sub>O<sub>2</sub>-induced cytotoxicity. *Pharmaceutical biology* 54, 1148-1155
5. Li, J. J., Zhou, S. Y., **Zhang, H.**, Lam, K. H., Lee, S. M. Y., Yu, P. H. F., and Chan, S. W. (2015) Cortex Fraxini (Qingpi) protects rat pheochromocytoma cells against 6-hydroxydopamine-induced apoptosis. *Parkinson's Disease* 532849
6. Zhao, Y. M., Xu, P. X., Hu, S. Q., Du, L. B., Xu, Z. Q., **Zhang, H.**, Cui, W., Mak, S. H., Xu, D. P., and Shen, J. G. (2015) Tanshinone II A, a multiple target neuroprotectant, promotes caveolae-dependent neuronal differentiation. *European journal of pharmacology* 765, 437-446
7. **Zhang, H.**, Li, C., Kwok, S. T., Zhang, Q. W., and Chan, S. W. (2013) A review of the pharmacological effects of the dried root of *Polygonum*

cuspidatum (Hu Zhang) and its constituents. Evidence-based complementary and alternative medicine 2013, 208349

- 8 **Zhang, H.**, Wu, M. Y., Guo, D. J., Wan, C. W., Lau, C. C., Chan, C. O., Mok, D. K. W., and Chan, S. W. (2013) Gui-ling-gao (turtle jelly), a traditional Chinese functional food, exerts anti-inflammatory effects by inhibiting iNOS and pro-inflammatory cytokine expressions in splenocytes isolated from BALB/c mice. Journal of Functional Foods 5, 625-632

### **Under review:**

**Zhang, H.**, Chan, S. W., Wong W.T. Luteolin on protecting human hepatocyte cells (LO2) from H<sub>2</sub>O<sub>2</sub>-induced cytotoxicity

### **Conference:**

1. Sham, T. T., Chan, C. O., **Zhang, H.**, Chan, S. W., and Mok, D. K. W. Serum metabolomics reveals the treatment effect of the water extract of Polygoni Cuspidati Rhizoma et Radix in hypercholesterolemic rats. 13<sup>th</sup> Annual Conference of the Metabolomics Society. June 25-29 2017 Brisbane, Australia.
2. **Zhang, H.**, Sham, T. T., NG, Y. F. Chan, C. O., Mok, D. K. W, Chan, S. W. Ultra-Performance Liquid Chromatography-Mass Spectrometry, a tool to estimate the treatment effect of the water extract of Polygonum cuspidatum (Hu Zhang) in diet-induced hypercholesterolemic rats. *The 3<sup>rd</sup> International Conference and Exhibition on Advances in Chromatography & HPLC Techniques*. July 13-14, 2017 in Berlin, Germany.

## Acknowledgments

It is my great honor to express my deep and sincere appreciation to those who have helped and supported me during the past three years in this university.

First of all, I would like to express my deepest gratitude to my supervisor, Prof. Wong Wing-Tak, and co-supervisor, Dr. Chan Shun-Wan, for their patience, understanding, guidance, and most of all the encouragement they have given me during my postgraduate studies.

Secondly, special thanks go to Prof. Mok Kam-Wah Daniel, Dr. Chan Chi-On, Ms. Sham Tung-Ting and Ms. Man Ka-Yi for their help on lipid metabolomics and HPLC studies. I would like to thank Ms. Lam Oi-Shan for her assistance with testing in *in vivo* study.

I would also like to thank committee members Prof. Chen Sheng for his advice, encouragement and support. Special thanks go to Prof. Kwan Yiu-Wa for his technical guidance, patience and time he put in throughout the study.

Great thanks are also given to Ms. Cheng Huan-Le, Mr. Ng Yam-Fung, Ms. Yu Wen-

Xuan, Ms. Lin Yun-Xiao, Ms. Zhang Xiao-Zhe, Ms. Sun Wen-Qin, Mr. Fan Zhu-Ming, Ms. Zhu Ling-Yan, Ms. Yuen Chui-Ying Alisa as well as to staff members from the Department of Applied Biology and Chemical Technology for their support.

My thanks would also go to my parents who have been showing constantly support, unconditional love and understanding. It would be much difficult walking alone throughout these years without their support and encouragement.

I also wish to express my appreciations to my mother-in-law for taking care of my two sons day and night, aunt-in-law's family for encouraging me and helping me take care of my babies.

Last but not least, I wish to express my special thanks to my husband Mr. Marvin Mak for his encouragement and spiritual support. I want to thank him for all the wonderful things that he did for me.

## Table of Contents

<b>Abstract</b> .....	<b>i</b>
<b>Publications</b> .....	<b>ix</b>
<b>Acknowledgments</b> .....	<b>xi</b>
<b>Table of Contents</b> .....	<b>xiii</b>
<b>List of tables</b> .....	<b>xix</b>
<b>List of figures</b> .....	<b>xx</b>
<b>List of Abbreviations</b> .....	<b>xxv</b>
<b>Chapter 1 Introduction</b> .....	<b>1</b>
<b>1.1 The pathogenesis of non-alcoholic fatty liver disease (NAFLD)</b> .....	<b>7</b>
<b>1.2 Common pathogenic mechanisms of NAFLD</b> .....	<b>8</b>
1.2.1 Dyslipidemia.....	9
1.2.2 Hepatic fat accumulation.....	11
1.2.3 Oxidative stress and mitochondrial dysfunction.....	12
<b>1.3 Lipophagy</b> .....	<b>13</b>

<b>1.4</b>	<b>Microbiota associated mechanisms of NAFLD .....</b>	<b>21</b>
<b>1.5</b>	<b>Bile acids metabolism .....</b>	<b>23</b>
<b>1.6</b>	<b>Therapeutic strategies for NAFLD .....</b>	<b>29</b>
1.6.1	Western medicine.....	29
1.6.2	Tradional Chinese Medicine (TCM).....	32
<b>1.7</b>	<b><i>Polygonum cuspidatum</i> (Hu Zhang)-a promising agent .....</b>	<b>37</b>
1.7.1	TCM theory.....	37
1.7.2	Potentially advantageous features .....	40
<b>1.8</b>	<b>The aims of the study .....</b>	<b>44</b>
<b>Chapter 2</b>	<b>Materials and Methods .....</b>	<b>46</b>
<b>2.1</b>	<b>Preparation of HZ sample.....</b>	<b>47</b>
<b>2.2</b>	<b>High performance liquid chromatography (HPLC) analysis .....</b>	<b>47</b>
<b>2.3</b>	<b>Determination of antioxidant properties.....</b>	<b>49</b>
<b>2.4</b>	<b><i>In vitro</i> study materials and methods .....</b>	<b>51</b>
2.4.1	Preparation FFA .....	51
2.4.2	Cell culture and measurement of cell viability.....	51

2.4.3	Nile Red staining.....	52
2.4.4	Intracellular TG and TC measurements .....	53
2.4.5	Measurement of intracellular ROS .....	54
2.4.6	GFP-LC3 transfection .....	54
2.4.7	RNA interference .....	55
<b>2.5</b>	<b><i>In vivo</i> study materials and methods.....</b>	<b>56</b>
2.5.1	Animals and experimental treatment.....	56
2.5.2	Measurement of serum biochemical markers.....	59
2.5.3	Liver histopathological examination.....	59
2.5.4	Hepatic lipid content evaluation .....	60
2.5.5	Measurement of antioxidative enzyme activities and MDA content .....	60
2.5.6	Isolation of thoracic aorta.....	61
2.5.7	Mesurement of endothelium-dependent vasorelaxtion.....	61
2.5.8	Quantification of NO production.....	62
2.5.9	Western blotting assay .....	63
<b>2.6</b>	<b>Metabolomics analysis .....</b>	<b>64</b>

2.6.1	Chemical and Reagent .....	64
2.6.2	Quality control sample preparation method.....	65
2.6.3	Serum sample extraction.....	65
2.6.4	UPLC-QTOF-MS condition.....	66
2.6.5	Data processing and analysis.....	67
<b>2.7</b>	<b>Data analysis and statistics.....</b>	<b>69</b>
<b>Chapter 3</b>	<b>Results .....</b>	<b>71</b>
<b>3.1</b>	<b>Quantitative determination of major components in HZ sample .....</b>	<b>72</b>
<b>3.2</b>	<b>Determination of antioxidant properties.....</b>	<b>74</b>
<b>3.3</b>	<b>HZ reduced lipid accumulation in steatotic LO2 cells .....</b>	<b>75</b>
<b>3.4</b>	<b>HZ inhibited lipid accumulation partially via autophagy induction <i>in vitro</i> .....</b>	<b>79</b>
<b>3.5</b>	<b>HZ ameliorated hepatic steatosis in HFD-induced steatosis Rats.....</b>	<b>87</b>
3.5.1	HZ supplementation alleviated HFD-induced fatty liver.....	87
3.5.2	HZ did not affect body weight and serum ALT, AST and glucose levels.....	89
3.5.3	HZ alleviated hyperlipidemia .....	91

3.6	<b>HZ inhibited fatty liver through alleviating oxidative stress .....</b>	<b>95</b>
3.7	<b>HZ reduced fatty liver via lipophagy activation <i>in vivo</i> .....</b>	<b>97</b>
3.8	<b>Serum metabolites change of bile acids after HZ treatment.....</b>	<b>102</b>
3.8.1	Reliability of the metabolomics MS platform.....	102
3.8.2	Serum bile acid metabolites change in HFD model.....	105
3.8.3	Serum metabolites change of bile acids after HZ treatment.....	106
<b>Chapter 4</b>	<b>Discussion .....</b>	<b>112</b>
4.1	<b>Experimental hepatic steatosis models.....</b>	<b>113</b>
4.2	<b>HZ exerted lipid lowering effect by its antioxidant properties.....</b>	<b>116</b>
4.3	<b>HZ reduced lipid accumulation partially by regulating autophagy induction.....</b>	<b>119</b>
4.4	<b>HZ decreased cholesterol accumulation by increasing bile acid synthesis and inhibiting intestinal cholesterol absorption .....</b>	<b>127</b>
4.5	<b>HZ improved endothelial function through attenuating dyslipidemia .</b>	<b>133</b>
4.6	<b>Study on active ingredients in HZ .....</b>	<b>135</b>
4.7	<b>Conclusion.....</b>	<b>139</b>

<b>4.8</b>	<b>Future studies.....</b>	<b>140</b>
	<b>References.....</b>	<b>142</b>

## List of tables

Table 1.5.1	Different kinds of bile acids.....	25
Table 1.6.1	Medications targeting NAFLD .....	30
Table 1.7.1	TCM theory in diagnosing and treatment of NAFLD-like symptom  40	
Table 1.7.2	Clinical and experimental studies of herbal formulas including HZ  or its monomers or extracts.....	43
Table 3.5.1	HZ reduced the lipid accumulation of fatty liver induced by HFD  90	
Table 3.8.1	Fold change of metabolites identified by UPLC-MS and GC-MS  103	

## List of figures

Fig. 1.2.1	Model for the TG accumulation in the liver at the early stage of NAFLD (Koo 2013).....	11
Fig. 1.2.2	Role of hepatic fatty acid metabolism in the development of hepatic steatosis (Tiniakos et al. 2010).....	12
Fig. 1.3.1	The molecular components of mammalian autophagic pathways (Singh and Cuervo 2011) .....	15
Fig. 1.3.2	Autophagy degrades lipid droplets (Ward et al. 2016) .....	16
Fig. 1.3.3	Hypothetical model of the contribution of autophagy to lipid metabolism in different lipogenic and nutritional states (Singh et al. 2009)	
		17
Fig. 1.3.4	Potential mechanisms involved in the decreased hepatic autophagy that occurs with HFD feeding or obesity (K. Liu and Czaja 2013).....	20

Fig. 1.5.1	Schematic overview of primary and secondary bile acid species (Kuipers et al. 2014) .....	24
Fig. 1.5.2	Bile acid Metabolism in Liver and Intestine (de Aguiar Vallim et al. 2013) 27	
Fig. 1.5.3	Schematic overview of bile acid signalling within the enterohepatic circulation (Kuipers et al. 2014) .....	27
Fig. 1.6.1	Medical therapies targeting NAFLD (Rotman and Sanyal 2017) ...	31
Fig. 1.6.2	Mechanisms of TCM in the pathogenesis of NAFLD (Hsu et al. 2016) 37	
Fig. 1.7.1	Photo of the dried root of <i>Polygonum cuspidatum</i> (Hu Zhang).....	39
Fig. 3.1.1	HPLC chromatograms of (A) five standard mixture and (B) HZ extract (10 mg/mL) .....	73
Fig. 3.2.1	Comparison of free radical scavenging capacity of HZ and vitamin C	

from DPPH assay .....	74
Fig. 3.3.1 FFA induced hepatic steatosis in FFA-induced LO2 cells .....	77
Fig. 3.3.2 HZ reduced lipid accumulation in FFA-induced steatotic LO2 cells	
78	
Fig. 3.4.1 Effects of HZ on expressions of lipid metabolism-related proteins in	
<i>in vitro</i> model.....	83
Fig. 3.4.2 HZ-induced autophagy regulates hepatic lipid accumulation in	
steatotic LO2 cells.....	85
Fig. 3.4.3 Effects of Atg5 siRNA on lipid metabolism-related proteins of HZ in	
LO2 cells.....	86
Fig. 3.5.1 HZ reduced lipid accumulation in the liver .....	88
Fig. 3.5.2 Role of endothelium in HZ-induced relaxation .....	92
Fig. 3.5.3 HZ promoted nitrite production in isolated aortas .....	94

Fig. 3.6.1	Effects of HZ on antioxidative enzyme activities and MDA content in liver	96
Fig. 3.7.1	Effects of HZ on expressions of lipid metabolism-related proteins in <i>in vivo</i> model	99
Fig. 3.7.2	Effects of HZ on protein expressions of autophagy in <i>in vivo</i> model	100
Fig. 3.7.3	HZ mediates MAPK activation in <i>in vivo</i> model	101
Fig. 3.8.1	(A) PCA score plot, (B) PLS-DA score plot in negative (1) and positive (2) ionization modes for UPLC-MS	104
Fig. 3.8.2	Heatmap of UPLC-MS identified bile acid in normal control, HFD and HZ group	109
Fig. 3.8.3	HZ regulated TC utilization by increasing bile acid synthesis via activating CYP7A1	110

Fig. 3.8.4 A simplified proposed diagram of bile acid biosynthesis affected by

HFD and HZ treatment ..... 111

Fig. 4.7.1 The potential mechanisms of anti-NAFLD of HZ..... 140

## List of Abbreviations

ALT	alanine transaminase
ABCG1	ATP binding cassette subfamily G member 1
ABCG8	ATP binding cassette subfamily G member 8
$\alpha$ -MCA	$\alpha$ -muricholic acid
AST	aspartate aminotransferase
ACC	acetyl-CoA carboxylase
apoB	apolipoprotein B
AMP	adenosine monophosphate
AMPK	adenosine 5'-monophosphate activated protein kinase
ANOVA	analysis of variance
ATP	adenosine triphosphate
ASBT	sodium/bile acid cotransporter
BA	bile acid
$\beta$ -MCA	$\beta$ -muricholic acid
CA	cholic acid
CDCA	chenodeoxycholic acid
CYP7A1	cytochrome P450 7A1
CV	coefficient of variations
CYP27A1	sterol 27-hydroxylase
CVD	cardiovascular disease
CAT	catalase
CMA	chaperone-mediated autophagy
C19:1n9c	cis-10-nonadecenoic acid
DAD	diode array detector
DCFH-DA	2',7'-dichlorodihydrofluorescein diacetate

DCA	deoxycholic acid
DCFH	dichlorofluorescein
DCF	2',7'-dichlorodihydrofluorescein
DPPH	1,1-diphenyl-2-picrylhydrazyl
DMEM	Dulbecco's Modified Eagle's Medium
DNL	de novo lipogenesis
ESI	electrospray ion source
ERK	extracellular regulated protein kinase
FFA	free fatty acid
FMT	faecal microbial transplant
FGF	fibroblast growth factor
FXR	farnesoid X receptor
FXRE	FXR response element
FBS	fetal bovine serum
FAS	fatty acid synthase
GAE	gallic acid equivalents
GC-MS	gas chromatography-mass spectrometry
GCA	glycocholate
GDCA	glycodeoxycholate
GCDCA	glycochenodeoxycholic acid
GUDCA	glycoursodeoxycholate
GHRH	growth hormone-releasing hormone
GPATs	glycerol 3-phosphate acyltransferases
GLP-1	glucagon-like peptide-1
GSH-Px	glutathione peroxidase
HC	Houttuynia cordata Thunb.
HDCA	hyodeoxycholate
HZ	<i>Polygonum cuspidatum</i> (Hu Zhang)
HPLC	high performance liquid chromatography
HDL	high density lipoprotein
HDL-c	high density lipoprotein cholesterol

HFD	high-fat diet
HCC	hepatocellular carcinoma
HMGCR	3-hydroxy-3-methylglutaryl-CoA reductase
IR	insulin resistant
IL-6	interleukin 6
JNK	c-Jun N-terminal kinase
KBG	Kampo formula keishibukuryogan
LDL	low density lipoprotein
LDL-c	low density lipoprotein cholesterol
LDLR	low density lipoprotein receptor
LC3	light chain 3
LC3-I	cytosolic form of LC3
LC3-II	LC3-phosphatidylethanolamine conjugate
LCA	lithocholic acid
LO2	human liver cell line
MDA	malondialdehyde
MS	mass spectrometry
MTT	3-(4, 5-Dimethylthiazol-2-yl)-2,5-Diphenyltetrazolium Bromide
mTOR	mammalian target of rapamycin
MAPK	mitogen-activated protein kinase
NAFLD	non-alcoholic fatty liver disease
NASH	nonalcoholic steatohepatitis
NF- $\kappa$ B	NF-kappaB
NO	nitric oxide
OA	oleic acid
OPLS-DA	orthogonal partial least squares-discriminant analysis
PA	palmitic acid
PI3K	phosphatidylinositol 3-kinase
PPAR $\alpha$	peroxisome proliferator activated receptor $\alpha$
PPAR- $\gamma$	peroxisome proliferator-activated receptor gamma

PPRE	PPAR response element
PBS	phosphate-buffered saline
PCA	principal component analysis
PLS-DA	partial least squares-discriminant analysis
QC	quality control
ROS	reactive oxygen species
QYHTTL	QuYuHuaTanTongLuo
QSHYD	Qushi Huayu Decoction
SD	Sprague-Dawley
SREBP-1c	sterol regulatory element- binding protein-1c
SOD	superoxide dismutase
SR	Scavenging Rate
SC <sub>50</sub>	50% scavenging concentration
TNF- $\alpha$	tumor necrosis factor- $\alpha$
TC	total cholesterol
TG	triglyceride
TCA	taurocholate
TCDCA	taurochenodeoxycholate
TUDCA	tauroursodeoxycholate
THDCA	taurohyodeoxycholate
TGR5	takeda G-protein-coupled receptor 5
TCM	traditional Chinese medicine
UDCA	ursodexoycholic acid
UPLC-QTOF-MS	ultra-performance liquid chromatography-quadrupole time-of-flight mass spectrometry
VLDL	very low density lipoprotein
VIP	variable importance in the projection
YCHT	Yin-Chen-Hao-Tang

# **Chapter 1 Introduction**

Nonalcoholic fatty liver disease (NAFLD) refers to a spectrum ranging from simple steatosis to nonalcoholic steatohepatitis (NASH), fibrosis, cirrhosis to hepatocellular carcinoma (HCC) (Vanni et al. 2015). NAFLD occurs in patients who consume little or no alcohol, in the absence of chronic viral hepatitis or other liver disease. In the western world, NAFLD affects up to 20 - 35% of adults and up to 5 - 17% of children (Finucane et al. 2011; Vernon et al. 2011). Due to change in the modern diet and people's lifestyle, NAFLD has become one of the leading causes of chronic liver diseases in China (~ 15%) and Hong Kong (~ 27.3%) (Farrell et al. 2013; Wong et al. 2012).

Although the pathogenesis of NAFLD is not entirely understood, disordered lipid metabolism appears to play a key role in the development of NAFLD (Lonardo et al. 2015). Recent studies have revealed that autophagy induction can promote degradation of excess lipid droplets to attenuate steatosis in the liver. Several studies have revealed that there is an interrelationship between lipid metabolism and autophagy. In addition to autophagy regulates lipid metabolism, a reverse relationship exists in which an abnormal increase in intracellular lipid impairs autophagic clearance (Singh et al. 2009). Moreover, bile acid signalling has drawn considerable attention for its regulation of

hepatic lipid and glucose metabolism in the past few years.

Current treatment recommendations for NAFLD are limited, which include weight loss, bariatric surgery, vitamin E and glitazone treatments. However, the latter is with a risk of significant adverse effect profile. Therefore, alternative therapeutic strategies are therefore warranted and intensively being sought. Using herbal medicine to prevent and treat NAFLD has received increasing attention due to its effectiveness and acceptable prices. To date, a number of traditional Chinese herbal formulae have been reported to be beneficial to NAFLD.

*Polygonum cuspidatum* Sieb. et Zucc. (HZ, Hu Zhang in Chinese), a traditional Chinese medicine (TCM), is clinically used in the treatment of hepatitis, jaundice, scald and bruises in oriental counties for centuries. A well-known traditional Chinese herbal formula, Qushi Huayu Decoction including HZ alleviated NAFLD via activation of adenosine 5'-monophosphate activated protein kinase (AMPK) signaling pathway, anti-inflammation and attenuating oxidative stress (Feng et al. 2013; Feng et al. 2017; H. S. Li et al. 2009; Hui Zhang et al. 2008a). Apart from this, traditional Chinese herbal

formulae, Danning Tablet (Fan 2004), Huganning tablet (L. W. Wang et al. 2005; Y. Zhang et al. 2017) and QuYuhuatan tong luo Decotion (S. J. Zhang et al. 2008b) were tested on their effect in the treatment for NAFLD. Interestingly, all these four herbal formulae contain HZ, indicating that HZ might play an important role for treating NAFLD. Additionally, the water extract of HZ was shown to have a significant lipid lowering effect by inhibiting malondialdehyde (MDA) level and increasing superoxide dismutase (SOD) activity in rats model of fatty liver (Yiyong 2016). Based on these findings, a potential role of HZ in the treatment of NAFLD is of considerable interest. However, most studies till date focused on lipid lowering effect by improving anti-oxidative activity, insulin resistance (IR), as well as decreasing inflammation and lipogenesis related genes or proteins expressions. However, the underlying mechanisms of anti-NAFLD effect of HZ on lipophagy, as well as bile acid synthesis still remain unknown.

It is the first time to be reported that (1) treatment with Atg5 siRNA significantly abolished the increased expressions of peroxisome proliferator activated receptor  $\alpha$  (PPAR $\alpha$ ), low density lipoprotein receptor (LDLR) and phosphorylation of acetyl-CoA

carboxylase (p-ACC) as compared to that of LO2 cells treated with HZ. Treatment of HZ was also able to upregulate LDLR and p-ACC expressions in the absence of autophagy, suggesting that HZ reduced lipid accumulation partially by regulating autophagy induction. (2) the restoration of the down-regulated phosphorylation of adenosine 5'-monophosphate activated protein kinase (p-AMPK), PPAR $\alpha$ , LDLR, and p-ACC protein expressions induced by high-fat diet (HFD) were achieved in animals treated with simvastatin or HZ. A cytosolic form of LC3 (LC3-I) is conjugated to form LC3-phosphatidylethanolamine conjugate (LC3-II) is regarded as the most reliable marker protein for autophagy. HZ induced LC3-II expression, which indicated HZ promote lipid clearance in the fatty liver by enhancing autophagy. (3) HZ also improved some cardiovascular disease (CVD) related symptoms such as aorta relaxation, nitric oxide (NO) dysfunction and atherogenic index. It may contribute to its liver protection effect. (4) using untargeted mass spectrometry (MS)-based metabolomic platforms, multivariate statistics revealed that HZ supplement to HFD rats resulted in significant increases in three primary bile acids [chenodeoxycholate (CDCA), glycochenodeoxycholate (GCDCA) and glycocholate (GCA)] and two secondary bile

acids [deoxycholate (DCA) and glycodeoxycholate (GDCA)]. HZ significantly promoted cholesterol 7 $\alpha$ -hydroxylase (CYP7A1) activity, which was, HZ accelerated transforming of cholesterol into bile acids. As for the cholesterol-lowering effect of HZ, another reason might be contributed by its inhibition on dietary cholesterol absorption in the small intestine by the binding effects of HZ and conjugated bile acids. Our result showed that HZ increased three conjugated bile acids (GCA, GDCA and GCDCA). These conjugated bile acids lowered the solubility of cholesterol, resulting in lowering the transfer of cholesterol from intestine to the hepatocytes.

Therefore, studies on key factors elucidating regulatory effect of HZ on lipid metabolism, with the aim to discover novel drug targets for the prevention and treatment of NAFLD are being carried out. In the following literature review sections, NAFLD will be first presented from the etiology to the pathogenetic mechanisms to the current therapeutics; further, the relationship between dyslipidemia, autophagy, gut microbiota, bile acid metabolomics and NAFLD will be presented as research background knowledge of this study. Secondly, the previous research findings on HZ will be shown as the foundations of this research. Finally, the aims of this research

project will be brought forward on the basis of the characteristics of the NAFLD disorders and the features of HZ.

## **1.1 The pathogenesis of non-alcoholic fatty liver disease (NAFLD)**

The pathogenesis of NAFLD is debatable: in the traditional ‘two-hit’ hypothesis, hepatic steatosis is the first ‘hit’. The accumulation of triglycerides in hepatocytes enhanced the hepatic susceptibility to a subsequent second hit, which is responsible for liver injury, inflammation and fibrosis and cellular death characteristics of NASH. The second hit involves several risk factors such as oxidative stress, endoplasmic reticulum stress, proinflammatory cytokines and gut-derived bacterial endotoxin. Recent studies, however, have confronted this view by the ‘multiple parallel hits’ hypothesis, in which various pathogenic events occur in parallel, not consecutively, to promote liver injury, is now favoured (Birkenfeld and Shulman 2014; Kirpich et al. 2015; Musso et al. 2016).

Studies of patient and animal models have indicated several common pathogenic mechanisms of NAFLD, including lipid accumulation, dyslipidemia, IR, oxidative

stress, proinflammation cytokines, lipotoxicity and endoplasmic reticulum stress.

Recent studies have revealed that autophagy induction can promote degradation of excess lipid droplets to attenuate steatosis in the liver. Moreover, gut microbiota has gained much attention, and bile acids have emerged as a crucial factor in NAFLD.

Although dyslipidemia and oxidative stress are typical risk factors found predominantly in NAFLD patients with high-fat diets and inactive lifestyles, the interplay between diet, gut microbiota and autophagy is more crucial for the development and progression of NAFLD.

We summarize the common pathogenic mechanisms, autophagy and gut microbiota, are relevant mechanisms (especially for bile acids) leading to NAFLD.

## **1.2 Common pathogenic mechanisms of NAFLD**

The first step in the pathophysiology of NAFLD results from imbalance between lipid acquisition and removal. Whether steatosis can progress toward NASH, or these entities represent two different diseases, is still highly debated. However, up to 20 - 30% of NAFLD patients with simple steatosis may transform to steatohepatitis at a certain

point (Yu et al. 2016).

Currently, both NAFLD patients and animal models have indicated several common pathogenic mechanisms of NAFLD, including lipid accumulation, dyslipidemia, IR, oxidative stress, proinflammation cytokines, lipotoxicity and endoplasmic reticulum stress.

### **1.2.1 Dyslipidemia**

Dyslipidemia, an established modifiable risk factor of CVD, is manifested as elevation or attenuation of plasma concentration of lipoproteins. Generally, dyslipidemia is determined as triglycerides  $\geq 1.70$  mmol/L ( $\geq 150$  mg/dL), and/or total cholesterol (TC)  $\geq 6.22$  mmol/L ( $\geq 240$  mg/dL), and/or high density lipoprotein cholesterol (HDL-c)  $< 1.04$  mmol/L ( $< 40$  mg/dL), and/or low density lipoprotein cholesterol (LDL-c)  $\geq 4.14$  mmol/L ( $\geq 160$  mg/dL), and/or use of lipid-lowering medications. Dyslipidemia phenotypes were defined as follows: isolated hypercholesterolemia (Type 1), isolated hyperglyceridemia (Type 2), mixed dyslipidemia (Type 3) and low HDL level alone (Type 4) (Gao et al. 2016). During the past several decades, with the rapid economic

development and changes in lifestyles, dyslipidemia has been shown to increase in absolute number in China. It was estimated that 31.5% or 308 million people had borderline high or high total cholesterol, whereas 20.4% or 196 million people have a borderline high, high, or very high level of LDL cholesterol in a cross-sectional study from 2007 to 2008 in a nationally representative sample of 46,239 adults aged  $\geq 20$  years among Chinese population (W. Y. Yang et al. 2012).

Unlike other forms of chronic liver diseases, NAFLD is also deemed to be hepatic manifestation of metabolic syndrome including IR and hyperlipidemia that are predictive risk factors of stroke, CVD and diabetes mellitus. Approximately 20 - 80% of NAFLD patients also have dyslipidemia (Souza et al. 2012).

Patients with NAFLD are at higher risk of CVD, particularly when NASH is present (VanWagner et al. 2012). Importantly, several longitudinal studies have demonstrated that CVD is one of the most important causes of mortality among NAFLD patients. Thus, the implementation with hypolipidemic agents should be considered in the overall management of these patients (Chatrath et al. 2012; Q. Q. Zhang and Lu 2015).

### 1.2.2 Hepatic fat accumulation

Hepatic steatosis can be stimulated via (1) excess dietary triglyceride (TG) intake (increased fatty acid uptake), (2) enhanced intrahepatic TG synthesis (fatty acids formed from *de novo* lipogenesis), (3) excess fatty acid influx into the liver from adipose tissue lipolysis [the hydrolysis of free fatty acid (FFA) and glycerol from TG], (4) diminished export of lipids from the liver [decreased very low density lipoprotein (VLDL) with the help of apolipoprotein B (apoB)] (Koo 2013) (Fig. 1.2.1). Mutation in apoB may lead to hepatic steatosis (Dowman et al. 2010; Vacca et al. 2015) (Fig. 1.2.2), and (5) reduced fatty acid oxidation through  $\beta$ -oxidation (Tiniakos et al. 2010).

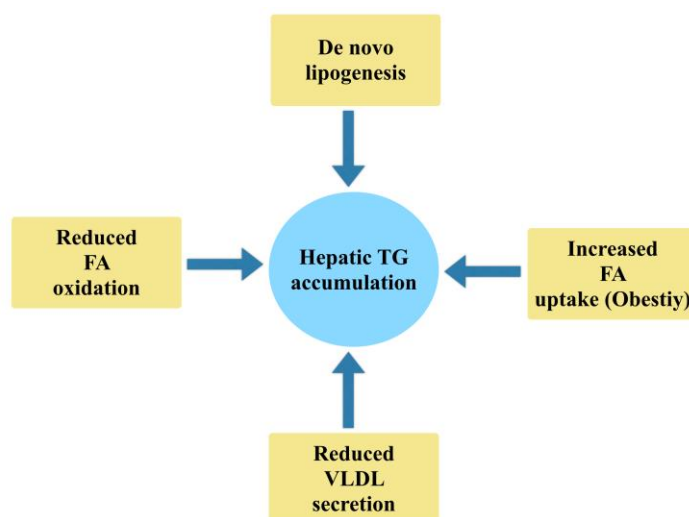


**Fig. 1.2.1 Model for the TG accumulation in the liver at the early stage of NAFLD (Koo 2013)**

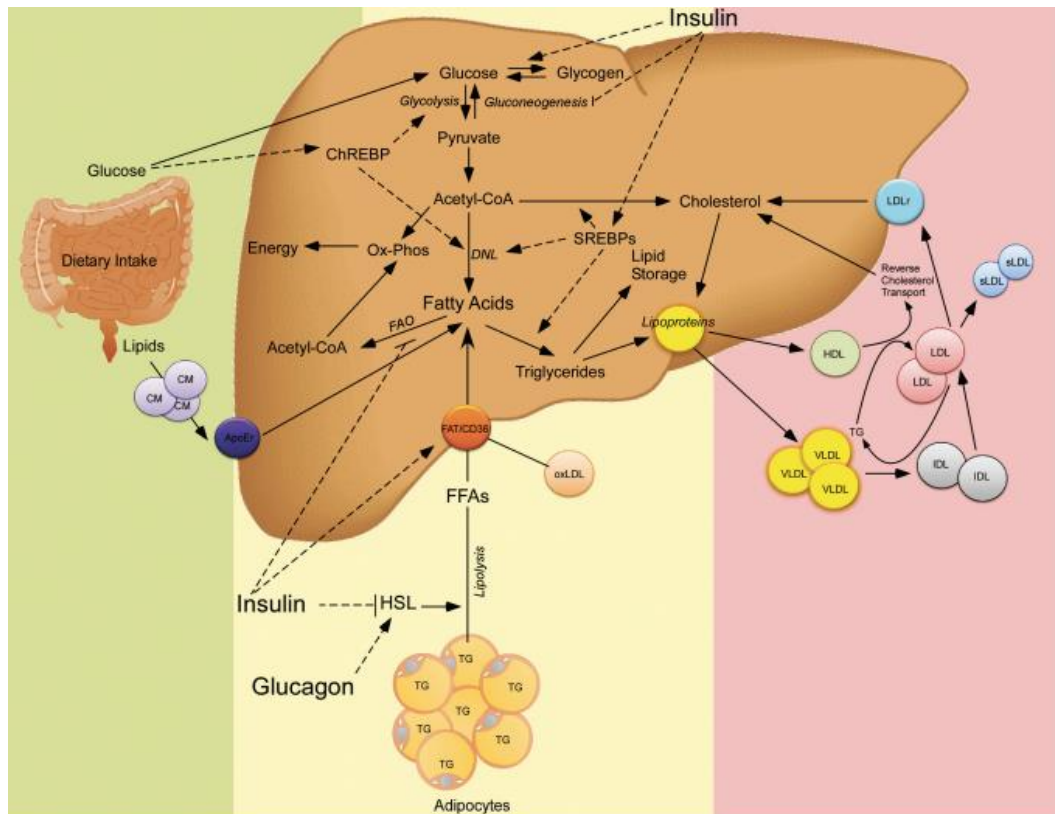


**Fig. 1.2.2 Role of hepatic fatty acid metabolism in the development of hepatic steatosis (Tiniakos et al. 2010)**

### 1.2.3 Oxidative stress and mitochondrial dysfunction

Clinical and experimental studies indicate a strong association between NAFLD and oxidative stress. The increased production of reactive oxygen species (ROS) induced lipid peroxidation, with subsequent activation of inflammatory pathways and stellate cells leading to fibrogenesis and mitochondrial damage. Mitochondria are responsible for oxidative phosphorylation and fatty acid  $\beta$ -oxidation and are the main source of cellular ROS. Therefore, dysfunction of liver mitochondria may play an important role

in the induction of hepatic steatosis and NASH. Oxidative phosphorylation and fatty acid  $\beta$ -oxidation within the normal liver takes place in the mitochondria, but this process may become overwhelmed as a result of increased FFA load, giving rise to ROS in the context of NAFLD (Gao et al. 2016). Although the molecular mechanism responsible for mitochondrial dysfunction remains elusive in NAFLD, a reduction in the activity of mitochondrial respiratory chain complexes and structural mitochondrial abnormalities (such as enlargement, loss of cristae, and paracrystalline inclusions) have been observed in human studies of NASH (Pérez-Carreras et al. 2003; Sanyal et al. 2001).

### **1.3 Lipophagy**

#### ***Autophagy***

In mammalian cells, there are three defined types of autophagy: macroautophagy, microautophagy and chaperone-mediated autophagy (CMA) (Fig. 1.3.1). Briefly, the first event of macroautophagy is the formation of the nucleation complex (beclin-1/VSP34-interacting complex), mediating of the phagophore. The second event is

elongation the formed phagophore into an autophagosome by two ubiquitin like conjugated complexes, modulated by Atg7: the Atg5/12 complex and the conjugation of LC3 to phosphatidylethanolamine. The third event is that degradation of cargo into their constituent components occurs when autophagosomes fuse with lysosomes (Singh and Cuervo 2011). A best-characterized modulator in microautophagy is the mammalian target of rapamycin (mTOR). This nutrient sensor kinase complex negatively regulates the initiation step of macroautophagy by phosphorylating UNC51-like kinase 1. However, AMPK is activated when adenosine monophosphate (AMP)/adenosine triphosphate (ATP) ratio increases under conditions of low energy status, leading to mTOR inhibition, thereby activating autophagy. A cytosolic form of LC3 (LC3-I) is conjugated to form LC3-PE conjugate (LC3-II), which is regarded as the most reliable marker protein for autophagy.

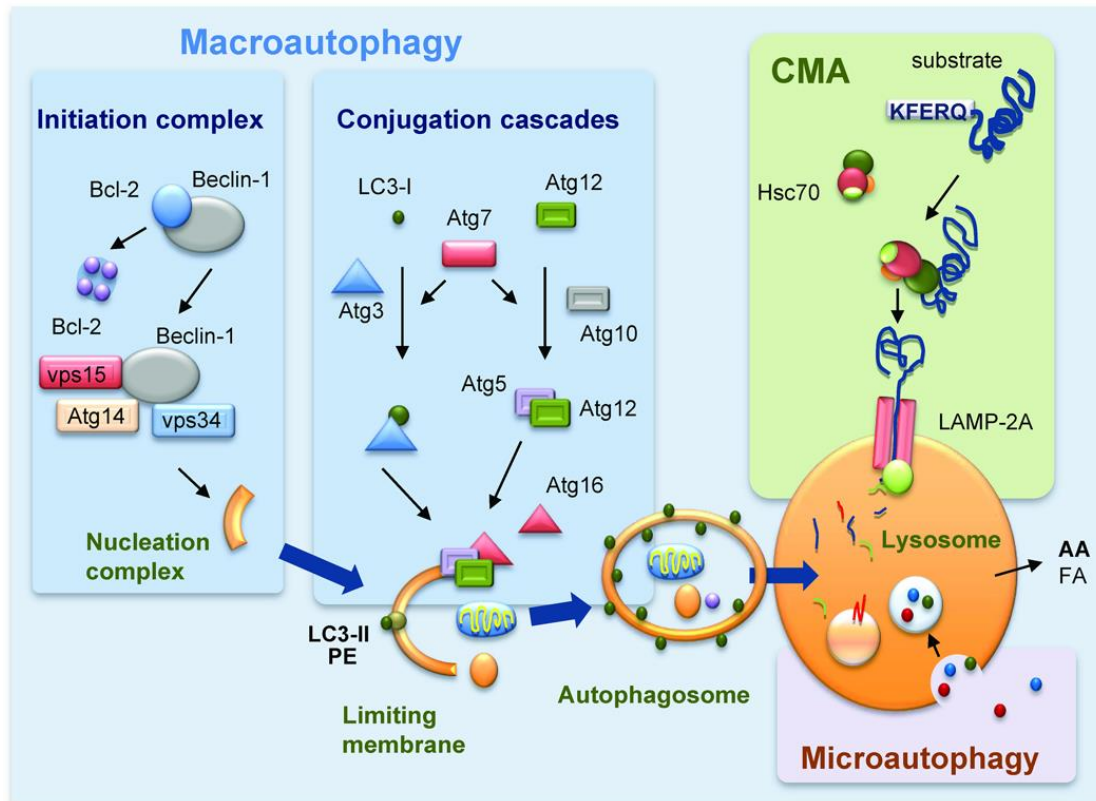


**Fig. 1.3.1** The molecular components of mammalian autophagic pathways (Singh and Cuervo 2011)

### *Lipophagy*

Triglycerides and cholesterol esters surrounded by a phospholipid and cholesterol monolayer are stored as neutral lipids in lipid droplets. Degradation lipid droplets by macroautophagy is termed lipophagy. Small lipid droplets or sequester portions of large lipid droplets were engulfed by LC3-II positive membranes. Autophagosomes deliver the lipid cargo to lysosomes wherein lysosomal acid lipase degrade lipids. Fatty acids

undergo mitochondrial  $\beta$ -oxidation with the production of energy once they are released into the cytosol (Fig. 1.3.2) (Ward et al. 2016).

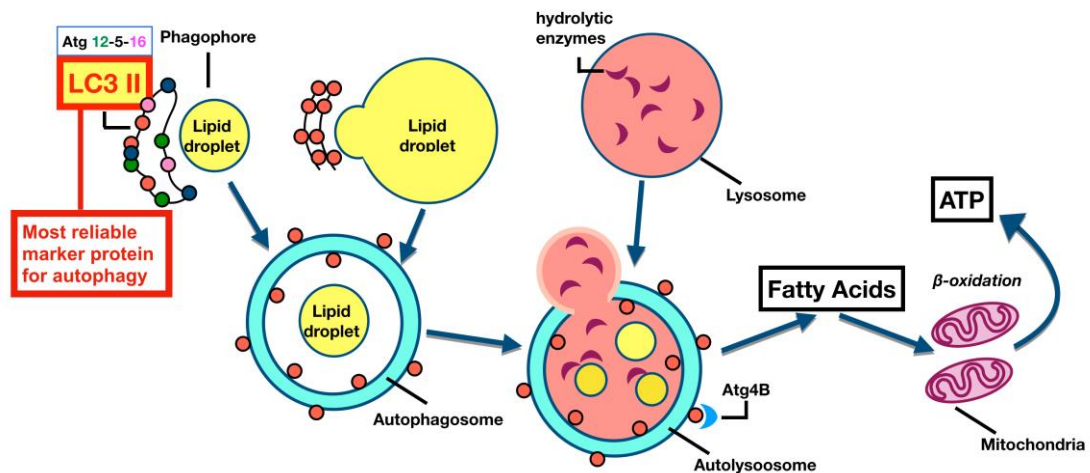


**Fig. 1.3.2 Autophagy degrades lipid droplets (Ward et al. 2016)**

Hepatic lipid metabolism has elicited a considerable interest in the interplay between autophagy and NAFLD. However, controversies of the exact role of autophagy in the lipid metabolism still exist: some publications claim a lipolytic function of autophagy, whereas others report a lipogenic function (Kwanten et al. 2014). In different lipogenic and nutritional states, the contribution of autophagy to lipid metabolism is different (Fig. 1.3.3). (a) Fed state: autophagy functions in the basal turnover of lipids from lipid droplets. (b) A short-term increase in lipid availability or during starvation state: autophagy is increased, leading to a greater breakdown of stored lipids to supply fatty

acids for  $\beta$ -oxidation or other uses. (c) Sustained increase in lipid availability (such as long-term HFD feeding) state: lipid accumulation also acts to inhibit autophagic function, thereby further promoting lipid accumulation (increased LD size; right panel) (Singh et al. 2009).

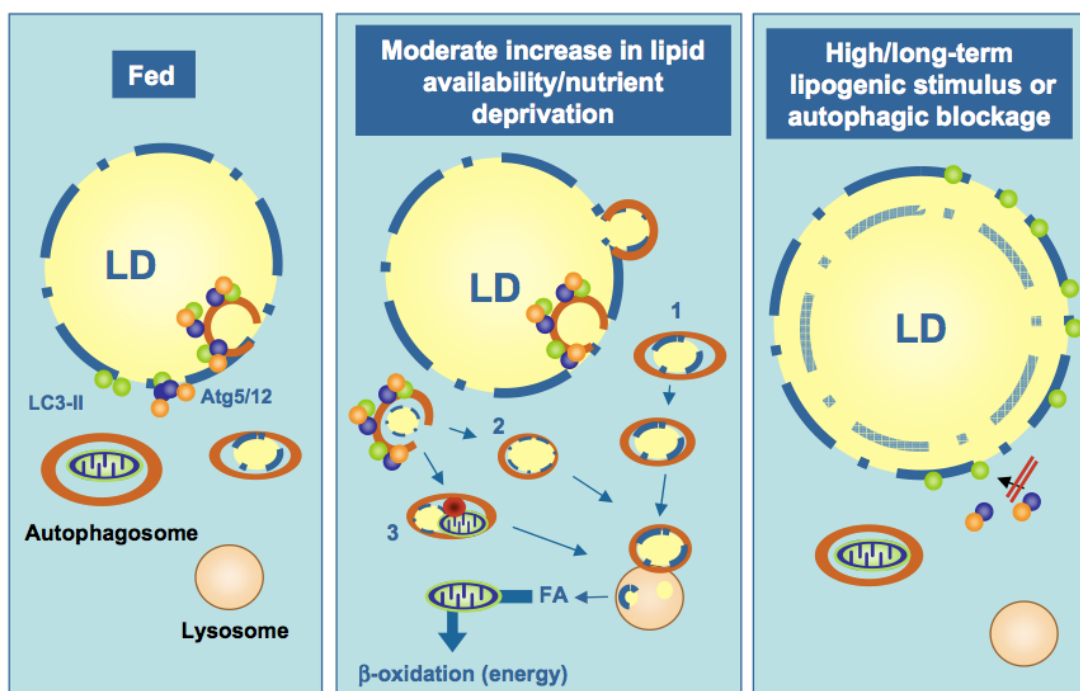


**Fig. 1.3.3 Hypothetical model of the contribution of autophagy to lipid metabolism in different lipogenic and nutritional states (Singh et al. 2009)**

In the fed state (left panel), a short-term increase in lipid availability or during starvation (center panel). A sustained increase in lipid availability (such as long-term HFD feeding), (increased LD size; right panel). Middle panel shows the three types of autophagic vesicles as identified in this study by their cargo: 1. autophagosomes carrying portions of a LD; 2. autophagosomes containing a whole small LD; and 3. autophagosomes containing lipids and other cytosolic components. LD: lipid droplet

Several studies have revealed that there is an interrelationship between lipid metabolism and autophagy. Initial evidence indicates that autophagy mediates lipid content because: (1) inhibition of autophagy increased triglycerides and lipid droplets accumulation not only in hepatocytes challenged with oleate methionine- and choline-deficient medium *in vitro* but also in Atg7<sup>F/F</sup>-Alb-Cre mice with a hepatocyte-specific knockout of the autophagy gene Atg7. (2) Loss of autophagy decreased TG  $\beta$ -oxidation and decay in siAtg5 cells. (3) Triglycerides and lipid droplets structural proteins were co-localized with autophagic compartments. (4) LC3 were associated with lipid droplets. In addition to autophagy regulates lipid metabolism, there is a reverse relationship exists in which an abnormal increase in intracellular lipid impairs autophagic clearance because of (1) decreased lipid droplet/LAMP1 co-localization, (2) the absence of autophagic upregulation in hepatocytes cultured with lipids, and (3) reduced association of autophagic vacuoles with lipid droplets in response to starvation

in HFD-fed mice (Singh et al. 2009).

Deletion of a hepatocyte-specific knockout of a gene essential for autophagosome formation, *atg7*, resulted in defective insulin signaling and elevated endoplasmic reticulum stress in both genetic (*ob/ob*) and dietary (HFD induced) models of murine obesity. The data demonstrated that reduced level of autophagy by decreasing autophagosome formation is a critical component of defective insulin action seen in obesity (L. Yang et al. 2010). In contrast, Inami et al. reported that autophagosome number increased with normal fusion of isolated autophagosomes and lysosomes, but autophagic function was suppressed due to a defect in autophagosomal acidification and cathepsin expression that impaired substrate degradation in autolysosomes in obese *ob/ob* mouse hepatocytes (Inami et al. 2011). Koga et al reported that up to 70% of autophagosome/lysosome fusion was reduced and this fusion defect was attributed to HFD or methyl-beta-cyclodextrin-induced changes in membrane lipid composition (Koga et al. 2010). Thus, there are three potential mechanisms (K. Liu and Czaja 2013) (Fig. 1.3.4) involved in the decreased hepatic autophagy that occurs with HFD feeding or obesity. (1) Obesity or HFD reduces levels of various autophagy factors (*Atg5* and

Atg7), resulting in decreased autophagosome formation and levels of autophagy (L. Yang et al. 2010). (2) The liver forms increased autophagosomes and autolysosomes, but levels of autophagy decreased due to the defective lysosomal that precluded degradation (Inami et al. 2011). (3) Autophagic flux decreases as a result of impaired autophagosome-lysosome fusion (Koga et al. 2010).

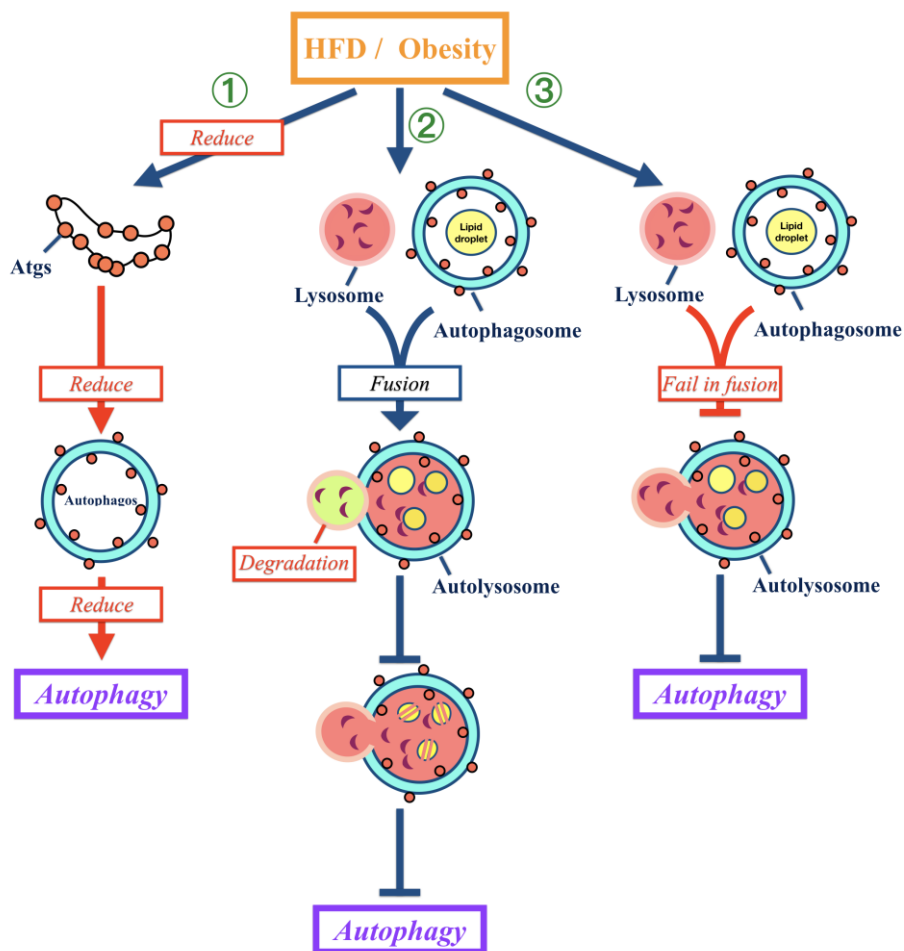


**Fig. 1.3.4 Potential mechanisms involved in the decreased hepatic autophagy that occurs with HFD feeding or obesity (K. Liu and Czaja 2013)**

## **1.4 Microbiota associated mechanisms of NAFLD**

The liver received a dual blood supply from the portal vein (70 - 80%) rich in nutrients and hepatic artery (20 - 30%) rich in oxygen. Since the liver receives 70% of its blood supply from the intestine via the portal vein, thus it is continually exposed to gut-derived factors including gut bacterial components, endotoxins (lipopolysaccharide, flagellin and lipoteichoic acid) and peptidoglycans.

NAFLD is a multifactorial disease that involves genetic and environmental contributions. Recent evidence demonstrates that gut microbiota dysbiosis can result in the development of NAFLD, and patients with NAFLD have increased intestinal permeability and small intestinal bacterial overgrowth (Miele et al. 2009). In the 1980s, gut microbiota was first found to be altered in patients with NASH, suggesting a possible role for the gut bacteria in NAFLD (Drenick et al. 1982). Disruption of the murine inflammasomes associated with intestinal microbiota results in exacerbation of hepatic steatosis and NASH in co-housing of inflammasome-deficient animals (Henao-Mejia et al. 2012).

Faecal microbiota analysis of patients with NAFLD revealed over-representation of *Lactobacillus* species and selected members of phylum Firmicutes (Lachnospiraceae; genera, *Dorea*, *Robinsoniella*, and *Roseburia*). One member of phylum Firmicutes (*Ruminococcaceae*; genus, *Oscillibacter*) was lower in the faecal microbiome of NAFLD patients compared with healthy subjects (Raman et al. 2013).

Since it is now evident that the gut microbiota plays an important role in energy storage and the subsequent development of obesity (Clarke et al. 2012), the role of gut microbiota in the development and progression of NAFLD has become a focus of research. Several mechanisms may lead to NAFLD through gut microbiota, including (1) increased production and absorption of gut short-chain fatty acids; (2) altered dietary choline metabolism by the microbiota; (3) altered bile acid pools by the microbiota; (4) increased delivery of microbiota-derived ethanol to liver; (5) gut permeability alterations and release of endotoxin; and (6) interaction between specific diet and microbiota (Gao et al. 2016).

## 1.5 Bile acids metabolism

Bile acids synthesized in the liver in humans include primary bile acids, cholic acid (CA; 3 $\alpha$ , 7 $\alpha$ , 12 $\alpha$  trihydroxycholanic acid) and chenodeoxycholic acid (CDCA; 3 $\alpha$ , 7 $\alpha$ -dihydroxycholanic acid). Their respective secondary bile acids, (DCA; 3 $\alpha$ , 12 $\alpha$ -dihydroxycholanic acid) and lithocholic acid (LCA; 3 $\alpha$ -monohydroxycholanic acid), which are formed by deconjugation and 7 $\alpha$ -dehydroxylation by intestinal bacteria (Kuipers et al. 2014) (Fig. 1.5.1) (Table 1.5.1). Ursodexoycholic acid (UDCA; 3 $\alpha$ , 7 $\beta$ -dihydroxycholanic acid) is a primary bile acid in some mammals (e.g., bear, nutria and beaver can be synthesized to a limited extent from CDCA. In mice and rats, the majority of CDCA is efficiently converted into alpha-Muricholic acid ( $\alpha$ -MCA) and beta-Muricholic acid ( $\beta$ -MCA) (Anwer 2012; Thomas et al. 2008) (Table 1.5.1).

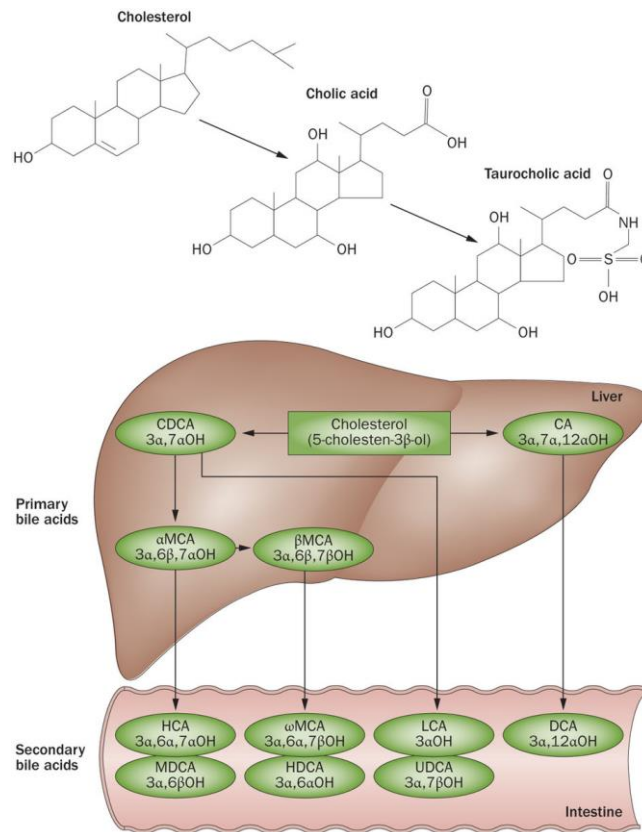


**Fig. 1.5.1 Schematic overview of primary and secondary bile acid species (Kuipers et al. 2014)**

**Table 1.5.1 Different kinds of bile acids**

Bile acids	Synthesis Organ	Abbreviation	Full name
Primary	Liver	CA	cholic acid; 3 $\alpha$ , 7 $\alpha$ , 12 $\alpha$ trihydroxycholanic acid
		CDCA	chenodeoxycholic acid; 3 $\alpha$ , 7 $\alpha$ -dihydroxycholanic acid
		$\alpha$ -MCA	Alpha-Muricholic acid
		$\beta$ -MCA	Beta-Muricholic acid
		G $\beta$ -MCA	glyco $\beta$ -muricholic acid
		T $\beta$ -MCA	tauro- $\beta$ -muricholic acid
		GCA	glycocholate
		TCA	taurocholate
		GCDCA	glycochenodeoxycholate
		TCDC	taurochenodeoxycholate
Secondary	Colon	DCA	deoxycholic acid; 3 $\alpha$ , 12 $\alpha$ -dihydroxycholanic acid
		HDCA	Hyodeoxycholate
		UDCA	ursodexoycholic acid; 3 $\alpha$ , 7 $\beta$ -dihydroxycholanic acid
		LCA	lithocholic acid; 3 $\alpha$ -monohydroxycholanic acid
		GDCA	glycodeoxycholate
		TDCA	taurodeoxycholate
		TUDCA	Tauroursodeoxycholate
		GHDCA	glycohyodeoxycholate
		THDCA	Taurohyodeoxycholate
GUDCA	glycoursodeoxycholate		

Within hepatocytes, bile acids are synthesized from cholesterol through the classic (neutral) and alternative (acidic) pathways that generate glycine-or taurine-conjugated bile acids (BA), including CA, CDCA and MCA. Then bile acids are conjugated with taurine or glycine before secretion into bile and released into the small intestine for absorption of triglycerides, cholesterol and lipid-soluble vitamins. In the small intestine, apart from their role in promoting in lipid absorption and transport, bile acids have also been reported for binding nuclear receptor and altering the microbiome (Fig.1.5.2) (de Aguiar Vallim et al. 2013). On the other hand, intestinal microbial organisms affect bile acid metabolism. The gut microbiota affects not only the composition of the bile acid pool but also the expression of genes controlled by the bile acid-activated farnesoid X receptor (FXR) (Fig. 1.5.3) (Kuipers et al. 2014; Swann et al. 2011).

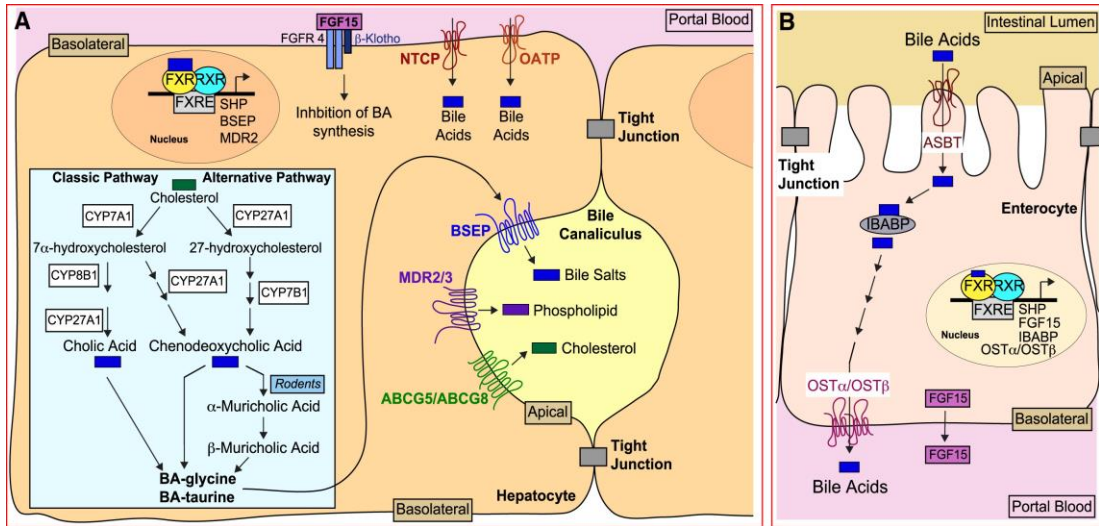


**Fig. 1.5.2 Bile acid Metabolism in Liver and Intestine (de Aguiar Vallim et al. 2013)**

(A) bile acid biosynthetic pathways: the classic (neutral) and alternative (acidic) bile acid biosynthetic pathways (B) bile acid absorption

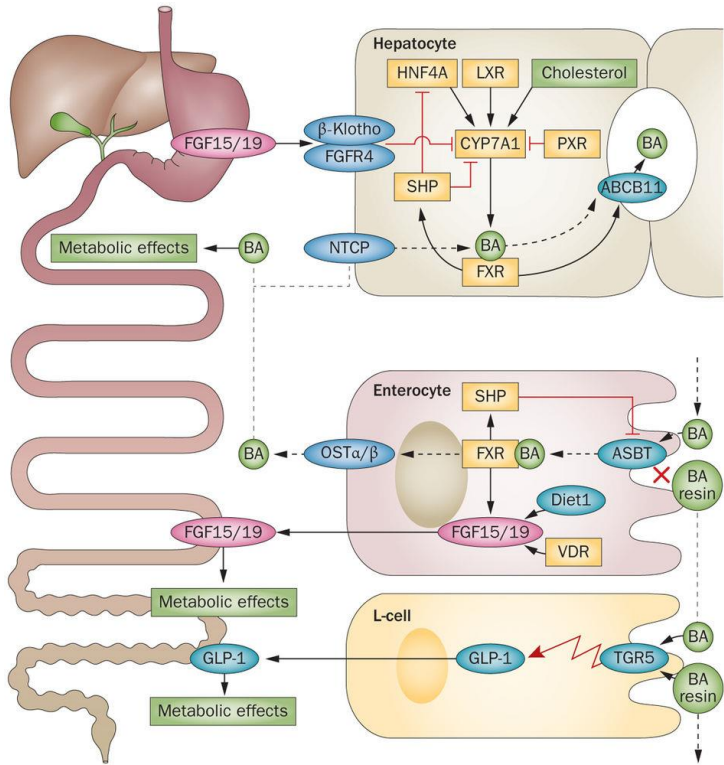


**Fig. 1.5.3 Schematic overview of bile acid signalling within the enterohepatic circulation (Kuipers et al. 2014)**

Extensive research has unveiled that bile acids play a number of roles in lipid metabolism. Bile acids are synthesized in hepatocytes from cholesterol, stored and concentrated in the gallbladder, and released into the duodenum. Most (95%) of bile acids are reabsorbed in the distal ileum following secretion of bile salts into the duodenum, mainly via apical sodium-dependent transporter (ASBT) but also through passive processes or excreted in the feces (Sayin et al. 2013).

It is well established that bile acids have profound effects on facilitating fat absorption.

Bile acids also function as signaling molecules regulating key metabolic pathways involved in lipid metabolism, drug, inflammatory response through activation of the FXR and cell surface G-protein coupled receptor 5 (TGR5) (Sayin et al. 2013).

McMahan et al. showed that activation of bile acid receptors with a dual FXR/TGR5 agonist was able to decrease liver steatosis and inhibit hepatic inflammation in a murine model of NAFLD (McMahan et al. 2013).

## **1.6 Therapeutic strategies for NAFLD**

### **1.6.1 Western medicine**

Although lifestyle interventions (including weight loss, dietary modification, and physical exercise) is the mainstay of treatment of NAFLD, it is difficult to maintain, prompting the need for pharmacotherapy as well. Researchers have identified four main pathways that opens the door to treat NAFLD according to their intended targets (Table 1.6.1) (Fig. 1.6.1) (Rotman and Sanyal 2017).

**Table 1.6.1 Medications targeting NAFLD**

Medications	Agents
With a primary metabolic target to reduce hepatic fat accumulation and metabolic stress	(1) inhibitors of de novo lipogenesis (DNL): (aramchol, NDI-010976) (2) peroxisome proliferator-activated receptor (PPAR) agonists (eg, pioglitazone, elafibranor, saroglitazar) (3) bile acid-farnesoid X receptor (FXR) axis (obeticholic acid) (4) hormones: glucagon-like peptide-1 (GLP-1): liraglutide ; fibroblast growth factor (FGF)-21 or FGF-19 analogues; growth hormone-releasing hormone (GHRH): tesamorelin;
Addressing oxidative stress or the inflammation and injury components of NASH	(1) antioxidants (vitamin E), (2) tumour necrosis factor $\alpha$ (TNF- $\alpha$ ) pathway (emricasan, pentoxifylline) (3) immune modulators (amlexanox, cenicriviroc)
With a primary gut target, modulating the interaction between the gut and the liver in NAFLD	(1) antiobesity agents such as orlistat (2) gut microbiome modulators (IMM-124e, (3) faecal microbial transplant (FMT): solithromycin
Antifibrotics, aiming to decrease the progressive fibrosis and resultant complications	antifibrotics (sintuzumab and GR-MD-02)

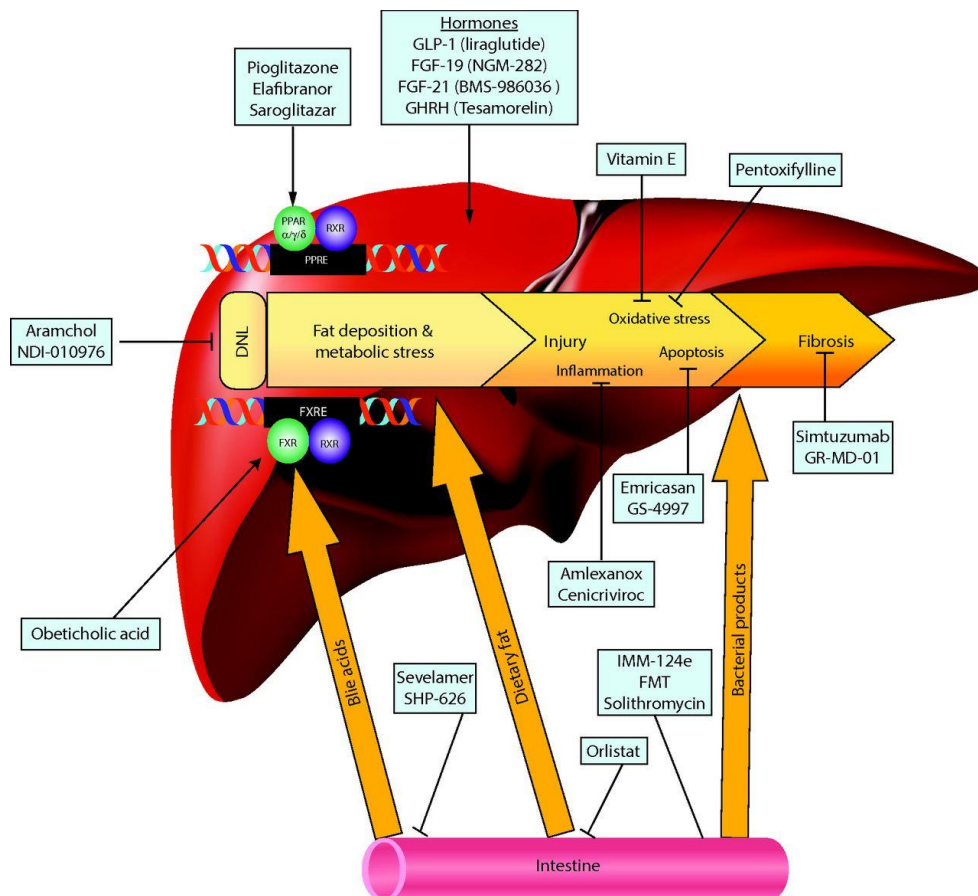


**Fig. 1.6.1 Medical therapies targeting NAFLD (Rotman and Sanyal 2017)**

FXRE, FXR response element; PPRE, PPAR response element; RXR, retinoid X receptor.

Data from other studies demonstrated that vitamin E may not be a completely risk-free intervention. Intake of vitamin E increased the risk of haemorrhagic stroke (Schürks et al. 2010), prostate cancer in men (Klein et al. 2011) and all-cause mortality (L Abner et al. 2011). Unfortunately, a side effect profile that pioglitazone includes increased the risk of bladder cancer in patients with type 2 diabetes and evidence of macrovascular disease was revealed in a large-scale randomized controlled trial (Dormandy et al.

2005). Recently, liraglutide, a glucagon- like peptide 1, was shown to reduce metabolic dysfunction, IR and lipotoxicity. Moreover, liraglutide was safe, well tolerated in a phase 2 trial conducted in four UK medical centres (26 patients were randomly assigned to receive liraglutide and 26 to placebo) between Aug 1, 2010, and May 31, 2013. Extensive and longer-term studies are needed to further evaluate the safety and efficacy of this drug (Matthew J Armstrong et al. 2016a; Matthew James Armstrong et al. 2016b).

### **1.6.2 Tradional Chinese Medicine (TCM)**

Since more effective new therapeutic options are lacking, patients with NASH should be encouraged to take traditional Chinese herbs, which are effective, safe and affordable.

#### **Clinical Studies**

In a multicenter clinical trial during the period of July 1999 to February 2000, short-term administration of Danning Pian for 3 months, a TCM herbal formula composed of Polygonum cuspidatum, Rheum palmatum L., Citrus reticulate Blanco, and Curcuma rchenyujin Y. was shown to improve clinical symptoms, reduce serum alanine

transaminase (ALT) and TG levels, and result in a mild reduction in degree of steatosis in patients with NAFLD. Mild adverse events, including diarrhea, skin rash and mild to moderate elevation of serum ALT level, were identified in the trial (Fan 2004). In a clinical trial comparing the effectiveness of QuYuHuaTanTongLuo (QYHTTL) decoction for 6 months (components: Radix Bupleuri 10 g, Radix Scutellariae 12 g, Rhizoma Pinelliae 10 g, Radix Codonopsis Pilosulae 30 g, Radix Glycyrrhizae Praeparata 6 g, Fructus Ziziphi Jujubae 9 g, Rhizoma Polygoni Cuspidati 30 g, Radix Morindae Officinalis 8 g, Herba Hedyotis Diffusae 30 g) with that of UDCA in patients with NASH, Zhang et al. found that patients who received the decoction had significantly lower levels of hepatic aminotransferases and significantly better lipid profiles than patients who received UDCA. The researchers also provided evidence that the effect of QYHTTL is due, at least in part, to its anti-inflammatory [down-regulating TNF- $\alpha$  and interleukin 8 (IL-8) level] and antioxidant properties [decreased MDA and increased SOD activity] (S. J. Zhang et al. 2008b). In a retrospective study, Fujimoto et al. (Fujimoto et al. 2010) reported that patients with NAFLD who received KBG (Guizhifulingwan) for 8 - 12 weeks showed significantly lower aspartate

aminotransferase (AST) and ALT levels after treatment.

However, a Cochrane review in 2013 (Z. L. Liu et al. 2013) showed that although some TCM formulas, such as Jiangzhi Ligan decoction, and Qingzhifugan decoction have positive effects on AST, ALT, and ultrasonographic findings in NAFLD patients, meta-analysis was not performed and no conclusions on the effectiveness of those TCM formulas could be reached because of the heterogeneity of the TCM trials included in the review, including different TCM formulas, the limited number of participants, and different outcome measures.

### **Experimental studies**

Both *in vitro* and *in vivo* studies have shown that a number of TCM on metabolic parameters is associated with NAFLD. For example, Wang et al. (M. J. Wang et al. 2012) reported that an extract of radix of *Polygoni multiflora* Moldenke (RPM) as well as its active components emodin, physcion and 2,3,5,4'-tetrahydroxystilbene-2-O- $\beta$ -D-glucoside could reduce TG, TC and LDL-c levels in LO2 hepatocytes that had been grown in medium containing fat emulsion and a high concentration of fetal bovine

serum. Kang and Koppula (H. Kang and Koppula 2014) reported that the hypolipidemic effects of ethanol extract of *Houttuynia cordata* Thunb. (HCE) was mediated through AMPK pathway. HCE attenuated the expression of fatty acid synthase (FAS), sterol regulatory element-binding protein-1c (SREBP-1c), and glycerol 3-phosphate acyltransferases (GPATs) in HepG2 cells exposed to 25 mM of glucose for 24 hours.

Kang et al. (O. Kang et al. 2013; O. H. Kang et al. 2015) found that curcumin and puerarin ameliorated oleic acid-induced lipid accumulation via activating the PPAR $\alpha$  and AMPK signaling pathways in HepG2 cells.

Lee et al. (Lee et al. 2010) found that the TCM herbal formula Yin-Chen-Hao-Tang (YCHT) administered to HFD-fed mice for 15 weeks resulted in an increase in level of adiponectin and endothelial progenitor cells, the upregulation of peroxisome proliferator-activated receptor gamma (PPAR- $\gamma$ ), inhibition of hepatic free fatty acid concentrations, elevated GSH level in hepatic tissue, and increased senescence marker protein-30 metabolism. Fujimoto et al. (Fujimoto et al. 2008) found that oral administration of Kampo formula keishibukuryogan (KBG) for twelve weeks resulted in significant reductions in hepatic TG, fibrosis and oxidative stress in a rabbit model

of NAFLD/NASH.

In addition, Zhang et al. (L. Zhang et al. 2014) showed that *Salvia-Nelumbinis naturalis* (SNN) alleviated hepatosteatosis by improving liver function and insulin signalling in rats fed with a high caloric diet. Chen et al. (S. D. Chen et al. 2013) demonstrated that administration of Yiqihuoxue formula for five weeks resulted in improved liver function and reducing the fatty deposition in liver via increasing expression of gastrin and motilin in rats fed with HFD.

The summary mechanisms of TCM in the pathogenesis of NAFLD is shown in Fig.1.6.2 (Hsu et al. 2016).

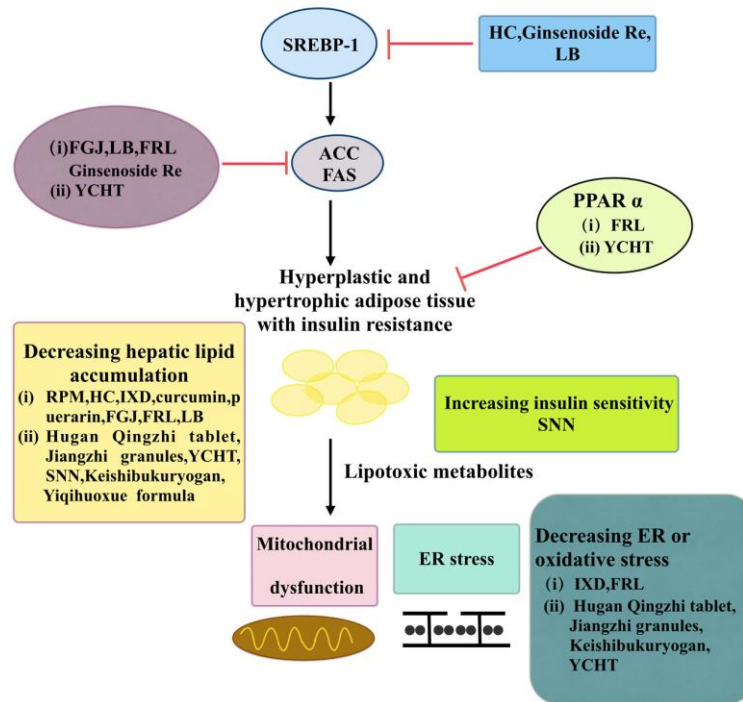


**Fig. 1.6.2 Mechanisms of TCM in the pathogenesis of NAFLD (Hsu et al. 2016)**

ACC: acetyl-CoA carboxylase; ER: endoplasmic reticulum; FAS: fatty acid synthase; FGJ: fruit of *Gardenia jasminoides* J. Ellis; HC: *Houttuynia cordata* Thunb.; IXD: *Ixeris dentata*; LB: *Lycium barbarum* L.; PPAR: peroxisome proliferator activated receptor; FRL: fruit of *Rosa laevigata* Michx.; RPM: radix of *Polygoni multiflora* Moldenke; SNN: *Salvia-Nelumbinis naturalis*; YCHT: Yin-Chen-Hao-Tang.

## 1.7 *Polygonum cuspidatum* (Hu Zhang)-a promising agent

### 1.7.1 TCM theory

In the theory of TCM, NAFLD is not recognized as a particular disease. Instead, the symptoms of NAFLD including obesity, right rib hypochondriac pain, discomfort, jaundice and fatigue have been classified as “Feiqi” “liver swelling”. According to the

book “Chinese medicine diagnosis” published in 1997, such symptoms have been named as liver swelling. According to TCM theory, eating disorders, work and restlessness, chronic illness physically weak, emotional disorders, lack of endowments caused liver qi stagnation, qiji is blocked by dampness-heat, which the passing of time blood stasis is induced.

Disease occurs in the liver and also involves the spleen, stomach and gall bladder. To sum up, dampness, heat and blood stasis are the key for NAFLD. Phlegm and blood stasis is considered as the main pathogenesis generally. It was mainly divided into five types: phlegm and blood stasis, liver and spleen deficiency, intrinsic damp heat, qi stagnation and blood stasis, liver and kidney deficiency. Treatments based on syndrome differentiation are mainly removing phlegm, or expelling blood stasis, dispersing stagnated liver qi, invigorating liver and kidney (Table 1.7.1).

*Polygonum cuspidatum* sieb. et Zucc. (HZ, Hu Zhang in Chinese) is a perennial herb with both medicinal and food dual value, native to Eastern Asia such as China, Japan and Korea, whose young stems are edible as a spring vegetable with a flavor similar to

lemon or rhubarb. The tropism of channel of the root of *Polygonum cuspidatum* (Fig. 1.7.1) is liver, gallbladder and lung. The tropism of taste of *Polygonum cuspidatum* is slightly bitter and cool. In TCM, the root of *Polygonum cuspidatum* was used for activating blood circulation, removing dampness and clearing hot, clearing heat and detoxification, relieving cough and resolving phlegm. It has been used for conditions of the heart and blood vessels including atherosclerosis and hyperlipemia and for digestion problems including constipation, liver disease (hepatitis), and gallstones. It is also used for scald and cancer.



**Fig. 1.7.1** Photo of the dried root of *Polygonum cuspidatum* (Hu Zhang)

**Table 1.7.1 TCM theory in diagnosing and treatment of NAFLD-like symptom**

TCM name of NAFLD	Feiqi; Phlegm, Liver swelling “Chinese medicine diagnosis” in 1997
NAFLD-like symptom	Obesity, hypochondriac pain, jaundicet, fatigue
Pathogenesis	Eating disorders, work and restlessness, chronic illness physically weak, emotional disorders, lack of endowments caused liver qi stagnation, damp heat accumulation
Types	Phlegm and blood stasis. Intrinsic damp heat, Qi stagnation and blood stasis, Liver and spleen, deficiency, Liver and kidney deficiency
Treatment based on syndrome differentiation	Removing phlegm or expelling blood stasis, Dispersing stagnated liver qi, Invigorating liver and kidney

### 1.7.2 Potentially advantageous features

A number of traditional Chinese herbal formulas have been reported to be beneficial to NAFLD. A well-known traditional Chinese herbal formula, Qushi Huayu Decoction (QSHYD), consists of five kinds of medicinal plants: *Artemisia capillaris* (Thunb), *Polygonum cuspidatum* Sieb. et Zucc., *Hypericum japonicum* (Thunb), *Curcuma Longa* L, and *Gardenia jasminoides* (Ellis). QSHYD alleviated NAFLD via activation of

AMPK signaling pathway, anti-inflammation and attenuating oxidative stress (Feng et al. 2017; H. S. Li et al. 2009) (Hui Zhang et al. 2008a). Apart from this, another traditional Chinese herbal formula, Danning Tablet containing *Polygonum cuspidatum* Sieb. et Zucc is also effective treatments for liver diseases such as cholecystitis and gallstones (Fan 2004). Zhang et al. found that patients who received the QYHTTL decoction for 6 months had significantly lower levels of hepatic aminotransferases and significantly better lipid profiles than patients who received UDCA. The researchers also provided evidence that the effect of QYHTTL is due, at least in part, to its anti-inflammatory (down-regulating TNF- $\alpha$  and IL-8 level) and antioxidant properties (decreased MDA and increased SOD activity) (S. J. Zhang et al. 2008b). In addition, Huganning tablet (L. W. Wang et al. 2005; Y. Zhang et al. 2017), alleviated NASH by reducing ALT, AST, LDL-c, TG, TC, Gamma-Glutamyl Transpeptidase ( $\gamma$ -GT) (Table 1.7.2).

Aqueous extracts of *Polygonum cuspidatum* compound could increase leptin mRNA level, decrease the adiponectin mRNA level to protect the liver from NAFLD (Jiang Qinglan et al. 2008). The water extract of HZ was shown to alleviate NAFLD by

inhibiting TNF $\alpha$  mRNA expression (Jiang et al. 2009), MDA level and increasing SOD activity in rats model of fatty liver (Yiyong 2016).

So we hypothesize that HZ might be effective for the treatment of fatty liver based on three reasons. First, tropism of channel of HZ is liver, which is consistent with the main site of fatty liver. Second, HZ can alleviate blood stasis and phlegm, which is consistent with pathogenesis and treatment of fatty liver. Third, it has been used as the components of a formula for treating hyperlipemia, liver disease (hepatitis).

**Table 1.7.2 Clinical and experimental studies of herbal formulas including HZ or its monomers or extracts**

	Study ID	Chinese Name	Botanical Name of Ingredient	Anti-NAFLD effects
Traditional Chinese herbal formulas	(Feng et al. 2017) (Feng et al. 2013)	Qushi Huayu Decoction	Polygonum cuspidatum, Artemisia capillaries Thunb, Gardenia jasminoides Ellis, Curcuma longa L., Hypericum japonicum Thunb	↑ GSH; ↓ Oxidative stress; ↓ Inflammation; ↓ lipid synthesis; ↑ Gut barrier function ↓ALT, AST; ↓SREBP-1 ↑p-AMPK, p-ACC;
	(L. W. Wang et al. 2005; Y. Zhang et al. 2017)	Huganning tablets	Lycopodium cernum, Polygonum cuspidatum, Saliva miltiorrhiza, Ganoderma lucidum.	↓ALT, AST, r-GT, ↓TG, TC, LDL-C
	(S. J. Zhang et al. 2008b)	QuYuHuaTanTongLuo Decoction	Polygonum cuspidatum, Bupleurum chinense, Scutellaria bicalensis, Pinellia ternate, Codonopsis pilosula, Glycyrrhiza uralensis, Ziziphus jujuba, Morinda officinalis, Hedyotis diffusa.	↓TNF- $\alpha$ , IL-8, MDA, ↑SOD
	(Fan 2004)	Danning Pian	Polygonum cuspidatum, Rheum palmatum L., Citrus reticulate Blanco, Curcuma rcenyujin Y., Crataegus pinnatifida Bunge	↓ ALT, TG

## 1.8 The aims of the study

Although clinical practice and modern experiments validate HZ or HZ combined with other herbs exhibits significantly hepatoprotective and cholagogic action, the anti-NAFLD effect of HZ still remains largely unknown. Based on previous findings, a potential role of HZ in the treatment of NAFLD is of considerable interest. However, the underlying mechanisms of anti-NAFLD effect of HZ on lipophagy and bile acid metabolism still remain unclear. Therefore, studies on key factors for elucidating regulatory effect of HZ on lipid metabolism, with the aim to discover novel drug targets for the prevention and treatment of NAFLD are being carried out.

To validate our hypothesis, we have designed and conducted experiments in this project.

There are three major objectives of my project:

1. Investigate the lipid reduction effects of HZ and characterize the molecular mechanisms of lipid reduction of HZ in normal human liver cell line (LO2 cells).
2. Evaluate the lipid reduction effects of HZ against fatty liver using high-fat diet (HFD)-induced steatosis in rats *in vivo*.

3. Investigate the possible mechanistic pathways of HZ on lipid reduction by using molecular and metabolomics approaches *in vivo*.

## **Chapter 2 Materials and Methods**

## 2.1 Preparation of HZ sample

HZ was obtained from Eu Yan Sang Company Limited (Hong Kong SAR, China). 1000 g of the dried roots of HZ was boiled for 2 h using 15 L water. The water extraction was centrifuged (at 4000 rpm, 10 min) and the supernatant was freeze-dried in a freeze drier (Labconco, Freezone 6). The dry weight was 75 g. Therefore, the yield is 7.5%.

## 2.2 High performance liquid chromatography (HPLC) analysis

### *Chemicals and reagents*

Standard of polydatin (> 98%) was purchased from Testing laboratory for Chinese Medicine (Hong Kong University of Science and Technology, Hong Kong, China). Emodin (> 97%), resveratrol (> 99%) is purchased from Sigma-Aldrich (St. Louis, MO, USA). Emodin 8-O- $\beta$ -D-glucopyranoside and physcion 8-O- $\beta$ -D-glucopyranoside were isolated in our laboratory and identified with NMR. The purities of these two compounds were determined to be higher than 98% by high performance liquid chromatography/diode array detector analysis (HPLC/DAD). Acetonitrile and

methanol (HPLC grade) were purchased from Duksan Pure Chemical. Co. Ltd. (Ansan, Korea). Distilled water was purified using a Milli-Q water purification system (Millipore, Bedford, MA, USA).

### ***Extraction and HPLC method***

0.1 g freeze-dried HZ water extract was accurately weighed and redissolved with 10 mL HPLC graded methanol. After 30 min ultra-sonication, the sample solution was filtrated through a syringe filter (0.45  $\mu\text{m}$ ). HPLC/DAD analysis was carried out on a Alltima HP C18 column (250 mm  $\times$  4.6 mm, 5  $\mu\text{m}$ ; Grace, USA) at room temperature using an Agilent 1100 liquid chromatography system equipped with a quaternary solvent delivery system, an autosampler and a DAD. The detection wavelength was 290 nm. The gradient elution of the mobile phase consisting of (A) water and (B) 0.05% (v/v) methanol in acetonitrile was as follows: 80% (A) at 0 - 15 min; from 80% to 50% (A) at 15 - 25 min, from 50% to 30% (A) at 25 - 30 min, from 30% to 0% (A) at 30 - 40 min, and 0% (A) at 40 - 45 min. 10 min re-equilibrium was allowed between injections. The flow rate was 0.8 mL/min. Aliquots of 10  $\mu\text{L}$  solution were injected into

the HPLC.

## 2.3 Determination of antioxidant properties

In order to measure the antioxidant properties of HZ, 1, 1-diphenyl-2-picrylhydrazyl (DPPH) free radical scavenging activity assay and total phenolic quantification is induced in this study following the procedures we described before (J. J. Li et al. 2015a).

For DPPH assay, various concentrations of HZ water extract and vitamin C were prepared by dissolving the dried powder with Milli-Q water. 50  $\mu$ L of sample solution was added to 950  $\mu$ L of DPPH• methanol solution (24 mg/L) and allowed to react for 1 h. The scavenging activity of each sample was measured by spectroscopic method.

Absorbance of sample ( $A_{\text{sample}}$ ) was determined by UV-visible spectrometer (Perkin Elemer Lambda 35) at 515 nm. Using 50  $\mu$ L of water as control ( $A_{\text{control}}$ ), the free radical scavenging Rate (SR%) of each concentration was calculated by the following equation:

$$\text{SR}\% = \left(1 - \frac{A_{\text{sample}}}{A_{\text{control}}}\right) \times 100\%$$

$A_{\text{control}}$ : absorbance value of DPPH• solution with 50  $\mu\text{L}$  of water

$A_{\text{sample}}$ : absorbance value of DPPH• solution with 50  $\mu\text{L}$  of herbal extract.

The 50% scavenging concentration ( $SC_{50}$ ) was calculated by GraphPad Prism 6.01 for Windows (GraphPad Software, San Diego California, USA).

For the determination of total phenolic content of HZ, Folin-Ciocalteu method was used to measure the total phenolic quantification of HZ water extract. 100  $\mu\text{L}$  of sample solutions [HZ water extract (0.3, 0.5 and 1.0 mg/mL) and gallic acid (0.01, 0.02, 0.03, 0.04, 0.05, 0.06, 0.07 and 0.08 mg/mL)] were mixed with 400  $\mu\text{L}$  of  $\text{Na}_2\text{CO}_3$  (75.05 g/L) and 500  $\mu\text{L}$  of Folin-Ciocalteu reagent (FCR) (1:10 diluted with water). The mixtures were then placed at room temperature for 2 h to allow reaction to take place. Absorbance of samples at 750 nm was determined by UV-visible spectrophotometer (Thermo Scientific Spectronic Genesys 20). A standard curve was prepared by using different concentrations of freshly prepared gallic acid solutions. Total phenolic content of the herb was expressed as gallic acid equivalents (mg GAE/g).

## **2.4 *In vitro* study materials and methods**

### **2.4.1 Preparation FFA**

Treatment of cells with an FFA mixture (oleate/palmitate, 2:1) induced efficient intracellular lipid accumulation that mimics benign chronic steatosis as found in human according to previously established methods (Gómez-Lechón et al. 2007; J. W. Wang et al. 2014).

Palmitic acid (100 mM) was dissolved in water/ethanol (1:1 v/v) at 80°C for 5 mins and then diluted to 10 mM with 10% FFA-free bovine serum albumin (BSA) at 37°C for 1 h. A stock concentration of oleic acid (10 mM) was conjugated with FFA-free BSA. FFA mixture containing oleate/palmitate, 2:1 was prepared. Control cells were cultured with DMEM containing equal amount of FFA-free BSA and ethanol.

### **2.4.2 Cell culture and measurement of cell viability**

Human liver cell LO2 (Shanghai Institute of Biological Sciences, China) were cultured in Dulbecco's Modified Eagle Medium (DMEM, Thermo Fisher Scientific, Waltham, MA, USA) supplemented with 10% fetal bovine serum (Thermo Fisher Scientific), and

100 U/mL penicillin and streptomycin (Thermo Fisher Scientific). Cells were grown in a humidified 37°C incubator with 5% CO<sub>2</sub> in air. Cells were seeded in the 96-well, 6-well plates or confocal dish containing 70 - 80% confluent

Cell viability at different treatment condition was examined by MTT (3-(4, 5-Dimethylthiazol-2-yl)-2,5-Diphenyltetrazolium Bromide) assay. Briefly, after treatment with HZ or FFA, the medium was removed and replaced by MTT solution at a final concentration of 0.5 mg/mL. After incubation at 37°C for 2 h, the MTT solution was discarded and 100 µL DMSO was added into each well to dissolve the formazan crystals. Cell viability was measured by observing colorimetric changes using a Bio-Rad Microplate Reader (Model 680, Bio-Rad Laboratories, Hercules, CA, USA) at a test wavelength of 570 nm with a reference wavelength at 655 nm. Data were calculated using control group as 100 %.

### **2.4.3 Nile Red staining**

To measure cellular neutral lipid droplet accumulation, LO2 cells were stained by the Nile Red staining method. After treatment, cells were washed once with phosphate-

buffered saline (PBS) and fixed with 4% paraformaldehyde for 20 min at room temperature. After fixation, cells were washed and stained with Nile Red (Sigma-Aldrich) solution (3  $\mu$ M) for 15 min at room temperature. After staining, cells were washed with PBS to remove unbound dye. Fluorescence was measured using the CLARIOstar microplate reader (BMG Labtech) at 488 nm excitation and 520 nm emission. Images were acquired with a confocal laser scanning microscope (TCS SP8, Leica) with HyD detectors.

#### **2.4.4 Intracellular TG and TC measurements**

To induce cellular fat-overloading, LO2 cells at 70 - 80% confluence were cultured with or without 0.3 mM FFA (oleic acid: palmitic acid, 2:1) in the presence or absence of HZ at 0.5 mg/mL. After 24 h, the cells were washed twice with 1 mL cold PBS.

Intracellular levels of TC and TG were determined using a colorimetric enzymatic kit (Nanjing Jiancheng Bioengineering Institute, Nanjing, China), according to the manufacturer's instructions.

#### **2.4.5 Measurement of intracellular ROS**

The intracellular ROS production was determined by oxidant-sensing fluorescent probe 2',7'-dichlorodihydrofluorescein diacetate (DCFH-DA). DCFH-DA is deacetylated to non-fluorescent dichlorofluorescein (DCFH) by cellular esterases and further subsequently oxidized by intracellular ROS and other peroxide to the highly fluorescent 2',7'-dichlorodihydrofluorescein (DCF). LO2 cells were seeded in black 96-well plates ( $1 \times 10^4$  cells/well) for 24 h, and then stained with 10  $\mu$ M DCFH-DA at 37°C for 1 h. After changing the medium, the cells were pretreated with FFA for 24 h in no phenol red DMEM medium. The fluorescence of DCF was detected at 485 nm excitation and 535 nm emissions using the CLARIOstar microplate reader (BMG Labtech) at 488nm excitation and 520 nm emission. The results were expressed as fold changes compared to control.

#### **2.4.6 GFP-LC3 transfection**

Lentivirus expressing GFP-LC3 (human; Ad-GFP-LC3) was used as described previously. GFP-LC3 cDNA was cloned into pLenti-CMV-Puro-DEST (Addgene).

Then 1  $\mu\text{g}$  of GFP-LC3 was transferred along with psPAX2 (1  $\mu\text{g}$ ) and pMD2.G (1 $\mu\text{g}$ ) into HEK293T cells for lentivirus production. After that, LO2 cells were seeded in 6-well plates at a density of  $4 \times 10^5$  cells/well. 500  $\mu\text{l}$  of GFP-LC3 lentivirus were added to 1mL fresh medium containing 8  $\mu\text{g}/\text{mL}$  polybrene the next day. After two-day incubation, cells infected with GFP-LC3 lentivirus were selected with 1  $\mu\text{g}/\text{mL}$  puromycin for 3 - 5 days. The puromycin resistant cells were collected and stored for further analysis. LO2 cells were infected with lentivirus GFP-LC3 in DMEM overnight followed by treatment HZ. Puncta was detected by fluorescent microscope (Nikon Eclipse 80i, Nikon Instrument Inc., NY). At least 50 cells were counted in each individual experiment.

#### **2.4.7 RNA interference**

LO2 cells were transiently transfected with siRNA for Atg5. Briefly, cells were seeded into a 6-well plate, with 10% FBS and 1% PS. Thereafter, cells were transfected with ON-TARGET plus Non-targeting Pool (No. D-001810-10-05, Dharmacon, Waltham, MA, USA) or SMARTpool ON-TARGET plus Atg5 siRNA (No. L-004374-00-0005,

Dharmacon), using DharmaFect 4 Transfection Reagent (No. T-2004-01) according to the manufacturer's instruction. After transfection for 48 h, cells were incubated by HZ for 24 h at 37°C in a 5% CO<sub>2</sub> atmosphere.

## **2.5 *In vivo* study materials and methods**

### **2.5.1 Animals and experimental treatment**

Sixty male Sprague-Dawley (SD) rats (weighing  $170 \pm 10$  g) were purchased from Guangdong Medical Laboratory Animal Center (Guangzhou, China). All animals were housed under standard conditions at a room temperature of  $20 \pm 1^\circ\text{C}$  with  $60\% \pm 10\%$  humidity and an alternating 12 h light-dark cycle for 1 week prior to the experiments. The rats were randomly assigned to six groups of 10 rats each. Control group of rats were fed with normal rat chow (Guangdong Provincial Medical Laboratory Animal Center, Guangzhou, China; protein: 14%, fat: 10% and carbohydrate: 76%); Five groups [high-fat diet, HFD; high-fat diet along with SIM-L (simvastatin, 3 mg/kg bw per day, p.o.), HFD + SIM-L; high-fat diet along with SIM-H (simvastatin, 10 mg/kg bw per day, p.o.), HFD + SIM-H; high-fat diet along with HL (150 mg/kg bw per day,

p.o., 10 mg/kg bw per day, p.o.), HFD + HL; high-fat diet along with HH (450 mg/kg bw per day, p.o., 10 mg/kg bw per day, p.o., HFD + HH) were fed with a high fat diet, which is a standard chow supplemented with 1% cholic acid, 2% pure cholesterol and 5.5% oil. All treatments were administered once daily by oral gavage for 4 weeks. After an overnight fast, the rats were killed by cervical dislocation at the end of the experimental period. Blood and tissue samples (livers and aortas) were collected for further analysis.

The experimental protocol was approved by the Health Department of the Hong Kong SAR Government and the Animal Subjects Ethics Sub-committee (ASESC No. 05/21) of The Hong Kong Polytechnic University. The care and treatment of the animals were performed in accordance with the Guide for the Care and Use of Laboratory Animals published by the US National Institutes of Health and the principles outlined in the Declaration of Helsinki.

In animal experiments, concentrations of HZ (150 and 450 mg/kg.bw) were selected that were based on several reasons. Firstly, they were based on the dosage (10 - 30 g)

in clinically prescribed to patients. The coefficient of proportionality for a dosage of 70 kg for humans and 0.2 kg for rats is 0.018. When the dosage for patients of raw herb of HZ (0.14 - 0.42 g/kg bw) is converted to rats, the dosage for rats is 0.9 - 2.7 g/kg bw. Because the yield of water extract of HZ is 7.5%, the final dosage of HZ water extract for rats is 67.5 - 202.5 mg/kg bw. The concentrations of our experiment selected (150 and 450 mg/kg bw) are closed to this interval (67 - 202 mg/kg bw) from clinical requirement. Secondly, it was based on the bioavailability of the major component (polydatin) identified from HZ. The effective concentration of HZ ranges from 0.1 to 0.5 mg/ml. The absolute bioavailability of polydatin was around 2.9%. The content of polydatin of HZ water extract is 7.9%. The yield of HZ water extract is 7.5%. Calculated as the result of effective cellular concentrations of HZ water extract and the bioavailability of polydatin, the dosage of HZ water extract ranges from 115 to 575 mg/kg bw. The concentrations of our experiment selected (150 and 450 mg/kg bw) are closed to this interval (115 - 575 mg/kg bw) from bioavailability data. Thirdly, based on the dosage used in two published paper. Jiang. et al ((Jiang et al. 2009) used 11 g raw herb of HZ and Song.et al. (Yiyong 2016) used 5 g raw herb of HZ. In our

experiment, the concentration selected (150 and 450 mg/kg bw), converted to the raw dosages of HZ are 2 and 6 g, are similar with previous studies.

### **2.5.2 Measurement of serum biochemical markers**

Then, blood samples were collected via cardiac puncture, stored at room temperature for 1 h, and then centrifuged at 1500 rpm for 10 minutes to obtain the serum samples, which were stored at -80°C until they were analyzed. Serum TC, TG, low density lipoprotein cholesterol (LDL-c) and high density lipoprotein cholesterol (HDL-c) were measured with the ALYCON<sup>®</sup> systems using Roche Reagents.

### **2.5.3 Liver histopathological examination**

Hepatic tissues from all animals were fixed in 4% paraformaldehyde and embedded in paraffin wax. Paraffin sections (5 µm) were stained with hematoxylin and eosin (H&E) and observed with a light microscope (Olympus BX43, Olympus, Tokyo, Japan) and photomicrographs (400 ×) were taken.

#### **2.5.4 Hepatic lipid content evaluation**

The sample of liver (~ 2 g) was dissected and homogenized with 2:1 chloroform-methanol mixture (v/v) to a final dilution of 1:20 w/v using Ultra-turrax T-25 homogenizer. After filtration, 10 mL of individual filtrate was added to 2 mL water and the mixture was centrifuged at 900 g for 20 min. The lower phase was dried and its weight was measured. Liver lipid content was expressed as weight of lipid per g of liver. Hepatic levels of TC and TG were measured using a colorimetric enzymatic kit (Nanjing Jiancheng Bioengineering Institute, Nanjing, China).

#### **2.5.5 Measurement of antioxidative enzyme activities and MDA content**

Isolated liver (~ 1 g) of each rat was homogenized and the homogenates were centrifuged (14,000 rpm, 5 min, 4°C). Then the supernatants were collected and stored at -20°C until enzyme activities analysis. SOD, CAT and MDA were measured using commercial kits (Nanjing Jiancheng Bioengineering Institute, Nanjing, China).

### **2.5.6 Isolation of thoracic aorta**

At the end of the treatment period, rats were sacrificed and their thoracic aortas were immediately removed and placed in 4°C Tyrode's solution composed of: (mM) NaCl, 118; KCl, 4.7 ; KH<sub>2</sub>PO<sub>4</sub>, 1.2; NaHCO<sub>3</sub>, 25; glucose, 11; CaCl<sub>2</sub>, 2.5; and MgSO<sub>4</sub>, 1.2. Adipose and connective tissues were removed, and several ring segments (~ 3 mm ring for endothelium-dependent vasorelaxation and ~ 15 mm ring for nitrite production) were dissected from the isolated aorta with care so as to not separate the endothelium from the luminal surface.

### **2.5.7 Measurement of endothelium-dependent vasorelaxation**

Ring segments were mounted in a 5 mL organ bath filled with Tyrode's solution , maintained at 37°C and aerated continuously with 95% O<sub>2</sub> and 5% CO<sub>2</sub> mixture. After equilibration for 60 min under 1.0 g resting tension, the aortic rings were challenged with 60 mM KCl twice to sensitize the preparations. And then the contraction of aortic rings response to 1 μM phenylephrine in the presence of indomethacin (1 μM, a nonselective cyclo-oxygenase inhibitor) and neostigmine (1 μM, an anticholinesterase)

was induced following 30 min of equilibration. Subsequently, the endothelium - dependent relaxation responses to cumulative concentrations (10 nM - 10  $\mu$ M) of acetylcholine were detected after the steady-state of phenylephrine-induced contraction. The relaxation in response to acetylcholine was expressed as a percentage of the phenylephrine induced-contraction. Isometric tension (in g) was monitored by isometric force-displacement transducers and a PowerLab data acquisition system.

#### **2.5.8 Quantification of NO production**

As we decription previously, NO production was detected by calculating the amount of content of nitrite ( $\text{NO}_2^-$ ) according to the Griess methods (Wu et al. 2010). Briefly, isolated aortas segments (~ 15 mm) were weighed and then incubated in a 24-well plate containing 2 mL Tyrode's solution per well with acetylcholine (1  $\mu$ M) and neostigmine (1  $\mu$ M). After incubation at 37°C for 2 h, each segment was blotted dry and weighed. The incubated culture solution of each well was collected and dried by vacuum freeze-drying. The resulting pellets were re-dissolved with distilled water (300  $\mu$ L) and Griess reagents were mixed and incubated at room temperature for 10 min. The absorbance

was measured using a spectrophotometer at 540 nm. The nitrite concentrations were determined at 540 nm using the standard solutions of sodium nitrite. The amount of nitrite formed was normalized to the weight of the respective aortic rings.

### **2.5.9 Western blotting assay**

Liver homogenates was subjected to western blotting analysis, as previously was described. The resultant proteins collected by centrifugation were separated on a 7.5 %, 10% or 15% SDS-PAGE gel and then transferred to polyvinylidene fluoride membranes. Membranes were incubated the following primary antibodies: rabbit anti-LDLR and rabbit anti-3-hydroxy-3-methylglutaryl-CoA reductase (HMG-CoA reductase, HMGCR) (Abcam), rabbit anti-SQSTM1/p62, rabbit anti-SREBP-1c, rabbit anti-SREBP-2, rabbit anti-phospho-AMPK $\alpha$  (Thr<sup>172</sup>), rabbit anti-PPAR $\alpha$ , rabbit anti-phospho-Acetyl-CoA Carboxylase (Ser<sup>79</sup>), rabbit anti-phospho-p44/42 MAPK (ERK1/2) (Thr<sup>202</sup>/Tyr<sup>204</sup>), rabbit anti-phospho-SAPK/JNK (Thr<sup>183</sup>/Tyr<sup>185</sup>), rabbit anti-phospho-p38 MAPK (Thr<sup>180</sup>/Tyr<sup>182</sup>) and rabbit anti- $\beta$ -actin (Cell Signaling Technology), rabbit anti-SREBP-2 and rabbit anti-CYP7A1 (Santa Cruz Biotechnology)

and rabbit anti-LC3B (Novus biologicals). Then signals were obtained by binding a secondary antibody. Protein bands were visualized using a Bio-Rad Clarity™ western ECL substrate on Azure™ Biosystems C600. The band intensities of proteins were normalized to  $\beta$ -actin and quantified with ImageJ software.

## **2.6 Metabolomics analysis**

### **2.6.1 Chemical and Reagent**

Formic acid, succinic acid-D4 and cis-10-nonadecenoic acid (C19:1n9c) was purchased from Sigma-Aldrich (St. Louis, MO, USA) while D-glucose (U-<sup>13</sup>C<sub>6</sub>), L-tryptophan (indole-D<sub>5</sub>) was purchased from Cambridge Isotope Laboratories (MA, USA). HPLC-graded acetonitrile and methanol were obtained from Fisher Scientific (Hampton, NH, USA). Water was purified in-house using a Milli-Q Advantage A10 water purification system (Millipore, Bedford, MA, USA).

### **2.6.2 Quality control sample preparation method**

An aliquot of 20  $\mu\text{L}$  of each serum sample was pooled, vortexed and aliquoted to provide quality control (QC) samples, and kept at  $-80^{\circ}\text{C}$  until use. For each analytical batch, QC samples went through extraction protocols as described below similar to all other samples. Before the start of the chemical analysis, five repeated injections of the same QC sample were used to verify the working condition of the instruments. Afterwards, a QC sample was injected to monitor the stability of the instruments after every five-sample runs.

### **2.6.3 Serum sample extraction**

Serum samples of normal, HFD model and HZ-treatment groups were thawed at  $4^{\circ}\text{C}$  before preparation. Each 100  $\mu\text{L}$  serum sample was mixed with 300  $\mu\text{L}$  methanol, which contained five in-house internal standards (100 ppm C19:1n9c and 40 ppm tryptophan-D5, succinic acid-D4 and glucose-C13) and vortexed for 30 s to precipitate the protein. Then, the mixture was stood at  $-20^{\circ}\text{C}$  overnight, and centrifuged at 14,000 rpm under  $4^{\circ}\text{C}$  for 20 min. Then, 340  $\mu\text{L}$  supernatant of each serum sample was

transferred into a new micro-centrifuge tube and evaporated to dryness under a gentle stream of nitrogen gas. The dried residue was finally reconstituted in 100  $\mu$ L of water-acetonitrile (95:5, v/v) and vortexed for further 30s. After centrifuged at 14,000 rpm under 4°C for 20 min, an aliquot of 5  $\mu$ L supernatant was ready for UPLC-QTOF-MS analysis.

#### **2.6.4 UPLC-QTOF-MS condition**

A 3  $\mu$ L aliquot was injected into a Waters ACQUITY UPLC system. The separation was performed on a Waters ACQUITY UPLC HSS T3 column (2.1 mm  $\times$  100 mm, 1.8  $\mu$ m) with HSS T3 pre-column (2.1 mm  $\times$  5 mm, 1.8  $\mu$ m, Waters Corporation, Milford, MA). The mobile phase consisted of combinations of A (0.1% formic acid in water, v/v) and B (0.1% formic acid in acetonitrile, v/v) at a flow rate of 0.3 mL/min with elution gradient as follows: 0 - 1 min, 5% B; 5 min, 35% B; 10 min, 50% B; 18 min, 65% B; 19-23 min, 95% B. A 3-min post-run time was set to fully equilibrate the column between injections. Column and sample chamber temperature were set at 40°C and 6°C, respectively.

Mass spectrometry (MS) was performed on a Waters SYNAPT G2 Q-IM-TOF HDMS system (Waters, Milford, USA) operating in an electrospray ion source (ESI) in both positive and negative modes. Nitrogen and argon were used as cone and collision gases. The desolvation gas flow was set to 600 L/h at a desolvation temperature of 400°C, and the cone gas was set to 40 L/h. The source temperature was set at 120°C. The capillary voltages in positive and negative ion modes were 3 kV and 2.2 kV, respectively. The sampling and extraction cone voltages were 40 V and 4 V, respectively. The scan time was 0.5 s with a 0.024 s interscan delay. Data scan range from m/z 50 to 1000 were recorded in the centroid data format. For accurate mass acquisition, a lock-mass of leucine enkephalin was used to monitor for positive ion mode ( $[M+H]^+$ : m/z 556.2771) and negative ion mode ( $[M-H]^-$ : m/z 554.2615) to ensure accuracy during the MS analysis. MS/MS analysis was carried out to study the structure of potential biomarkers. In this section, the collision energy was set between 5 to 50 eV according to the situation.

### **2.6.5 Data processing and analysis**

Peak picking and alignment of all raw UPLC-MS data were conducted by Progenesis

QI software (Nonlinear Dynamics, United Kingdom) in both ionization modes in two separate analyses. Data were imported in the following setting prior to peak picking: resolution (full width at half maximum), 15000; adduct, [M-H]<sup>-</sup>; retention time limit, 0.3 - 23 min; data type, centroided while other settings were set default. All ion abundance was normalized by internal standards of its own sample to generate a data matrix that consisted of the retention time, m/z value, and the normalized ion abundance.

Quality screening was done by filtering out those metabolites which coefficient of variations (CV) was greater than 30% in quality control samples to reduce the contribution of unstable peaks and eliminate noise from the dataset (Dunn et al. 2011).

The resultant data matrices were introduced to Extended Statistical tool EZinfo v2.0 software (Umetrics AB, Sweden) for multivariate statistics. The data were scaled to unit variance for principal component analysis (PCA), to give an overview of the repeatability of QC samples. The QC samples with high repeatability should cluster together in the score plot of PCA. The samples excluding QC samples were pareto-scaled for partial least squares-discriminant analysis (PLS-DA) and orthogonal partial least squares-discriminant analysis (OPLS-DA). Potential markers of interest were

extracted from the variable importance in the projection (VIP) values (threshold of VIP  $\geq 1$ ) and the location in S-loading plot of OPLS-DA based on their contribution to the variation and correlation in the data set. The markers were identified by LC-MS/MS and matched with the METLIN (<http://metlin.scripps.edu>), the MassBank ([www.massbank.jp](http://www.massbank.jp)) and the Human Metabolome Databases ([www.hmdb.ca](http://www.hmdb.ca)) and/or confirmed by literatures and authentic standards based on retention times, mass fragmentation pattern and accurate masses (mass error  $\leq 5$  ppm).

Statistical analyses were performed using SPSS PASW Statistics 18 (Chicago, IL, USA). After logarithmic transformation [ $\log_2$  (normalized ion abundance)] followed by filtering out outliers (1.5 times of the interquartile range) and, statistical differences were analysed at a univariate level by one-way analysis of variance (ANOVA); least significant difference or Tamhane's T2 post-hoc test was used based on homogeneity of variances with a  $p$  value less than 0.05 as statistically significant.

## **2.7 Data analysis and statistics**

All data were expressed as means  $\pm$  SEM of three independent experiments. Statistic

analysis was carried out using Student's t test or one-way ANOVA followed by post-hoc Bonferroni test (GraphPad Prism version 6.01 for Windows, SanDiego, CA, USA).

Values of  $p < 0.05$  or less were considered to be statistically significant.

## **Chapter 3 Results**

### **3.1 Quantitative determination of major components in HZ sample**

A representative HPLC chromatogram of HZ sample and standard mixture were shown in Fig. 3.1.1. Totally, five peaks were identified from the sample with authentic standards. Their contents relative to dried crude drug weight were polydatin (10.64 mg/g  $\pm$  0.23 mg/g), emodin 8-O- $\beta$ -D-glucopyranoside (4.77 mg/g  $\pm$  0.04 mg/g), resveratrol (0.67 mg/g  $\pm$  0.01 mg/g), emodin (0.57 mg/g  $\pm$  0.01 mg/g) and physcion 8-O- $\beta$ -D-glucopyranoside (0.53 mg/g  $\pm$  0.05 mg/g).

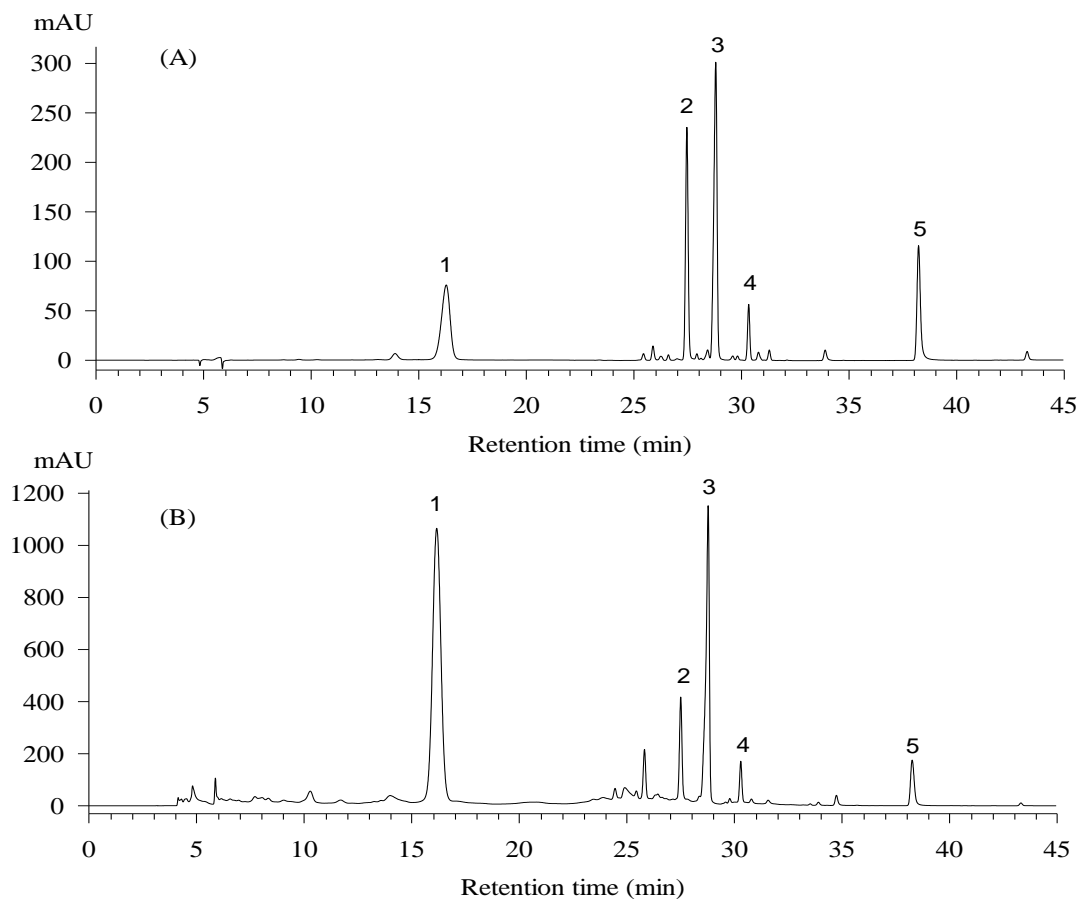


**Fig. 3.1.1 HPLC chromatograms of (A) five standard mixture and (B) HZ extract (10 mg/mL)**

Peak 1: polydatin; 2: resveratrol; 3: emodin 8-O- $\beta$ -D-glucopyranoside; 4: physcion 8-O- $\beta$ -D-glucopyranoside; and 5: emodin.

### 3.2 Determination of antioxidant properties

For DPPH assay, as is shown in Fig. 3.2.1, HZ exerted a concentration-dependent scavenging activity against DPPH free radicals with  $SC_{50}$  of 0.051 mg/mL compared with that of ascorbic acid (vitamin C, a positive control), which is 0.003 mg/mL. In addition, the total phenolic content of HZ water extract was found to  $26.83 \pm 5.03$  mg GAE/g dry extract.

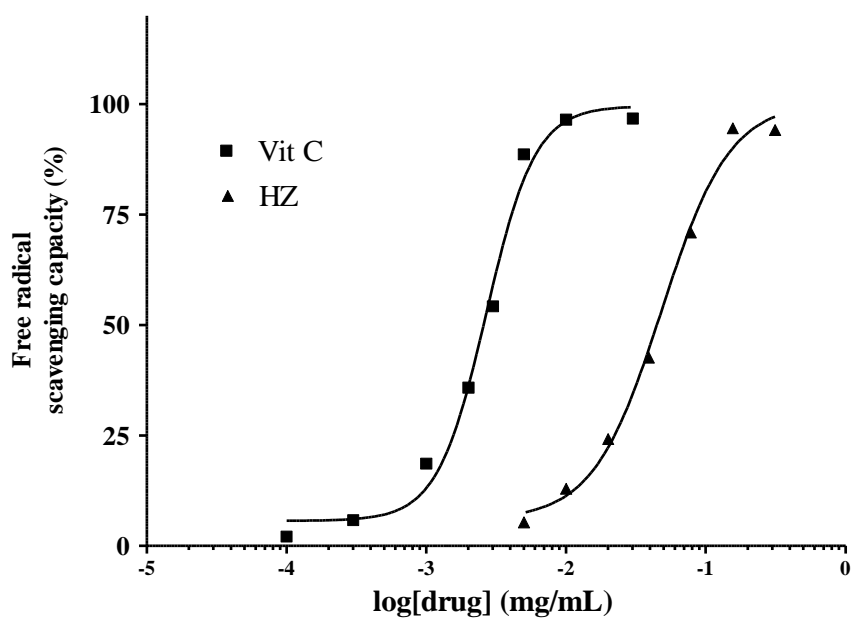


**Fig. 3.2.1 Comparison of free radical scavenging capacity of HZ and vitamin C from DPPH assay**

### **3.3 HZ reduced lipid accumulation in steatotic LO2 cells**

To determine the optimal concentration of FFA to induce steatosis, LO2 cells were cultured with FFA (oleate: palmitate, 2:1) at a concentration of 0.05, 0.1, 0.2 or 0.3 mM for 24 h. Nile red staining of LO2 cells confirmed the formation of intracellular lipid droplets in FFA-treated cells (Fig. 3.3.1 A). We observed a large quantity of green lipid droplets in LO2 cells in the model group (Fig. 3.3.1 B). For maximal intracellular lipid accumulation with minimal cytotoxicity, cells were treated with 0.3 mM FFA for 24 h in subsequent experiments. There was no significant increase in intracellular oxidative stress, following FFA treatment (Fig. 3.3.1 E). To evaluate the apoptotic effect of FFA treatment on LO2 cells, the cells were incubated with 0.3 mM FFA mixture for 24 h. Apoptosis related proteins (bcl-2 and bax) were measured by western blot assay. As shown in Fig. 3.3.1 C&D), FFA treatment had no apparent effect on apoptosis in LO2 cells.

So a steatotic hepatocyte model was that LO2 cells would be incubated with FFA mixture at the concentration of 0.3 mM for 24 h. As shown in Fig. 3.3.2 A&B HZ

treatment (0.1 - 0.5 mg/mL) reduced lipid accumulation in steatotic LO2 cells. As shown in Fig. 3.3.2 C&D, the intracellular TG level was significantly higher in the model group than in the normal group, HZ (0.1 - 0.5 mg/mL) significantly reduced TG level. However, no differences of cholesterol between normal group and model group. The amount of cholesterol in LO2 cells in the presence of HZ was reduced by 15% in comparison with the control after 24 h incubation.

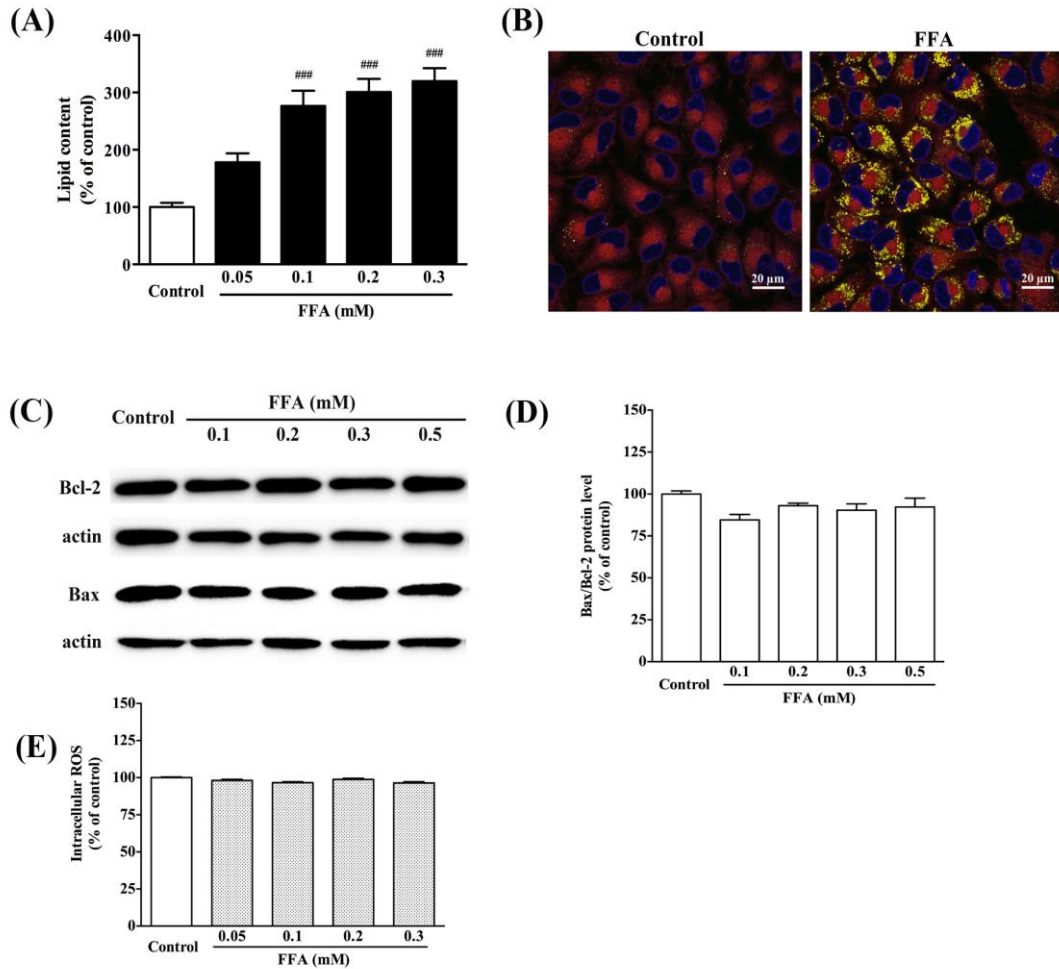


**Fig. 3.3.1 FFA induced hepatic steatosis in FFA-induced LO2 cells**

(A) Cells were treated with FFA at 0.05, 0.1, 0.2, 0.3 mM for 24 h. Lipid accumulation was analyzed by Nile red staining. The yellow color indicated the neutrolipid. The blue color indicated nucleus and red color indicated polar membrane lipid. (B) Cells treated with 0.3 mM FFA were stained with Nile red and viewed under a microscope at 400 × magnification. (C) Apoptosis protein (bcl-2 and bax). (D) Protein levels are expressed relative to actin. (E) Intreacullar ROS level detected by DCFH-DA staining. ###  $p < 0.001$  versus the control group.

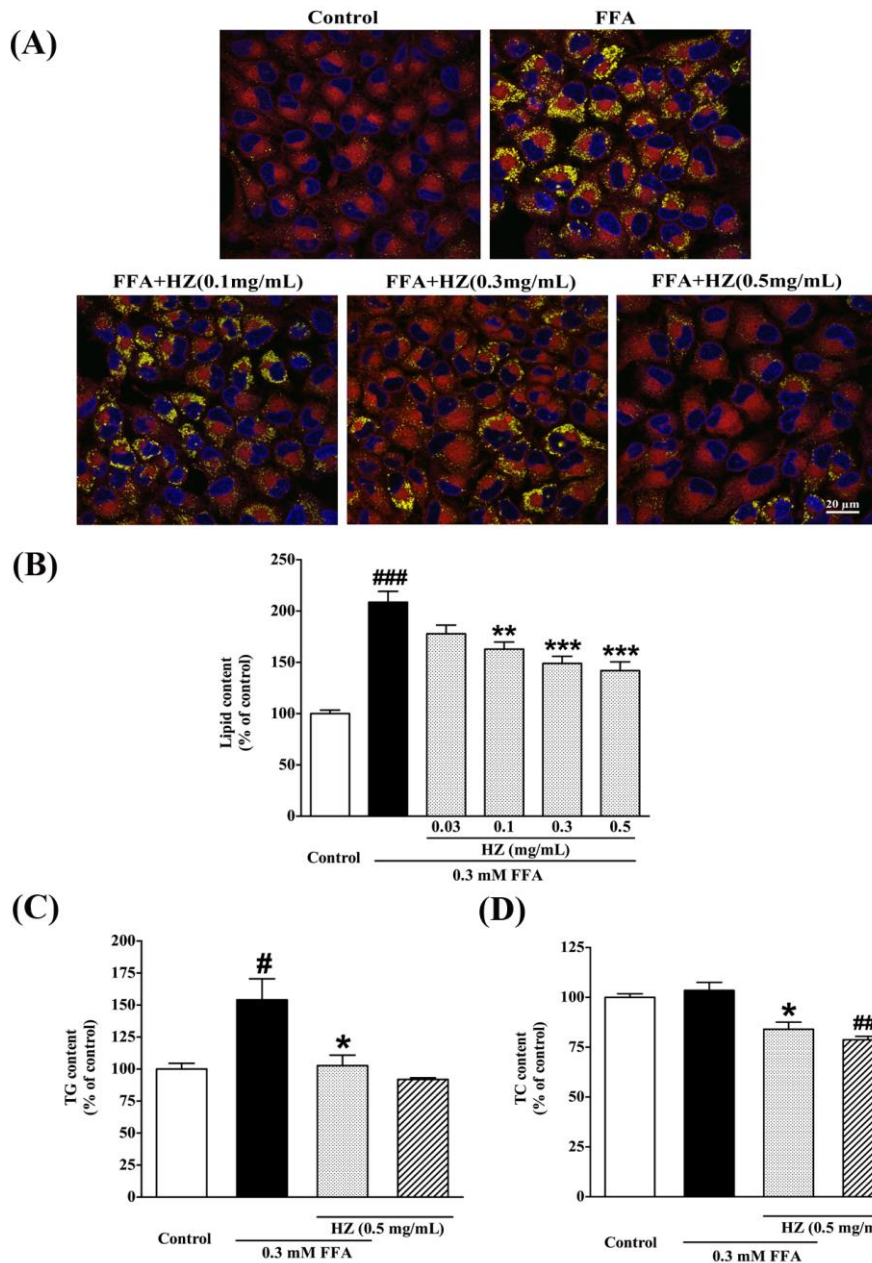


**Fig. 3.3.2 HZ reduced lipid accumulation in FFA-induced steatotic LO2 cells**

(A) Cells were treated with FFA (0.3 mM) and 0.1, 0.3 or 0.5 mg/mL for 24 h. Lipid accumulation in LO2 cells was visualized under a microscope at 400 × magnification. The yellow color indicated the neutral lipid. The blue color indicated nucleus and red color indicated polar membrane lipid. (B) Lipid content detected using Nile red staining. (C) Intracellular TG content measured with a TG-detection kit in LO2 cells. (D) Intracellular TC content measured with a TC-detection kit in LO2 cells. Data are expressed as means ± SEM. <sup>#</sup> $p < 0.05$ , <sup>###</sup> $p < 0.001$  versus the control group. <sup>\*</sup> $p < 0.05$ , <sup>\*\*</sup> $p < 0.01$  and <sup>\*\*\*</sup> $p < 0.001$  versus the FFA group.

### **3.4 HZ inhibited lipid accumulation partially via autophagy induction *in vitro***

In this study, we observed the effect of HZ on autophagy and the related pathways in hepatic lipid metabolism in FFA-induced steatotic LO2 cells.

Similar results were obtained that protein expressions of the p-AMPK, p-ACC, LDLR and PPAR $\alpha$  were increased by HZ treatment both *in vitro* (Fig. 3.4.1). However, HZ had no significant ( $p > 0.05$ ) effects on the altering of protein expressions of SREBP-2, SREBP-1c and HMGCR as compared with the FFA-treated cells (Fig. 3.4.1).

To elucidate the hypothesis stating that HZ could attenuate FFA-induced steatosis via lipophagy induction, three independent approaches for measuring autophagy were developed. First, LC3B-II conversion of LO2 cells treated with HZ for 24 h was increased in a dose-dependent manner, monitored by western blotting. As shown in Fig. 3.4.2 A & B, the LC3B-II protein expression levels in the HZ group were significantly higher than those of control group ( $p < 0.001$ ). These results were confirmed using LO2 cells stably transfected with an autophagic marker green fluorescent protein-LC3 (GFP-

LC3) plasmid and visualized by fluorescence microscopy. As presented in Fig. 3.4.2 C & D, untreated LO2 cells showed a diffuse distribution of green fluorescence within the cytoplasm and a few dots (2 dots/cell), consistent with the cytoplasmic delipidated form of the protein. On the other hand, a punctate pattern of GFP-LC3 accumulated upon the challenge with HZ, an excessive number of dots (9 dots/cell) appeared in HZ-treated cells compared with the control group ( $1.90 \pm 0.31$  vs.  $9.63 \pm 0.51$ ,  $p < 0.001$ ).

Second, we investigated its autophagic role in the presence or absence of (1) rapamycin for autophagy activation and (2) siRNA against Atg5 for the inhibition of autophagosome formation and autophagy activation. Pharmacological activation of autophagy with rapamycin significantly decreased lipid content in the presence of exogenous lipid supplementation with FFA (Fig. 3.4.2 E). Similar to previous results, in Fig. 3.3.2, 0.3 mM FFA significantly increased lipid accumulation; however, HZ partially attenuated FFA-induced lipid accumulation. In the treatment of Atg5 knockdown, siRNA against Atg5 significantly increased the inhibition of HZ against FFA-induced lipid accumulation ( $179.4 \pm 11.09$  vs.  $124.7 \pm 3.11$ ,  $p < 0.001$ ) in Fig. 3.4.2 F. Consistent with the increased lipid levels, lipid staining with Nile red revealed

increased lipid content in cells that were further increased by Atg5 knockdown and a significant difference in lipid content was found between cells treated with FFA + HZ and those with FFA + HZ + siAtg5 (Fig. 3.4.2 G).

Third, PPAR $\alpha$ , LDLR and ACC are key proteins responsible for lipid metabolism, we checked if they are involved in the HZ-induced autophagy. We investigated its effects under Atg5 knockdown conditions. We transfected LO2 cells with siRNA molecules against Atg5 and then incubated them in the presence or absence of HZ. As shown in Fig. 3.4.3 A&C, siRNA against Atg5 significantly decreased the expression of Atg5, LC3-II, p-ACC, PPAR $\alpha$  and LDLR, significantly in Atg5 ( $55.63 \pm 6.52$  vs.  $100.0 \pm 2.38$ ,  $p < 0.01$ ), LC3B-II ( $51.48 \pm 2.55$  vs.  $100.0 \pm 2.38$ ,  $p < 0.001$ ), p-ACC ( $59.16 \pm 10.30$  vs.  $100.0 \pm 2.38$ ,  $p < 0.01$ ), PPAR $\alpha$  ( $68.41 \pm 4.34$  vs.  $100.0 \pm 2.38$ ,  $p < 0.05$  and LDLR ( $66.32 \pm 6.39$  vs.  $100.0 \pm 2.38$ ,  $p < 0.01$ ). The results suggested that PPAR $\alpha$ , LDLR and p-ACC are regulated by autophagy.

As shown in Fig. 3.4.3 B&D, in the treatment of siAtg5, statistical differences were found between cells treated with HZ and those with HZ + siAtg5, significantly in Atg5

( $94.48 \pm 3.50$  vs.  $13.27 \pm 4.81$ ,  $p < 0.001$ ), LC3B-II ( $141.1 \pm 7.25$  vs.  $98.91 \pm 12.30$ ,  $p < 0.05$ ), p-ACC ( $120.4 \pm 5.75$  vs.  $79.51 \pm 1.90$ ,  $p < 0.001$ ), PPAR $\alpha$  ( $119.3 \pm 2.04$  vs.  $65.58 \pm 4.10$ ,  $p < 0.001$ ) and LDLR ( $144.9 \pm 7.56$  vs.  $100.2 \pm 3.31$ ,  $p < 0.001$ ). Moreover, in the treatment of siAtg5, statistical differences were found between cells treated with HZ + siAtg5 and those with siAtg5, significantly in Atg5 ( $13.27 \pm 4.81$  vs.  $13.75 \pm 2.72$ ,  $p > 0.05$ ), LC3B-II ( $98.91 \pm 12.30$  vs.  $51.09 \pm 1.42$ ,  $p < 0.05$ ), p-ACC ( $79.51 \pm 1.90$  vs.  $56.27 \pm 2.74$ ,  $p < 0.01$ ), PPAR $\alpha$  ( $65.58 \pm 4.10$  vs.  $75.67 \pm 3.94$ ,  $p > 0.05$ ) and LDLR ( $100.2 \pm 3.31$  vs.  $70.04 \pm 1.39$ ,  $p < 0.001$ ). These results showed that although autophagy was blocked, HZ was still able to upregulate LDLR and p-ACC expressions compared with siAtg5 group, suggesting that HZ reduced lipid accumulation partially by regulating autophagy induction. However, treatment of HZ was not able to upregulate PPAR $\alpha$  expression in the absent of autophagy, suggesting that HZ upregulated PPAR $\alpha$  expression by regulating autophagy induction.

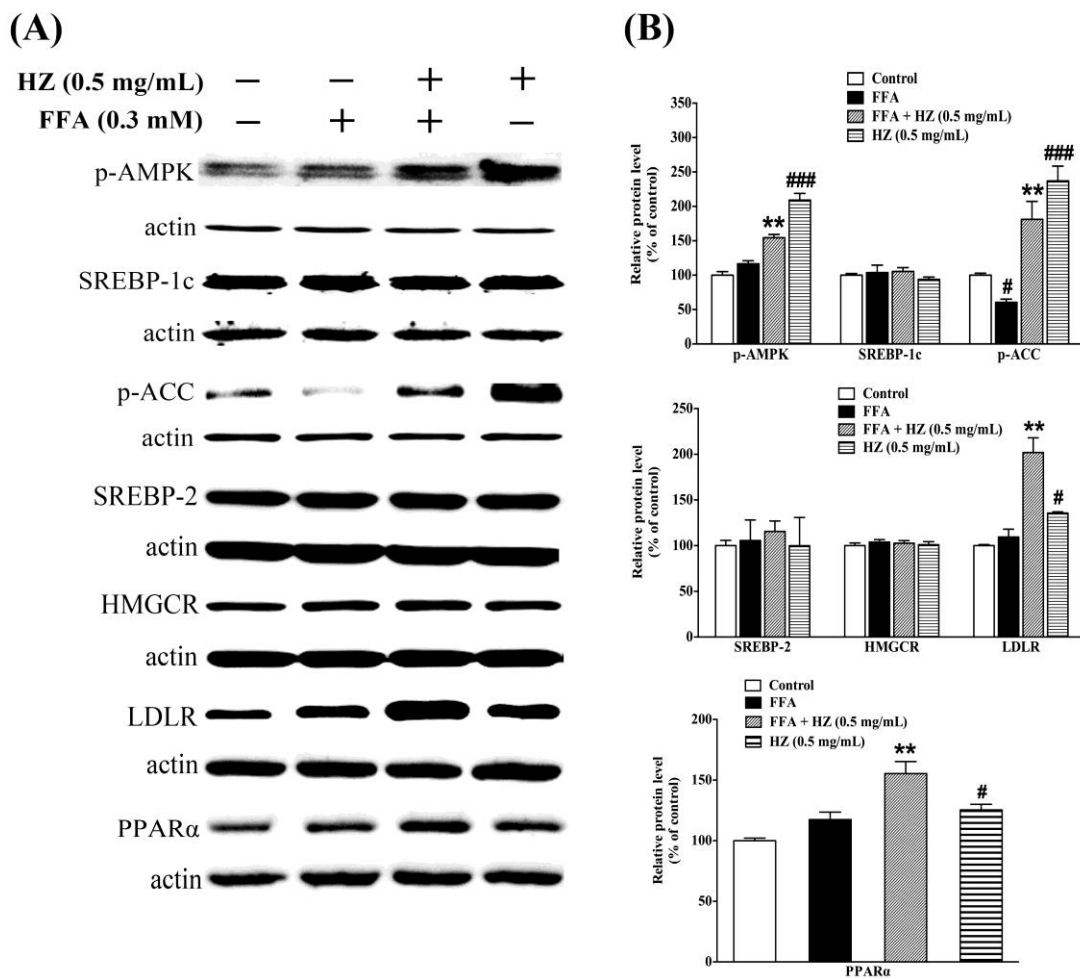


**Fig. 3.4.1** Effects of HZ on expressions of lipid metabolism-related proteins in *in vitro* model

(A) Protein expression of lipid metabolism-related proteins (p-AMPK, SREBP-1c, p-ACC, HMGCR, SREBP-2, LDLR, PPAR $\alpha$ ) in LO2 cells were changed by HZ and FFA.

(B) The protein levels were expressed relative to actin. Data are expressed as means  $\pm$  SEM. #  $p < 0.05$ , ###  $p < 0.001$  versus the control group. \*\*  $p < 0.01$  versus the FFA group.

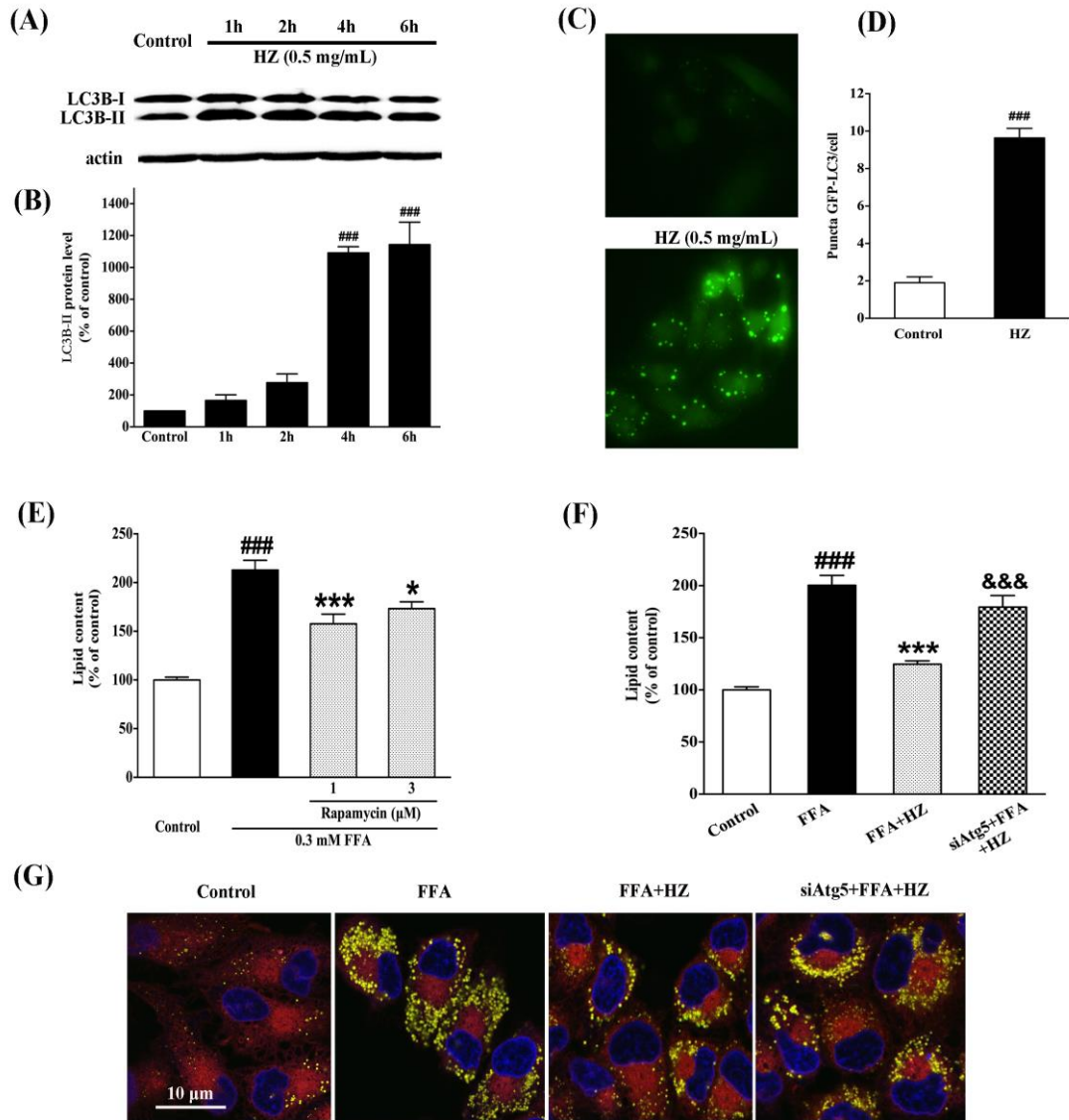


**Fig. 3.4.2 HZ-induced autophagy regulates hepatic lipid accumulation in steatotic LO2 cells**

(A) LC3B protein expression level in the groups given various treatments. Actin was used as a loading control. Cells treated with HZ (0.5 mg/mL) for different time point. (B) Protein levels of LC3B-II. (C) Representative GFP-LC3 images. (D) Number of GFP-LC3 dots per cell. LO2 cells were first infected with Ad-GFP-LC3 overnight and then treated with vehicle control or HZ (0.5 mg/mL) for 24 h followed by fluorescence microscopy. (E) Lipid content detected using Nile red staining. Cells treated with 1, 3  $\mu$ M rapamycin (autophagic enhancer). (F) LO2 cells were transfected with negative control siRNA or Atg5-specific siRNA (Atg5 siRNA) and experiments were performed 48 h after transfection. After application of control siRNA or Atg5 siRNA for 48 h, LO2 cells were exposed to HZ (0.5 mg/mL) for another 24 h, and subsequently lipid content was detected by Nile red staining and (G) visualized by confocal microscopy.  $###p < 0.001$  versus the control group.  $*p < 0.05$ ,  $***p < 0.001$  versus the FFA group.  $$$$p < 0.001$  versus the FFA + HZ group.

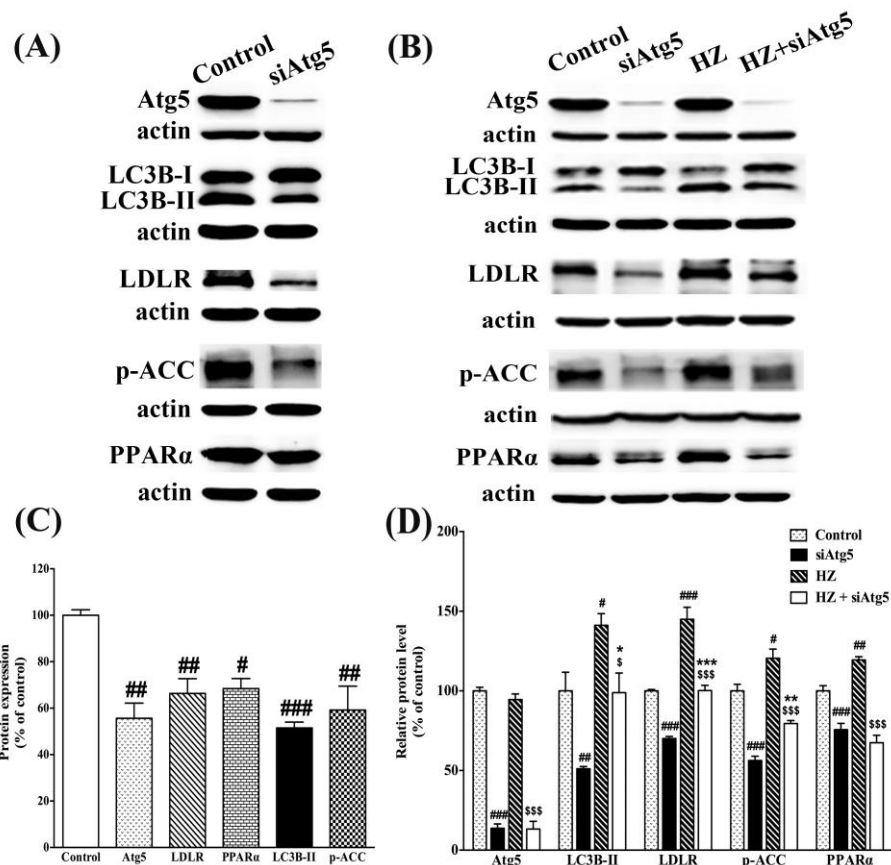


**Fig. 3.4.3 Effects of Atg5 siRNA on lipid metabolism-related proteins of HZ in LO2 cells**

(A) Testing of Atg5 knock-down efficiency. Cell lysates were probed by Western blotting for Atg5, LC3B, LDLR, PPAR $\alpha$  and p-ACC expression and actin as a control. (B) After application of Control siRNA or Atg5 siRNA for 48 h, LO2 cells were exposed to HZ (0.5 mg/mL) for another 24 h, and subsequently cell lysates were probed by Western blotting for Atg5, LC3B, LDLR, PPAR $\alpha$  expression and actin as a control. (C) Protein levels of Atg5, LC3B-II, LDLR, PPAR $\alpha$  after Atg5 siRNA. (D) Protein levels of Atg5, LC3B-II, LDLR, PPAR $\alpha$  after Atg5 siRNA in the absence or presence of HZ. Data are expressed as means  $\pm$  SEM. # $p$  < 0.05, ## $p$  < 0.01, ### $p$  < 0.001 versus the control group. \* $p$  < 0.05, \*\* $p$  < 0.01, \*\*\* $p$  < 0.001 versus the FFA group. \$ $p$  < 0.05, \$\$\$ $p$  < 0.001 versus the HZ group.

## **3.5 HZ ameliorated hepatic steatosis in HFD-induced steatosis Rats**

### **3.5.1 HZ supplementation alleviated HFD-induced fatty liver**

The hepatic pathological alterations from the six groups were evaluated by measuring hepatic TG and TC contents and circulating liver enzyme levels. In this study, HFD cannot induce liver injury which was manifested as increased plasma AST and ALT levels. But HFD induced fatty liver in the rats, which was manifested as increased hepatic TG, TC and lipid content. In response to HZ supplementation, both hepatic TG and TC accumulation, lipid content were significantly reduced in the HFD-fed group ( $p < 0.05$ ) (Fig. 3.5.1 C&D, Table 3.5.1). Furthermore, histological examination of H&E stained liver sections revealed that the rats fed with 4 week HFD demonstrated severe hepatic microvesicular and macrovesicular fat, whereas HZ supplementation significantly reduced hepatic steatosis (Fig. 3.5.1 A&B).

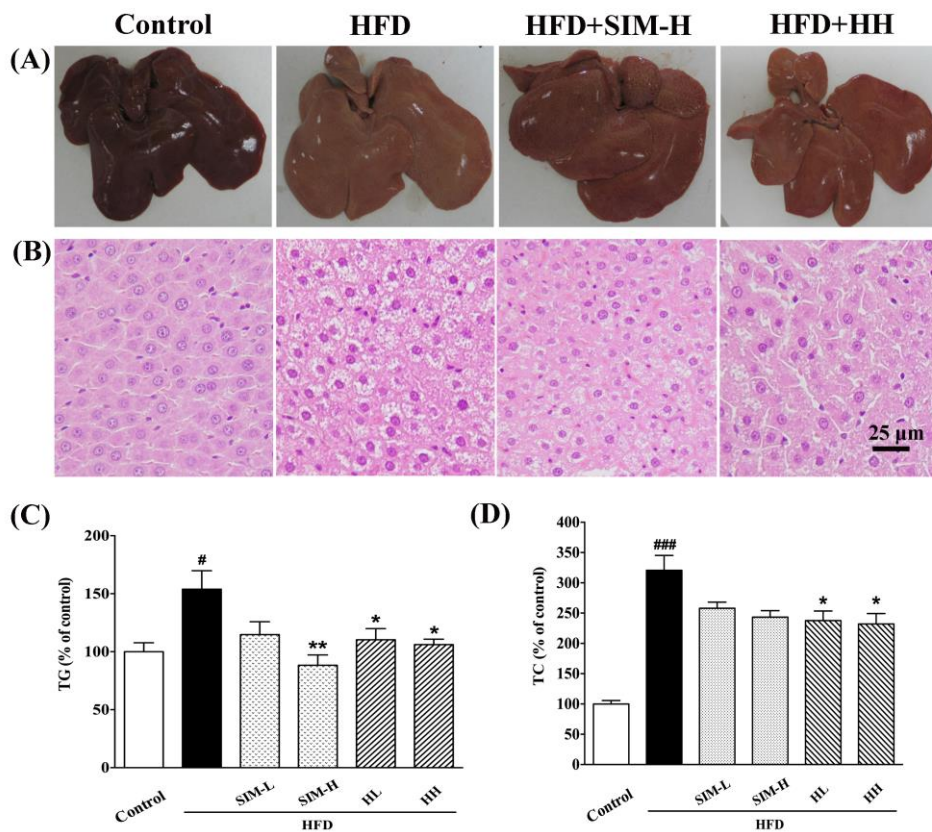


**Fig. 3.5.1 HZ reduced lipid accumulation in the liver**

(A) Gross appearance and (B) Hepatic pathological (H&E staining) from different groups and (C) hepatic TG and (D) TC contents. Rats were fed with normal chow diet (control), HFD, HFD plus 3 mg/kg SIM (HFD + SIM-L), HFD plus 10 mg/kg SIM (HFD + SIM-H), HFD plus 150 mg/kg HZ (HFD + HL), with HFD plus 450 mg/kg HZ (HFD + HH) for 4 weeks. <sup>#</sup> $p < 0.05$ , <sup>###</sup> $p < 0.001$  versus the control group. <sup>\*</sup> $p < 0.05$ , <sup>\*\*</sup> $p < 0.01$  versus the HFD group.

### **3.5.2 HZ did not affect body weight and serum ALT, AST and glucose levels**

As shown in Table 3.5.1, no significant difference was observed in the rat body weight gain. Four weeks of HFD feeding increased liver/body weight ratio (liver index) ( $p < 0.001$ ) and body weight ( $p > 0.05$ ), while HZ intervention decreased liver index but caused a moderate decrease in body weight. Moreover, no significant differences in ALT, AST and glucose levels were detected between the control, HFD and HZ groups.

**Table 3.5.1 HZ reduced the lipid accumulation of fatty liver induced by HFD**

	Control	HFD	SIM-L	SIM-H	HL	HH
Body weight gain (g)	187.8 ± 9.12	207.1 ± 13.65	179.6 ± 6.94	181.5 ± 5.58	199.6 ± 14.99	202.6 ± 10.13
Liver						
Liver/body (g/kg)	26.63 ± 0.45	39.42 ± 1.83 <sup>###</sup>	35.45 ± 0.64	32.79 ± 1.97 <sup>**</sup>	35.06 ± 0.63	33.38 ± 0.99 <sup>**</sup>
Liver lipid content (g/g of liver)	0.159 ± 0.01	0.34 ± 0.03 <sup>###</sup>	0.24 ± 0.01 <sup>*</sup>	0.14 ± 0.04 <sup>***</sup>	0.18 ± 0.02 <sup>***</sup>	0.21 ± 0.02 <sup>***</sup>
Liver TG (% of control)	100.0 ± 7.77	153.9 ± 15.96 <sup>#</sup>	114.7 ± 11.07	88.34 ± 8.91 <sup>**</sup>	110.3 ± 9.62 <sup>*</sup>	106.2 ± 4.62 <sup>*</sup>
Liver TC (% of control)	100.0 ± 5.78	320.6 ± 24.71 <sup>###</sup>	258.0 ± 10.12	243.3 ± 10.68	237.7 ± 15.89 <sup>*</sup>	232.0 ± 17.40 <sup>*</sup>
Serum						
TC (mmol/L)	1.36 ± 0.09	2.93 ± 0.29 <sup>###</sup>	2.11 ± 0.27	1.76 ± 0.15 <sup>**</sup>	1.98 ± 0.10 <sup>*</sup>	1.93 ± 0.19 <sup>*</sup>
TG (mmol/L)	0.57 ± 0.03	0.54 ± 0.11	0.36 ± 0.02	0.48 ± 0.05	0.47 ± 0.04	0.51 ± 0.06
LDL-c (mmol/L)	0.21 ± 0.02	0.56 ± 0.07 <sup>###</sup>	0.35 ± 0.08	0.22 ± 0.02 <sup>**</sup>	0.28 ± 0.03 <sup>**</sup>	0.30 ± 0.04 <sup>*</sup>
HDL-c (mmol/L)	1.10 ± 0.04	1.42 ± 0.05	1.24 ± 0.08	1.45 ± 0.06	1.40 ± 0.09	1.35 ± 0.13
ALT (U/L)	42.13 ± 2.78	42.38 ± 1.28	44.08 ± 1.51	42.63 ± 2.81	39.38 ± 2.08	40.25 ± 2.58
AST (U/L)	147.8 ± 6.02	155.8 ± 3.36	147.9 ± 8.49	150.4 ± 7.63	124.1 ± 4.21	126.1 ± 10.92
Glucose (mmol/L)	5.96 ± 0.33	6.42 ± 0.30	5.91 ± 0.40	6.05 ± 0.35	6.07 ± 0.35	5.85 ± 0.27

Data are expressed as means ± SEM. n = 6 - 9. <sup>#</sup>*p* < 0.05, <sup>###</sup>*p* < 0.001 versus the control group. <sup>\*</sup>*p* < 0.05, <sup>\*\*</sup>*p* < 0.01 and <sup>\*\*\*</sup>*p* < 0.001 versus the HFD group.

### 3.5.3 HZ alleviated hyperlipidemia

#### *HZ promoted vasorelaxing effect of HZ*

To evaluate the vasorelaxing effect of HZ on endothelium-intact rat aortic rings, acetylcholine (10 nM - 10  $\mu$ M) was added cumulatively to the aortic preparation in the presence of neostigmine (1  $\mu$ M) after phenylephrine - induced contraction reached plateau levels. As illustrated in Fig. 3.5.2, acetylcholine induced relaxation in a dose-dependent manner for endothelium-intact aorta of various groups of rats with ~ 45 - 75% maximum relaxation at 10  $\mu$ M. A significantly smaller magnitude of relaxation caused by acetylcholine was observed in aortas from HFD rats as compared with those observed in other groups ( $p < 0.001$ ). HZ (150 or 450 mg/kg bw. per day,  $p < 0.001$ ) improved the acetylcholine - induced relaxation in rats with HFD. Ameliorations in the acetylcholine-induced relaxation were only observed in animals treated with simvastatin (10 mg/kg bw. per day) (Fig. 3.5.2).

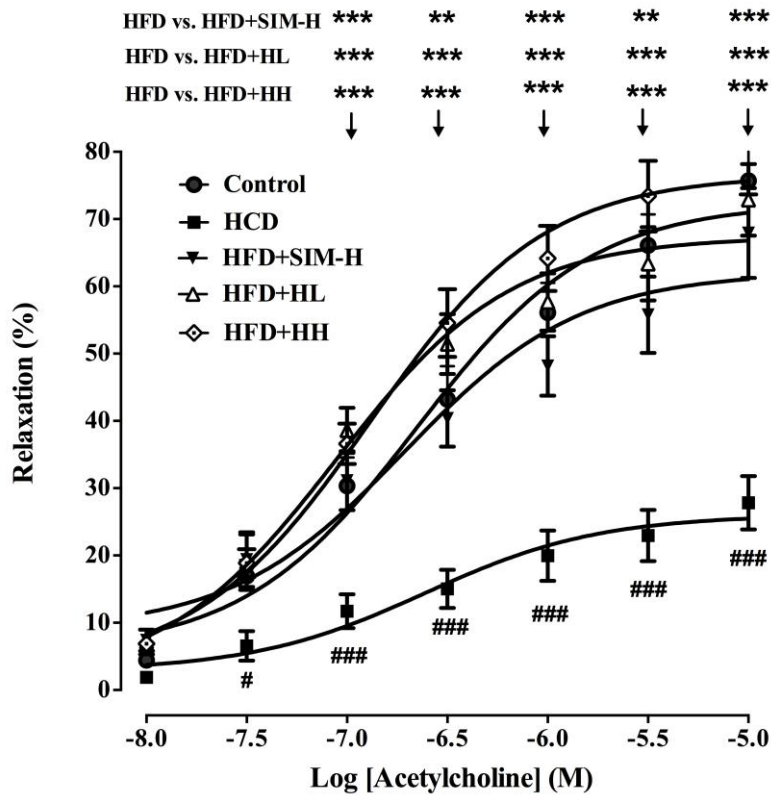


**Fig. 3.5.2 Role of endothelium in HZ-induced relaxation**

Data are expressed as decrease in (percentage) steady state tension obtained with 1  $\mu$ M phenylephrine pre-contracted thoracic aortic rings from the control, HFD, SIM-H (10 mg/kg bw per day), HL (150 mg/kg/day) and HH (450 mg/kg/day). Data are expressed as means  $\pm$  SEM, n = 8. # $p$  < 0.05 and ### $p$  < 0.001 versus the control group. \*\* $p$  < 0.01 and \*\*\* $p$  < 0.001 versus the HFD group.

***HZ reduced nitrite production level in the isolated thoracic aortas***

Without acetylcholine (1  $\mu\text{M}$ ), aortic rings released undetectable levels of nitrite after 2 h of incubation (data not shown). When acetylcholine (1  $\mu\text{M}$ ) was added to the incubation medium, nitrite production in the control group increased dramatically to  $75.99 \pm 5.75$  nmol/g of aortic tissue after the 2 h incubation period. It was found that HFD markedly attenuated nitrite production ( $30.78 \pm 2.87$  nmol/g of aortic tissue,  $p < 0.001$ ). As shown in Figure 3.5.3, aortas from the simvastatin (3 and 10 mg/kg bw. per day) treatment group significantly potentiated nitrite production. There was a significant increase in the HZ treatment groups (both dosages) as compared with the HFD group (HL:  $64.78 \pm 7.01$  nmol/g of aortic tissue,  $p < 0.05$ ; HH:  $74.34 \pm 7.37$  nmol/g of aortic tissue,  $p < 0.01$ ) (Fig. 3.5.3).

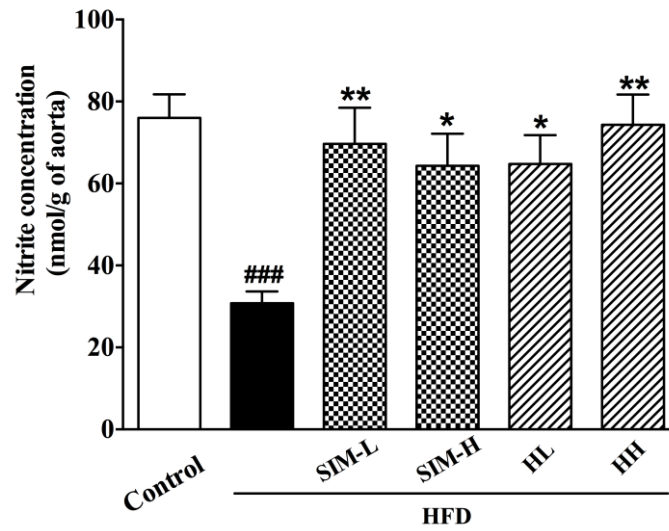


**Fig. 3.5.3 HZ promoted nitrite production in isolated aortas**

*In vitro* nitrite production from various groups' isolated aortas was determined under challenge with acetylcholine (1  $\mu$ M). Data are expressed as means  $\pm$  SEM, n = 6 - 8. ### $p$  < 0.001 versus the control group. \* $p$  < 0.05 and \*\* $p$  < 0.01 versus the HFD group.

### **3.6 HZ inhibited fatty liver through alleviating oxidative stress**

Fig. 3.6.1 depicts the activities of antioxidant enzymes: CAT and SOD in the livers of rats from the control, HFD, SIM-L, SIM-H, HL and HH groups. There was a marked decrease in CAT ( $p < 0.001$ ) but insignificant decrease in SOD ( $p > 0.05$ ) activity in the HFD group as compared with the control rats. For the activity of CAT, treating the animals with SIM ( $p > 0.05$ ) or HH ( $p < 0.001$ ) managed to restore the HFD-induced reduction of CAT activity (Fig. 3.6.1 A). No significant changes ( $p > 0.05$ ) in SOD activities were found between the control group with the HFD group (Fig. 3.6.1 B). Comparing with the HFD rats, treating the animals with SIM, but not HZ, could significantly raise the liver SOD activity (SIM-L:  $p < 0.001$ , SIM-H:  $p < 0.05$ ). A marked increase of MDA content in the HFD group was recorded as compared with the control rats ( $p < 0.05$ ). Treating the animals with SIM (SIM-L,  $p < 0.01$ ; SIM-H,  $p < 0.05$ ) or HZ (HL,  $p < 0.01$ ; HH,  $p < 0.05$ ) significantly decreased the MDA content as compared with the HFD rats (Fig. 3.6.1 C).

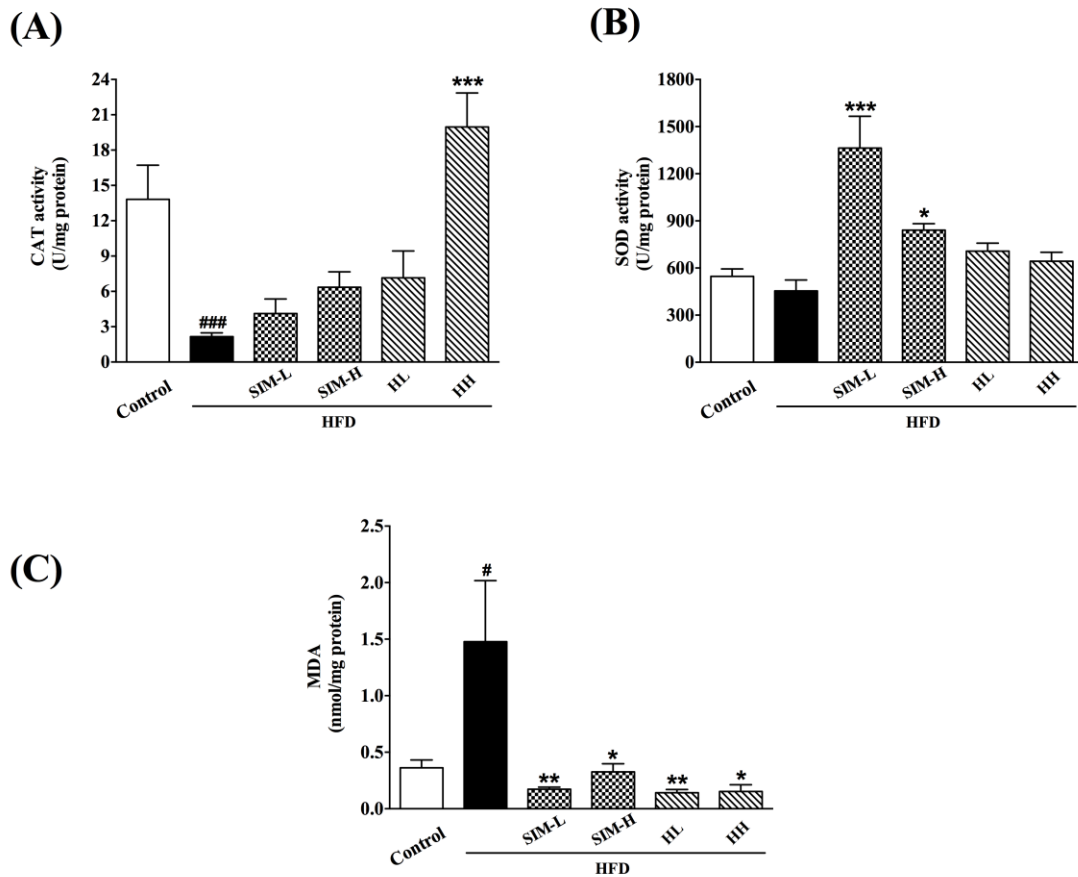


**Fig. 3.6.1 Effects of HZ on antioxidative enzyme activities and MDA content in liver**

(A) CAT, (B) SOD and (C) MDA contents of isolated livers from the control, HFD, SIM-L, SIM-H, HL and HH groups. Data are expressed as means  $\pm$  SEM,  $n = 6 - 8$ . # $p < 0.05$ , and ### $p < 0.001$  versus the control group. \* $p < 0.05$ , \*\* $p < 0.01$  and \*\*\* $p < 0.001$  versus the HFD group.

### **3.7 HZ reduced fatty liver via lipophagy activation *in vivo***

To investigate the potential mechanisms by which HZ activated AMPK, the phosphorylation on the Thr<sup>172</sup> residue of AMPK, an essential marker of AMPK activity, was determined. Activation of AMPK leads to inactivate ACC activity by phosphorylation of Ser<sup>79</sup>. We found that ACC phosphorylation was suppressed by HFD treatment. The decreased phosphorylation of AMPK and ACC by HFD was largely prevented by addition of SIM or HZ (Fig. 3.7.1).

In addition, SREBP-2, HMGCR and LDLR are key regulatory factors for cholesterol synthesis or uptake in the liver. The expression level of LDLR was significantly decreased in the NAFLD rats and HZ significantly upregulated the protein expression level of LDLR (Fig. 3.7.1). However, both simvastatin and HZ had no significant ( $p > 0.05$ ) effects on the altering of protein expressions of SREBP-1c, SREBP-2 and HMGCR as compared with the HFD fed rats. Furthermore, HZ was shown to increase the protein expression level of PPAR $\alpha$ , which is associated with fatty acid oxidation (Fig. 3.7.1).

The autophagy was expected to involve in the effect of HZ on HFD-treated rats, thus expression levels of proteins (LC3B-II and p62) involved in autophagy were determined by western blots analysis (Fig. 3.7.2). HFD could not markedly decrease protein expression level of LC3B-II and increase p62 expression level ( $p > 0.05$ ) compared with control. HZ treatment increased LC3B-II level ( $p < 0.05$ ) but did not decrease p62 expression. In this study, HZ was found to increase phosphorylated MAPKs (p-ERK1/2, phosphorylated ERK1 and ERK2; p-JNK1/2, phosphorylated JNK1 and JNK2; p-p38, phosphorylated p38) expressions (Fig. 3.7.3).

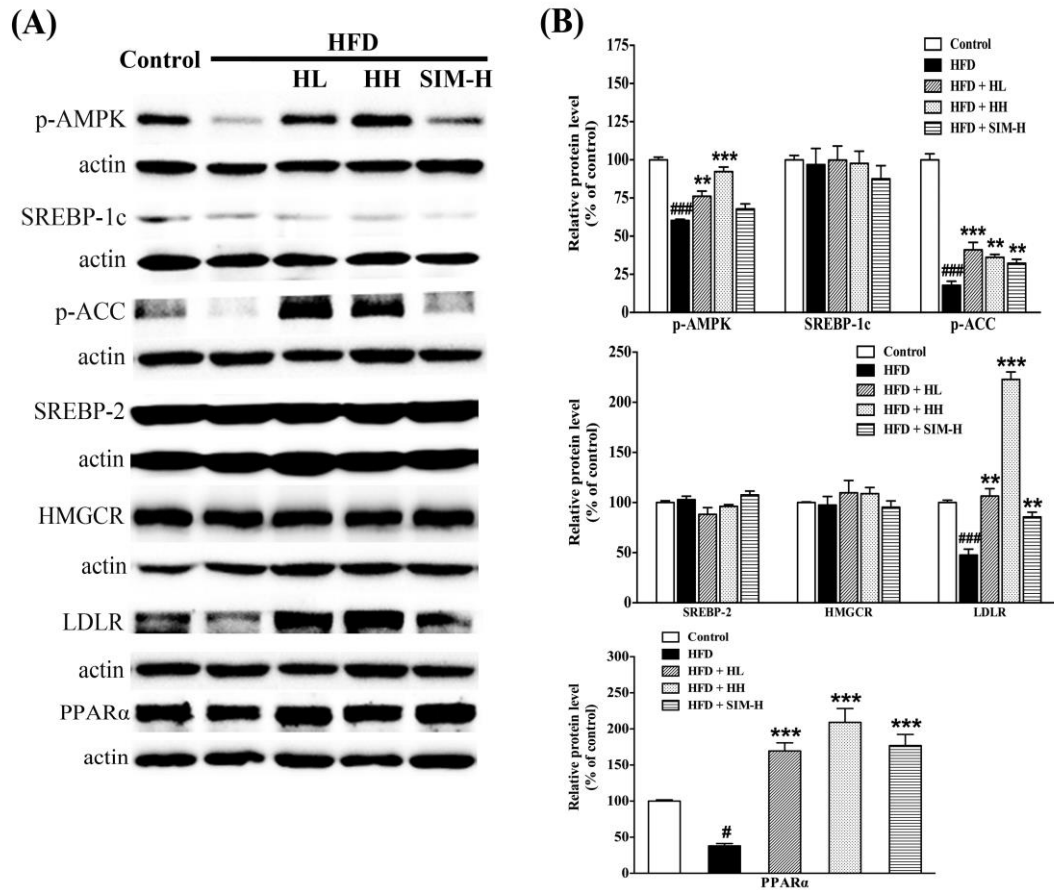


**Fig. 3.7.1** Effects of HZ on expressions of lipid metabolism-related proteins in *in vivo* model

(A) Protein expressions of lipid metabolism-related proteins (p-AMPK, SREBP-1c, p-ACC, HMGCR, SREBP-2, LDLR, PPAR $\alpha$ ) in the liver of rats were changed by SIM-H, HL and HH. (B) The protein levels were expressed relative to actin. Rats were fed with normal chow diet (control), HFD, HFD plus 10 mg/kg SIM (HFD + SIM-H), HFD plus 150 mg/kg HZ (HFD + HL), HFD plus 450 mg/kg HZ (HFD + HH) for 4 weeks. # $p < 0.05$  and ### $p < 0.001$  versus the control group. \*\* $p < 0.01$  and \*\*\* $p < 0.001$  versus the HFD group.

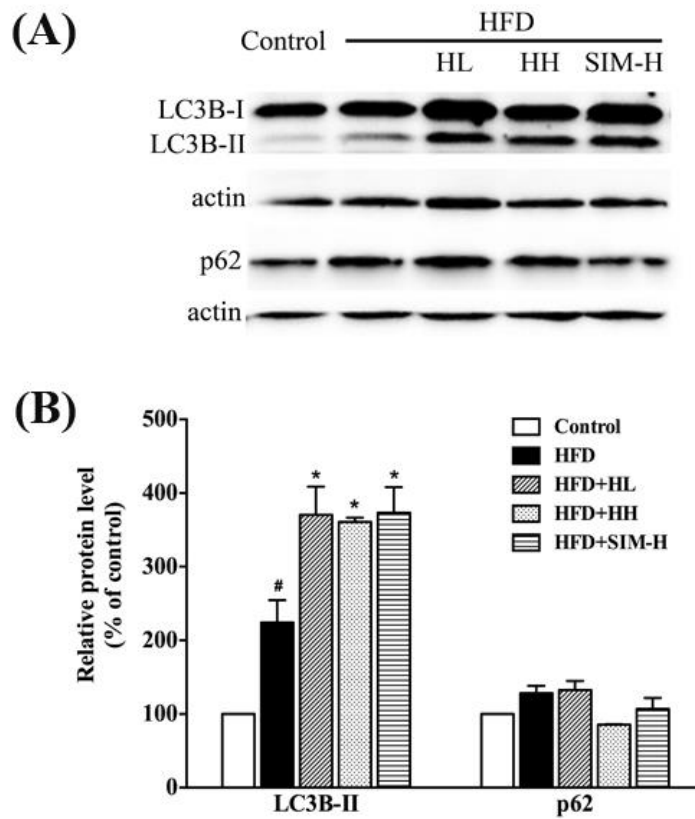


**Fig. 3.7.2 Effects of HZ on protein expressions of autophagy in *in vivo* model**

(A) Protein expressions of autophagy proteins (LC3B-II and p62) in the liver of rats were changed by SIM-H, HL and HH. (B) The protein levels were expressed relative to actin. Rats were fed with normal chow diet (control), HFD, HFD plus 10 mg/kg SIM (HFD + SIM-H), HFD plus 150 mg/kg HZ (HFD + HL), with HFD plus 450 mg/kg HZ (HFD + HH) for 4 weeks. <sup>#</sup> $p < 0.05$  versus the control group. <sup>\*</sup> $p < 0.05$  versus the HFD group.

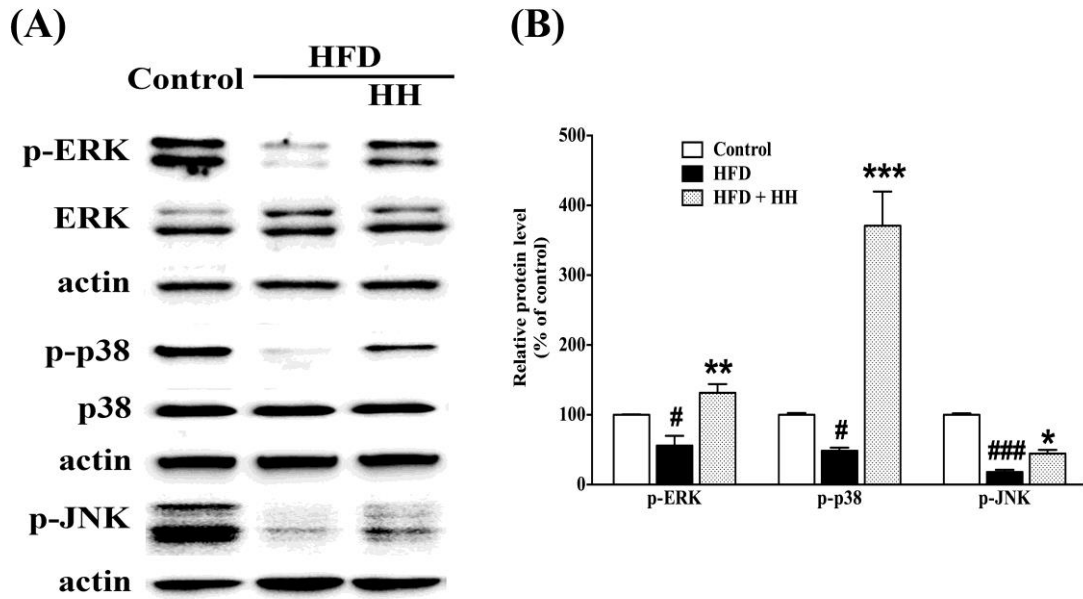


**Fig. 3.7.3 HZ mediates MAPK activation in *in vivo* model**

(A) Western blot analysis of phosphorylated MAPKs (p-ERK1/2, pJNK1/2, p-p38) in the liver of rats were changed by HH. (B) The protein levels were expressed relative to actin. Rats were fed with normal chow diet (control), HFD, HFD plus 150 mg/kg HZ (HFD + HL), HFD plus 450 mg/kg HZ (HFD + HH) for 4 weeks. # $p < 0.05$ , ### $p < 0.001$  versus the control group. \* $p < 0.05$ , \*\* $p < 0.01$  and \*\*\* $p < 0.001$  versus the HFD group.

## **3.8 Serum metabolites change of bile acids after HZ treatment**

### **3.8.1 Reliability of the metabolomics MS platform**

The stabilities of UPLC-MS detections were assessed by inter-day measurement of the pooled QC sample injections and internal standards, respectively. PCA score plot was used to evaluate the stability of the analytical instruments and Fig. 3.8.1 showed the QC sample injections of inter-day experiments acquired in negative ESI mode were clustered together in PCA score plot better than that in positive ESI mode. Overall negative ESI results indicated high reproducibility was achieved across the runs and this ensured the changes among the different groups observed from the statistical analysis were biologically related. 13 metabolites from QC samples were selected for comparison (Table 3.8.1). The CV% of metabolites detected under negative modes of UPLC-MS listed in Table 3.8.1 were mostly less than 5% except glycocholate (< 30%) while the CV% of internal standards was 7.05 - 16.23% without normalization and 2.98 - 9.68% after normalization.

**Table 3.8.1 Fold change of metabolites identified by UPLC-MS and GC-MS**

Metabolites	Adducts	Retention time/min	Theoretical m/z	Measured m/z	Mass error/ppm	Fold change		QC CV (%)
						Control / HFD	HZ / HFD	
<b>Taurocholate</b>	[M-H] <sup>-</sup>	7.18	514.2844	514.2839	-0.97	1.71 <sup>##</sup>	1.20	4.25
<b>Taurohyodeoxycholate/ Tauroursodeoxycholate</b>	[M-H] <sup>-</sup>	7.02	498.2895	498.2880	-3.01	1.58	0.98	3.49
<b>Alpha-Muricholic acid</b>	[M-H] <sup>-</sup>	8.31	407.2803	407.2796	-1.72	0.56	1.69	4.06
<b>Glycocholate</b>	[M-H] <sup>-</sup>	8.28	464.3018	464.3013	-1.08	0.66 <sup>#</sup>	1.25 <sup>*</sup>	29.32
<b>Glycohyodeoxycholate/ Glycoursodeoxycholate</b>	[M-H] <sup>-</sup>	8.36	448.3068	448.3062	-1.34	0.74	1.10	3.82
<b>Taurochenodeoxycholate/ /Taurodeoxycholate</b>	[M-H] <sup>-</sup>	9.14	498.2895	498.2891	-0.80	0.43 <sup>#</sup>	1.05	4.48
<b>Cholic acid</b>	[M-H] <sup>-</sup>	10.21	407.2803	407.2796	-1.72	0.66 <sup>##</sup>	1.23	3.41
<b>Glycochenodeoxycholate</b>	[M-H] <sup>-</sup>	10.46	448.3068	448.3062	-1.34	0.39 <sup>###</sup>	2.16 <sup>***</sup>	4.48
<b>Hyodeoxycholate/ Ursodeoxycholate</b>	[M-H] <sup>-</sup>	10.67	391.2854	391.2848	-1.53	0.64	1.25	3.41
<b>Glycodeoxycholate</b>	[M-H] <sup>-</sup>	10.91	448.3068	448.3063	-1.12	0.31 <sup>###</sup>	1.64 <sup>*</sup>	4.34
<b>Beta-Muricholic acid</b>	[M-H] <sup>-</sup>	8.59	407.2803	407.2796	-1.72	0.54	1.49	3.15
<b>Chenodeoxycholate</b>	[M-H] <sup>-</sup>	13.51	391.2854	391.2848	-1.53	0.53 <sup>#</sup>	1.96 <sup>***</sup>	3.97
<b>Deoxycholate</b>	[M-H] <sup>-</sup>	14.02	391.2854	391.2848	-1.53	0.36 <sup>###</sup>	1.71 <sup>***</sup>	3.73

One-way ANOVA, equal variance: LSD; equal variance: Tamhane: <sup>#</sup> $p < 0.05$ , <sup>##</sup> $p < 0.01$  and <sup>###</sup> $p < 0.001$  versus the control group. <sup>\*</sup> $p < 0.05$  and <sup>\*\*\*</sup> $p < 0.001$  versus the HFD group. n = 7 - 9.

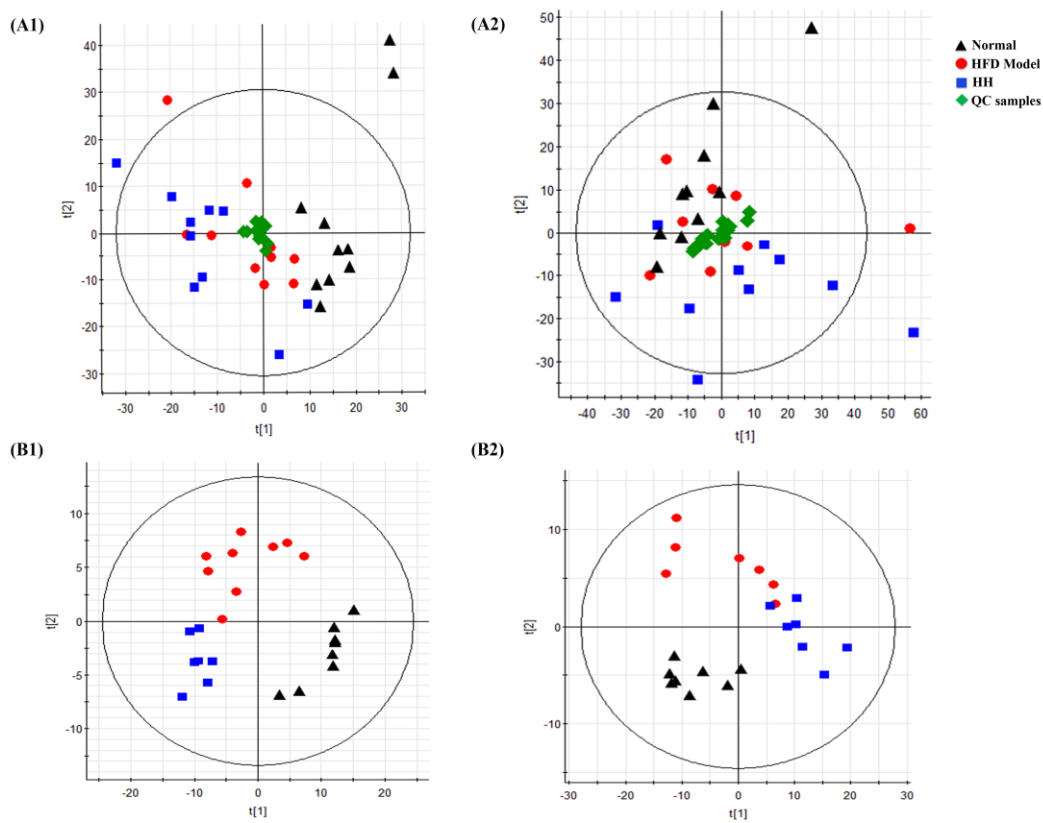


**Fig. 3.8.1 (A) PCA score plot, (B) PLS-DA score plot in negative (1) and positive (2) ionization modes for UPLC-MS**

### 3.8.2 Serum bile acid metabolites change in HFD model

The PCA method was first applied to explore the influence of treatment on the variation in serum metabolites over the duration of the study. It is noted that in the PLS-DA score plot, the sham group and HFD models were separated in the second principal component (accounted for 8.7% of explained variance), whereas the HZ treatment groups were deviated away from the HFD model from the first component (accounted for 27.9% of explained variance).

Metabolite changes in the blood serum between HFD model and sham group were investigated using orthogonal partial least-squared discriminant analysis (OPLS-DA).

Metabolites with significant contribution to the differentiation of two groups by OPLS-DA [ $R^2X(\text{cum}) = 0.50$ ,  $R^2Y(\text{cum}) = 0.94$ ,  $Q^2(\text{cum}) = 0.64$ ] are usually identified based on their VIP values (threshold of  $VIP \geq 1$ ). Variables with higher VIP values have greater the importance for the separation of two groups. According to the results obtained by VIP value, over 10 bile acids and their conjugated derivatives were identified and showed in Table 3.8.1.

### 3.8.3 Serum metabolites change of bile acids after HZ treatment

Bile acids and their metabolites were significantly affected by HFD as well as the HZ treatment. The fold changes for these metabolites are listed in Table 3.8.1 and more details could be found in a heatmap in the Fig. 3.8.2. Fig. 3.8.4 shows the proposed pathway of bile acid biosynthesis and indicates the bile acids affected by HFD and HZ treatment.

HFD rats resulted in significant increases in three primary bile acids and their conjugated derivatives (CDCA, GCDCA and GCA) and two secondary bile acids and conjugated derivatives (DCA and GDCA) ( $p < 0.05$ ). Our findings are consistent with the previous reports that dietary cholesterol increased bile acid pool size and faecal bile acid excretion. HZ supplement to HFD rats resulted in significant increases CDCA, GCDCA, GCA, DCA and GDCA ( $p < 0.05$ ). The increased levels of primary and secondary bile acids in HFD group might be the results of increased stimulation of dietary absorbed cholesterols for bile acid synthesis but the elimination rate was not high enough to cope with the influx of cholesterol from diet. It should be clarified that

increased bile acid pool is the consequence of dysregulation of bile acid metabolism and altered metabolic homeostasis.

Regarding the mechanism of bile acid disturbance, cytochrome P450 7A1 (CYP7A1), the rate-limiting enzyme in the classical pathway of bile acid biosynthesis, was thought to be upregulated by HZ, which affects the bile acid synthetic pathway and enhances the excretion of faecal bile acids to lower cholesterol (Fig. 3.8.3). The CYP7A1 protein expression of HZ-treated group was higher than that of the HFD group ( $p < 0.01$ ). This indicated that HZ might rely on CYP7A1 action in removal of cholesterol (Fig. 3.8.3).

Bile acids and their metabolites were significantly affected by HFD as well as the HZ treatment. The fold changes for these metabolites were listed in Table 3.8.1 and more details could be found in a heatmap in the Fig. 3.8.2. Fig. 3.8.4 showed the proposed pathway of bile acid biosynthesis and indicated the bile acids affected by HFD and HZ treatment.

To study the effect on HZ, PLS-DA was further carried out to examine the difference of metabolite profiles among the normal control, HFD and piceatannol groups. As

shown in Fig. 3.8.1 B, the results of PLS-DA score plot showed a clear distinction of the normal control, HFD and HZ groups.

HFD rats resulted in significant increases in three primary bile acids (CDCA, GCDCA and GCA) and two secondary bile acids (DCA and GDCA) ( $p < 0.05$ ). Our findings are consistent with the previous reports that dietary cholesterol increased bile acid pool size and faecal bile acid excretion. HZ supplement to HFD rats resulted in significant increases CDCA, GCDCA, GCA, DCA and GDCA ( $p < 0.05$ ). The increased levels of primary and secondary bile acids in HFD group might be the results of increased stimulation of dietary absorbed cholesterols for bile acid synthesis but the elimination rate was not high enough to cope with the influx of cholesterol from diet. It should be clarified that increased bile acid pool is the consequence of dysregulation of bile acid metabolism and altered metabolic homeostasis.

Regarding the mechanism of bile acid disturbance, cytochrome P450 7A1 (CYP7A1), the rate-limiting enzyme in the classical pathway of bile acid biosynthesis, was thought to be upregulated by HZ, which affects the bile acid synthetic pathway and enhances

the excretion of faecal bile acids to lower cholesterol (Fig. 3.8.3). The CYP7A1 protein expression of HZ-treated group was higher than that of the HFD group ( $p < 0.01$ ). This indicated that HZ might rely on CYP7A1 action in removal of cholesterol.

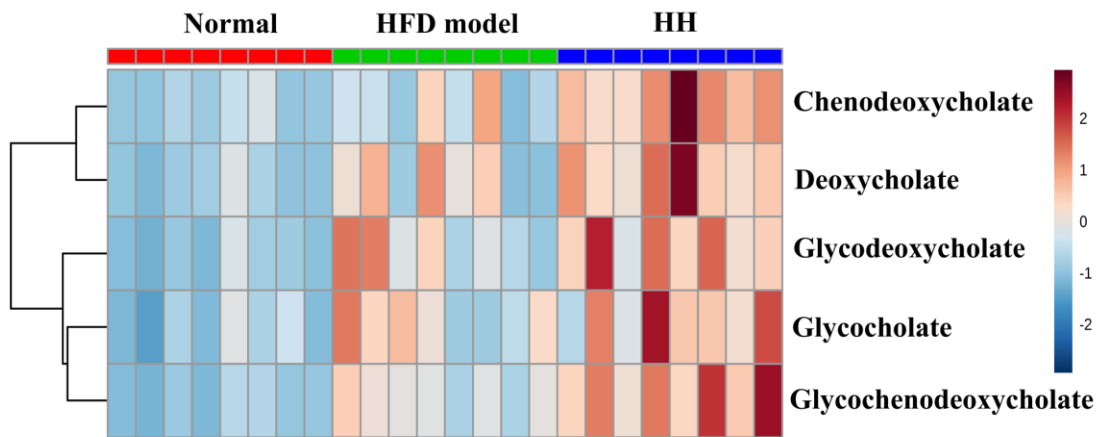


**Fig. 3.8.2** Heatmap of UPLC-MS identified bile acid in normal control, HFD and HZ group

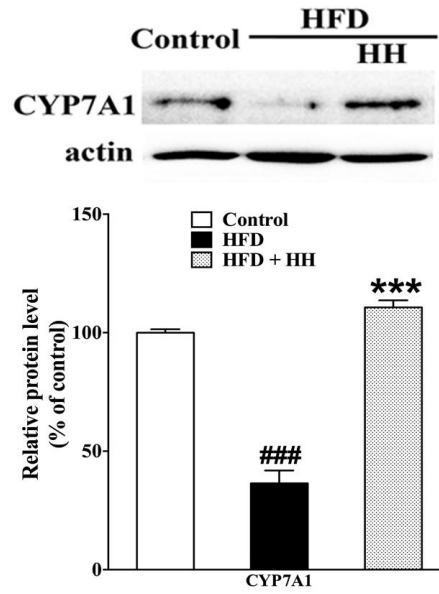


**Fig. 3.8.3 HZ regulated TC utilization by increasing bile acid synthesis via activating CYP7A1**

Representative Western blots (A) and the graph (B) representing the quantitative comparison of protein expression of CYP7A1 in the livers of the normal control, HFD and HZ-treated group. Data are expressed as means  $\pm$  SEM. ### $p < 0.001$  versus the control group. \*\*\* $p < 0.001$  versus the HFD group.

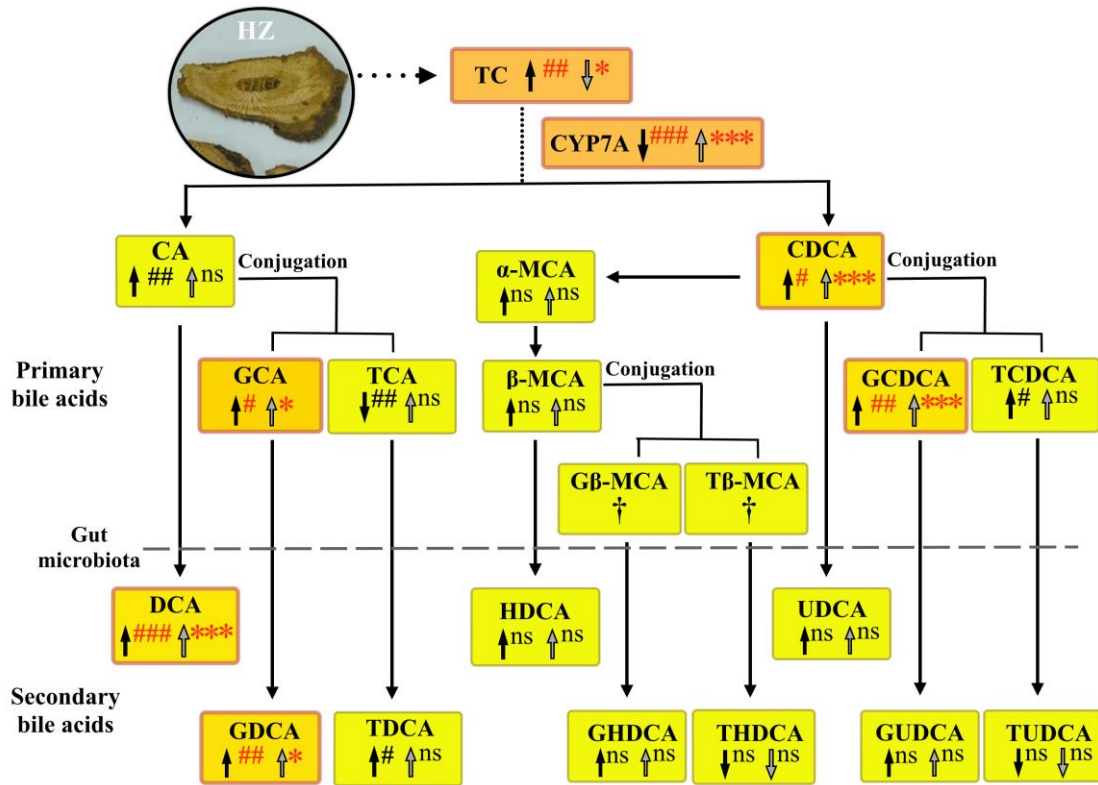


**Fig. 3.8.4** A simplified proposed diagram of bile acid biosynthesis affected by HFD and HZ treatment

↑↓: trend of HFD model group compared to normal control group. : ↑↓ trend of HZ group compared to HFD group. ns: no significant difference. † not detected. Dotted line: skipped pathway. #  $p < 0.05$ , ##  $p < 0.01$  and ###  $p < 0.001$  versus the control group. \*  $p < 0.05$ , \*\*\*  $p < 0.001$  versus the HFD group.

## **Chapter 4 Discussion**

## 4.1 Experimental hepatic steatosis models

NAFLD refers to a spectrum ranging from simple steatosis to NASH, fibrosis, cirrhosis and HCC (Vanni et al. 2015). Whether steatosis can progress toward NASH, or these entities represent two different diseases, is still highly debated. However, up to 20 - 30% of NAFLD patients with simple steatosis may transform to steatohepatitis at a certain point. This breakthrough-like process is mediated by the interplay of multiple hit factors (Gao et al. 2016) .

In the present study, the impact of HZ on NAFLD was examined through a series of *in vitro* and *vivo* experiments using LO2 (normal human liver cell line) and HFD-fed rats models.

In order to study further mechanism of HZ improving hepatic lipid metabolism *in vitro*, LO2 cells, a kind of normal human hepatocyte, were incubated with an FFA mixture (oleate/palmitate, 2:1) to develop cellular steatosis. LO2 cells were induced by a mixture of oleic acid and palmitic acids as they are the most abundant FFAs of hepatic TG pool in both normal subjects and patients suffering from NAFLD (Gambino et al.

2016). In a previous study, treatment of LO2 cells with an FFA mixture (oleate/palmitate, 2:1) induced efficient intracellular lipid accumulation that mimics benign chronic steatosis as found in human (J. W. Wang et al. 2014). In agreement with this, we found that exposure of LO2 cells to a mixture of FFA (oleate/palmitate, 2:1) for 24 h resulted in significant increase in intracellular lipid accumulation by Nile red staining. Concomitantly, FFA-treated cells significantly augmented intracellular TG levels compared to untreated cells. Meanwhile, LO2 cells had apparent steatosis by incubating with 0.3 mM FFA mixture for 24 h, with minor toxic, oxidative and apoptotic effects FFA mixture. This cellular steatosis model was similar to that observed in simple hepatic steatosis in humans by Farrell and Larter (Farrell and Larter 2006).

The rat model of high-fat diet-induced fatty liver was considered a good model for the study of NAFLD (Lau et al. 2016) (Lieber et al. 2004). Furthermore, previous studies reported the rat model of high-fat diet-induced fatty liver was considered a good model for the study of NAFLD. Rats fed with HFD showed similar clinical characteristics observed in human NAFLD with dyslipidemia, IR, obesity, augmented expression of regulators of lipogenesis and proinflammatory cytokines (R. J. Zhang et al. 2016)

(Longato et al. 2012).

In keeping with these, we found that SD rats fed with HFD lasting 4 weeks had marked increases in liver index (liver weight as a percentage of body weight), hepatic fat deposition, liver content of TG, serum contents of TC, as well as the activities of SOD and MDA. Further, histological analyses (H&E staining) of liver suggested hepatic fatty degeneration in HFD group. Steatosis in *in vivo* model was assessed by gross liver appearance, liver index (liver weight as a percentage of body weight) and HE staining for lipid accumulation. The HFD generated a dramatic increase in the liver size and weight, as well as in the percentage of lipid content compared with controls. Gross livers from rats maintained on regular diet for 4 weeks retained dark red coloration of the liver and showed in either the gross appearance or the size and weight. Consumption of HFD resulted in an increase in gross liver size and yellowish coloration of the liver (Fig. 3.5.1). H&E stained sections from livers demonstrate the enlarged hepatocytes and an increasing degree of steatosis represented by the vacuolation in hepatocytes, which correlated with consuming the high fat diet (Fig. 3.5.1). Graphical comparison of the liver weights over total body, as well as liver as lipid content showed a significant

1.5 fold ( $p < 0.001$ ) and 2 fold ( $p < 0.001$ ) increase respectively in the rats fed with high-fat diet when compared with rats fed with regular diet. Consumption of a high fat diet induced lipid accumulation such that an increased TG ( $p < 0.05$ ) and TC ( $p < 0.001$ ) content compared with regular diet (Table 3.5.1).

ALT and AST elevations usually reflect the presence of hepatocellular injury. However, HFD can not lead to significant increase in ALT and AST levels, which indicates no liver injury. Moreover, it was found that the serum glucose did not change after a 4-week HFD treatment. Considering the findings, we proposed that a 4-week HFD induced simple hepatic steatosis, the early stage of NAFLD, and potentiated metabolic dysfunction with the resultant development of NAFLD.

## **4.2 HZ exerted lipid lowering effect by its antioxidant properties**

Another major contributing factor to the pathogenesis of NAFLD is the oxidative stress (W. S. Liu et al. 2015). Clinical and experimental studies indicate a strong association between NAFLD and oxidative stress. The increased production of ROS induced lipid

peroxidation, with subsequent activation of inflammatory pathways and stellate cells leading to fibrogenesis, and also mitochondrial damage. Oxidative phosphorylation and fatty acid  $\beta$ -oxidation within the normal liver takes place in the mitochondria, but this process may become overwhelmed as a result of increased FFA load, giving rise to ROS in the context of NAFLD (Gao et al. 2016).

In this study, the antioxidative capacities of HZ were measured by using both a cell-free assay [2,2-diphenyl-1-(2,4,6-trinitrophenyl) hydrazyl (DPPH) assay and total phenols assay by Folin-Ciocalteu reagent (FCR)] and biological methods [hepatic lipid oxidation (MDA level) and CAT activities in HFD-fed rats]. DPPH (2,2-diphenyl-1-picryl-hydrazyl-hydrate) free radical assay is an easy and accurate method based on electron-transfer (ET) that produces a violet solution in methanol. The violet color DPPH solution is reduced to yellow colored product, diphenylpicryl hydrazine, in presence of an antioxidant in a concentration dependent manner. DPPH assay has been used extensively to predict the capacity of an antioxidant because of the relatively short time required for analysis (Huang et al. 2005). Our results revealed that the water extract of HZ had a similar free radical scavenging activity ( $SC_{50} = 0.05$  mg/mL) when

compared with standard Vit C.

Total phenols assay by Folin-Ciocalteu reagent (FCR) is a routine assay in studying phenolic antioxidants. Several studies have indicated that the antioxidant activities of TCM were highly correlated to their total phenolic contents (D. J. Guo et al. 2008; Jacobo - Velázquez and Cisneros - Zevallos 2009). The total phenolic content of HZ water extract was found to  $26.83 \pm 5.03$  mg GAE/g dry extract. The polyphenolic constituents of HZ (Resveratrol and polydatin) may be the major contributors to the antioxidant activity in free radical neutralization.

A series of studies have demonstrated that hepatic lipid peroxidation enhanced, as observed by increased MDA level, and antioxidant defenses decreased, as observed by reduction of GSH, SOD and CAT activities in the presence of NAFLD (S. Li et al. 2015b). In our study, HZ exhibited marked antioxidant properties to suppress the hepatic lipid oxidation (MDA level), and increase CAT level in HFD-fed rats.

Earlier literature (Huan Zhang et al. 2013) reveals that HZ is rich in anthraquinones and stibenes. Anthraquinones (emodin and physcion) (Alisi et al. 2012) and stilbenes

(resveratrol and polydatin) have been reported to exert antioxidant and hypolipidemic effects (Nishikawa et al. 2013)

Based on the above information, it is presumed that because of its appreciable antioxidant activities, HZ can combat steatosis. Such an event has been reflected in a study reporting that the water extracts of HZ at doses of 5 g/kg b.w. attenuated lipid lowering effect in rats model of fatty liver by its antioxidant activity (Yiyong 2016).

### **4.3 HZ reduced lipid accumulation partially by regulating autophagy induction**

Until now, the underlying mechanisms of anti-NAFLD effect of HZ on lipophagy remains unclear. Studies to date have revealed that impaired lipophagy, indeed, may be a fundamental mechanism of disorders of lipid metabolism such as NAFLD and the metabolic syndrome. Lipophagy may therefore represent a potential therapeutic target for the treatment of NAFLD.

To elucidate the hypothesis that HZ could attenuate lipid accumulation via lipophagy induction, autophagy inhibition by transfection with autophagy-related (Atg5) small

interfering RNA was used in FFA-induced steatotic LO2 cells. Rapamycin, as an inhibitor of mTOR, activates autophagy. Our study showed that treatment with HZ enhanced autophagy and reduced lipid accumulation in steatotic LO2 cells, which was similar to rapamycin. Moreover, we inhibited autophagy with siRNA for Atg5, which is essential for autophagosome formation and autophagy activation. siRNA against Atg5 significantly increased the inhibition of HZ against FFA-induced lipid accumulation. Therefore, the activation of autophagy plays a significant role in the anti-steatosis effect of HZ *in vitro*. Taken together, these findings establish for the first time that HZ was still able to upregulate PPAR $\alpha$ , LDLR and p-ACC expressions in the absence of autophagy, suggesting that HZ reduced lipid accumulation partially by regulating autophagy induction.

In our *in vitro* study, the protein expression of LC3-II was markedly elevated but no alteration in the downstream events regulating autophagosomal degradation. For example, the levels of p62 were observed in FFA-treated cells upon co-exposure to HZ, which was in agreement with our *in vivo* findings as stated above, suggesting that this effect may be mediated through increased autophagosomes synthesis but rather to a

blockage in the autophagic flux. Our findings agree with previous reports obesity or HFD reduce levels of various autophagy factors (Atg5, Atg7), resulting in decreased autophagosome formation and levels of autophagy (L. Yang et al. 2010). However, there are two more potential mechanisms involved in the decreased hepatic autophagy that occurs with HFD feeding or obesity. (1) The liver form increased autophagosomes and autolysosomes, but levels of autophagy decreased due to the defective lysosomal that precluded degradation (Inami et al. 2011). (2) Autophagic flux decreased as a result of impaired autophagosome-lysosome fusion (Koga et al. 2010).

In our study, the protein expression of LC3-II was markedly elevated but no alteration in the level of p62 was observed in both *in vivo* and *in vitro* upon co-exposure to HZ. SQSTM1/p62 protein serves as a link between LC3 and ubiquitinated substrates. P62 and p62-bound polyubiquitinated proteins become incorporated into the completed autophagosome and are degraded in autolysosomes, thus serving as an index of autophagic degradation. However, p62 should be used as an indicator of autophagy flux with caution, as its level is regulated by a number of factors. P62 may be transcriptionally upregulated under certain conditions, further complicating the

interpretation of results (Sahani et al. 2014). For example, activation of a signaling pathway, e.g., RAF1/Raf-MAP2K/MEK-MAPK/ERK and JNK, can also upregulate SQSTM1 transcription, where there is an increase in autophagic flux (Kim et al. 2014; Puissant et al. 2010). In this study, HZ was found to promote JNK/ERK expression which indicates HZ may up-regulate p62 transcription and expression (Fig. 3.7.3). Aberrant p38 activation also can induce autophagy flux, where p62 expression is decreased. HZ could induce p38 activation (Gonnella et al. 2015) (Fig. 3.7.3). Besides, evidences showed high autophagic flux would also lead to up-regulation of p62 transcription. Overall, even though autophagic degradation causes decrease in p62 level, p62 both at transcriptional and expression level is up-regulated via ERK and JNK activation under autophagic process (Kim et al. 2014; Puissant et al. 2010).

So the SQSTM1 protein level may restore to the basal level resulting in no significant changes when compared with the control. If only the measurement of p62 protein level will lead to an incorrect interpretation of autophagic flux, the level of p62 mRNA should be simultaneously determined along with the p62 protein level as an autophagy indicator. Further study of p62 mRNA level will be warranted.

However, our findings agree with those of other studies in which there is an interrelationship between lipid metabolism and autophagy. Notably, our laboratory reported (for the first time) that treatment with Atg5 siRNA significantly abolished the increased expressions of PPAR $\alpha$ , LDLR and p-ACC compared to that of steatotic cells treated with HZ treatment.

Activation of AMPK by phosphorylation at Thr<sup>172</sup> in the alpha subunit leads to the stimulation of hepatic fatty acid oxidation and inhibition of cholesterol synthesis, lipogenesis, and autophagy activation (T. Y. Liu et al. 2016). Activation of AMPK inactivates acetyl-CoA carboxylase (ACC) by phosphorylation of ACC1 at Ser<sup>79</sup> and ACC2 at Ser<sup>218</sup> and 3-hydroxy-3-methylglutaryl-CoA reductase (HMG-CoA reductase, HMGCR), which are the rate-limiting enzymes of fatty acid and sterol synthesis, respectively (Srivastava et al. 2012; Viollet et al. 2006) .

Experimental evidence suggests that AMPK activation increased phosphorylation of ACC and decreased SREBP and HMGCR, which were correlated with decreased hyperlipidemia and NAFLD (Y. Li et al. 2011; Pan et al. 2012; Tang et al. 2016).

Report revealed that resveratrol, bioactive compound isolated from HZ, strongly activated AMPK phosphorylation and downregulated SREBP-1c in HepG2 cells and in High-fat-diet feeding rats (Shang et al. 2008). Polydatin, a stilbenoid compound derived from HZ, inhibited SREBP-1c mRNA expression in high-fat diet-induced fatty liver (Hong Zhang et al. 2012a). Therefore, it is logical to hypothesize that AMPK may be involved in the HZ-induced hypolipidemic effects by reducing TG and cholesterol levels.

Despite these compounds effects on AMPK signaling or SREBP-1c activity, the extent to which HZ improves hepatic steatosis has not been well studied.

The synthesis and cellular uptake of fatty acids and cholesterol are regulated by sterol regulatory element-binding proteins (SREBPs, including SREBP1a, SREBP1c, and SREBP2) (Ye and DeBose-Boyd 2011). Activation of hepatic expression of SREBP-1c and its target lipid synthesis genes, FAS and ACC are highly related to elevated TG level; thus, inhibition of these proteins remains a promising target for future therapies of dyslipidemia (Ahmed and Byrne 2007; Shang et al. 2008; C. M. Wang et al. 2016a).

SREBP-1c activation stimulates hepatic lipogenesis and leads to fatty liver under high-fat diet (W. Li et al. 2014). Our study showed that HFD-fed rats or FFA-treatment LO2 cells did not stimulate hepatic expression of SREBP-1c at protein levels *in vivo* and *in vitro*, suggesting that SREBP-1c is not responsible for the low TG level of HZ in NAFLD.

Agonist for PPAR $\alpha$  related to  $\beta$ -oxidation of fatty acid such as fibrates may potentially be useful in the management of NAFLD and co-morbidities such as CVD (Souza-Mello 2015). Consistent with these reports, our results showed that HZ promoted the phosphorylation of AMPK followed by the downregulation of ACC, thus preventing hepatic TG synthesis both *in vivo* and *in vitro*. Moreover, a significant increase in PPAR $\alpha$  level was observed in FFA-induced cells when co-treated with HZ and in HFD-fed rats, suggesting that upregulation of PPAR $\alpha$  may contribute to the anti-steatosis effect of this herbal medicine via promoting fatty acids  $\beta$ -oxidation.

Current concepts on NAFLD pathogenesis are evolving as new information is the role abnormal cholesterol metabolism has attracted wide attention (Min et al. 2012; Wouters

et al. 2008).

Puri et al.(Puri et al. 2007) reported a significant stepwise increment in free cholesterol in the liver of patients with NAFLD quantified by capillary gas chromatography. Caballero et al. (Caballero et al. 2009) verified that free cholesterol increased in patients with NAFLD and correlated with SREBP-2 induction significantly. However, HMGCR and SREBP-2 proteins were similar across our study groups suggesting that other mechanisms are responsible for the low cholesterol level of HZ in NAFLD.

It is well known that LDL cholesterol is taken up via LDLR and then de-esterified in late endosomes and the free cholesterol returned to the plasma membrane or used for cellular needs (Ikonen 2008). Min et al reported that expression of LDL receptors significantly decreased in contrast to the increase in HMGCR expression in a total of 20 subjects with NAFLD or NASH (Min et al. 2012). Consistent with the reports, the protein level of LDLR was significantly decreased in rats treated with HFD, and there was a significantly increase in the protein level of LDLR in both groups with HZ and

SIM. The results indicated that upregulated cholesterol uptake pathway was responsible for the cholesterol-lowering effect of HZ. A similar effect was also observed in FFA-induced steatosis cell model. These results indicated that HZ might activate lipophagy via activating AMPK/autophagy pathway.

#### **4.4 HZ decreased cholesterol accumulation by increasing bile acid synthesis and inhibiting intestinal cholesterol absorption**

Previous studies indicated that a combination of increased production (HMGCR), decreased utilization (bile acid synthesis due to CYP7A and CYP27A) and transport [ATP binding cassette subfamily G member 1 (ABCG1) and ATP binding cassette subfamily G member 8 (ABCG8)] could contribute to the accumulation of free cholesterol in NAFLD (Min et al. 2012).

Bile acids are synthesized from cholesterol in the liver. About 95% of bile-secreted bile acids are reabsorbed in the ileum via ileal ASBT and return to the liver through the portal vein, maintaining the bile acid pool. Bile acid composition is regulated by

numerous factors, including FXR-dependent pathways in the liver and metabolism by the gut microbiota.

Disruption of normal bile acid synthesis and metabolism is associated with hypercholesterolemia. Bile acid sequestrants are approved for treatment with hypercholesterolemia. These resins impaired bile acid reabsorption, resulting in increased bile acid excretion and reduced plasma LDL levels (Staels et al. 2010).

HFD group had a higher level of primary (CDCA, GCA and GCDCA) and secondary (DCA and GDCA) bile acids ( $p < 0.05$ ). Our findings are consistent with the prior research showing that dietary cholesterol increased bile acid pool and faecal bile acid excretion (J. Guo et al. 2011; Sham et al. 2017; Tiemann et al. 2004). The increased levels of bile acids in HFD group might be because the rate of bile acid synthesis and excretion for cholesterol removing from the body is not high enough to cope with the influx of cholesterol from diet.

Bile acids are amphipatic molecules that can be as well detrimental to cells. The beneficial effects include solubilization and absorption of lipids and certain vitamins,

cell survival, while the toxic effects include inhibition of bile formation, apoptosis, necrosis, and oxidative stress. Not all bile acids are toxic due to minor chemical structure changes (Thomas et al. 2008).

CDCA, the major hydrophobic primary bile acids in cholestatic liver injury, serves as endogenous danger signal to activate NLRP3 inflammasome and induce secretion of pro-inflammatory cytokine-IL-1 $\beta$  in macrophages (Gong et al. 2016). However, CDCA is the most potent natural bile acid in activating FXR- $\alpha$  to treat gallstones (Shaw et al. 1981).

In contrast, hydrophilic ursodeoxycholic acid (UDCA), has been widely used for the treatment of hepatopathies of a cholestatic nature, and the only one approved by U.S. FDA (Food and Drug Administration) to treat PBC (primary biliary cirrhosis) (Gitto et al. 2015; Roma et al. 2011).

Tauroursodeoxycholic acid (TUDCA), synthesized in the hydrophilic conjugation pathway of ursodeoxycholic acid, has been effectively used for treating several liver disease such as cholelithiasis, HCC (Vandewynckel et al. 2015) and improving liver

insulin sensitivity in obese men and women (Kars et al. 2010)

HZ supplement to HFD rats resulted in significant increases in three primary bile acids (CDCA, GCA and GCDCA) and two secondary bile acids (DCA and GDCA) ( $p < 0.05$ ).

Although HZ can significantly increase hydrophobic bile acids such as CDCA, it can also increase hydrophilic bile acid such as GUDCA. Bile acids exhibiting varying degrees of cytotoxicity was depended on their hydrophobic-hydrophilic balance. By combining the data of HZ attenuated lipid level in HFD-fed rats and relevant mechanism, these strongly suggest that HZ reduced steatosis through its ability to induce bile acids synthesis and increase its detergent effect rather than its ability to induce cytotoxicity. Strikingly, these results can also be used to explain HZ in clinical practice for the treatment of gallstones.

Regarding the mechanism of bile acid disturbance, up-regulated CYP7A1 may affect the bile acid synthetic pathway as for the cholesterol-lowering effect of HZ. CYP7A1 (cytochrome P450, family 7, subfamily A, polypeptide 1) is the rate-limiting enzyme in the classical bile acid biosynthetic pathway, a major efflux pathway for the

elimination of cholesterol from the body. HZ significantly promoted CYP7A1 activity, indicating that HZ accelerated transforming of cholesterol into bile acids.

In this study, we found that CYP7A1 protein expression was significantly decreased in HFD-fed rats compared with normal diet-fed rats. Supplementation of the HFD with HZ caused a significant induction of CYP7A1 protein expression compared with the HFD alone. As a result, hepatic and serum cholesterol levels were reduced and the bile acid level was increased in HZ-fed rats compared with HFD-fed rats. A similar activity in resveratrol and emodin (components in HZ) was reported in literatures. Resveratrol (Q. Chen et al. 2012) and emodin (J. Wang et al. 2016b) has been shown to up-regulate CYP7A1 which affects the bile acid synthetic pathway and enhances the excretion of faecal bile acids to lower cholesterol (Zhu et al. 2008).

Scientists discovered that there was a region-specific interaction of polyphenols in tea (Ogawa et al. 2015) and grapes (Ngamukote et al. 2011) with conjugated bile acids.

These binding effects decrease the solubility of cholesterol in bile acid micelle, resulting in delayed cholesterol absorption. Since HZ extract contains polydatin and

resveratrol, which belong to polyphenol, it might also interact with the conjugated bile acids and lower the solubility of cholesterol micelles. In our study, the conjugated bile acids in HZ group were higher than that of the other groups, which may result in lowering the transfer of cholesterol from intestine to the hepatocyte. It was found that resveratrol enhanced the excretion of faecal bile acids to lower cholesterol (Zhu et al. 2008). Further study for bile acids of faeces, the liver and small intestine of HZ group is needed to be done.

It is well known that primary bile acids secreted into intestinal lumen are metabolized to secondary bile acids by intestinal microflora. We speculated that HZ improved the HFD-induced fatty liver by modifying the gut microbial composition as well. Modification of gut microbial composition caused by HZ may play an important role in the health benefits of these plant polyphenols. The present study provides some evidence of this and further study is certainly necessary to provide a better picture on the role of gut microbiota in improving the health of the host through the consumptions of phytochemicals.

## **4.5 HZ improved endothelial function through attenuating dyslipidemia**

It has previously been reported that dyslipidemia is a common pathogenic risk factor for the rising of NAFLD. The mechanisms underlying the relationship between dyslipidemia and hepatic steatosis remain unclear.

The current study demonstrated that HZ improved endothelium-dependent vasodilatation on high fat diet-induced hypercholesterolemia in rats. The improvement in endothelial function induced by HZ was evident under a blunted acetylcholine-induced vascular relaxation which represented an endothelial/NO dysfunction. Interestingly, HZ treatment induced greater improvement than simvastatin group with hypercholesterolemia in rats.

Patients with hypercholesterolemia are known to have impaired receptor- and endothelium-dependent vascular relaxation in both the absence and presence of coronary artery disease (Pompilio et al. 2001). Accumulating evidence suggests that endothelial dysfunction has been identified as an important early event in patients with

hypercholesterolemia as a result of reduced bioavailability of NO (Drexler 1999). We observed that administration of HZ for 4 weeks in hypercholesterolemic rats dose-dependently enhanced NO production, leading to improve endothelial function. These mechanistic data are in line with our previous study in which turtle jelly improved acetylcholine-induced relaxation on isolated aortic rings and increased NO production (Wu et al. 2012). Furthermore, the observations suggest that HZ is a promising therapeutic option for improving endothelial function in patients with hypercholesterolemia.

Patients with NAFLD are at higher risk of CVD, particularly when NASH is present (VanWagner et al. 2012). Importantly, several longitudinal studies have demonstrated that CVD is one of the most important causes of mortality among NAFLD patients. Thus, the implementation with hypolipidemic agents should be considered in the overall management of these patients (Q. Q. Zhang and Lu 2015)

The present study demonstrated that long-term high-fat diet-feeding rats resulted in a significant increase in plasma TC and LDL cholesterol levels, which are key indicators

of dyslipidemia. HZ attenuated dyslipidemia and yielded improvement in endothelial function and an up-regulation of NO production under hypercholesterolaemic condition.

Moreover, HZ was also shown to alleviate hepatic steatosis. The results indicated that HZ treatment improved endothelial function amongst fatty liver disease.

## **4.6 Study on active ingredients in HZ**

In this study, five major compounds were identified from the sample with authentic standards. Their contents relative to dried crude drug weight were polydatin (10.64 mg/g  $\pm$  0.23 mg/g), emodin 8-O- $\beta$ -D-glucopyranoside (4.77 mg/g  $\pm$  0.04 mg/g), resveratrol (0.67 mg/g  $\pm$  0.01 mg/g), emodin (0.57 mg/g  $\pm$  0.01 mg/g) and physcion 8-O- $\beta$ -D-glucopyranoside (0.53 mg/g  $\pm$  0.05 mg/g).

Literature review showed that its active components such as polydatin, resveratrol and emodin also showed a similar effect. The protective effects of polydatin against high-fat diet HFD-induced hepatic steatosis may be partly associated with reduced liver TNF- $\alpha$  expression, lipid peroxidation level and SREBP-1c-mediated lipogenesis (Chatrath et al. 2012; J. M. Zhang et al. 2012b). Zhang *et al* (2015) reported that

polydatin supplementation alleviated IR and advanced hepatic steatosis through increasing expression levels of insulin receptor substrate 2 and improving abnormal adipokine production in HFD-induced fatty liver in rats (Q. Zhang et al. 2015). Emodin attenuated systemic and liver inflammation in hyperlipidemic mice administrated with lipopolysaccharides (Dong et al. 2005). Alisi et al. reported that in a high-fat/high-fructose diet fed rat model, emodin administration via drinking water for 10 weeks reduced hepatosteatosis and metabolic derangement. Emodin also reduced plasma TNF- $\alpha$  concentration, slightly increased body weight but reduced liver weight/body weight ratio, reduced blood levels of ALT, triglycerides, insulin, glucose and homeostasis model of assessment for IR index (Alisi et al. 2012). Furthermore, resveratrol is a polyphenol present in high concentration in grape seeds, peanuts, and various other plants such as HZ. Studies have demonstrated that resveratrol can be used to ameliorate NAFLD by improving IR (Shang et al. 2008) as well as decreasing lipogenesis (ACC, PPAR- $\gamma$  and SREBP-1) and inflammation [TNF- $\alpha$ , interleukin 6 (IL-6) and nuclear factor-kappa B (NF- $\kappa$ B)] expressions (Andrade et al. 2014; Nishikawa et al. 2013).

There is a general consensus concerning the positive effects of resveratrol on liver steatosis in animal models. The range of doses used in experiments carried out on rats has been very huge (10 - 450 mg/kg bw per day). The treatment periods were from 4 to 10 weeks (Aguirre et al. 2014). Compared to resveratrol, relative fewer studies about polydatin and emodin effects on liver steatosis were conducted in rats. Alisi et al. reported that emodin (40 mg/kg/day) in 5 weeks pre-treated rats that received the treatment with SD or HFD for an additional 10 weeks prevent hepatosteatois, preserving liver from pro-inflammatory and pro-oxidant damage caused by HFD/HF diet (Alisi et al. 2012). Zhang et al. reported that 30 and 90 mg/kg polydatin treatment for 8 weeks alleviated hepatic steatosis and reduced plasma and liver TG, TC and FFA concentration significantly in HFD rats (J. M. Zhang et al. 2012b).

In our *in vivo* study, we found that 150 mg/kg/day and 450 mg/kg/day HZ treatment for 4 weeks alleviated hepatic steatosis in HFD rats. In the 150 mg/kg/day and 450 mg/kg/day of HZ, the relative content of resveratrol, polydatin and emodin is 1.3 - 4.0 mg/kg/day, 21.2 - 63.7 mg/kg/day, 1.1 - 3.4 mg/kg/day respectively, is much lower than the concentration in previous studies (10 - 450 mg/kg/day, 30 - 90 mg/kg/day, 40

mg/kg/day) respectively. In *in vitro* studies, among the compounds isolated from HZ, few studies addressed the lipid-lowering action of resveratrol under *in vitro* steatosis conditions. In human cancer cell line (HepG2) of steatosis induced by palmitate treatment and incubated with 40  $\mu$ M of resveratrol for 24 h, Wang et al observed resveratrol reduced TG accumulation and inhibit SREBP1 expression via Sirt1-FOXO1 pathway (G. L. Wang et al. 2009). Zang et al et al showed that incubation of HepG2 hepatocytes exposed to high concentrations of glucose to get a cell steatosis model, with 10  $\mu$ M of resveratrol for 24 h prevented lipid accumulation. Resveratrol prevented steatosis by activation of AMPK and down-regulation of ACC (Zang et al. 2006).

However, we found that HZ (0.1 - 0.5 mg/mL) but not the five compounds isolated from HZ (1 - 100  $\mu$ M) reduced lipid accumulation in this cell line model (data not shown). This may due to two reasons. First, we used different cell line models. In our study, we use FFA to get a cell steatosis model in normal human cell line (LO2) different from cancer liver cell line (HepG2). Second, there are not studies about the anti-steatosis effect of the other four compounds besides resveratrol in *in vitro* steatosis model. Resveratrol content relative to dried weight is 0.67 mg/g, so the effective

contraction of HZ (0.1 - 0.5 mg/mL) contain (3.9 - 19.5  $\mu$ M) resveratrol, concentration lower than those used in other studies conducted in HepG2 cell line (10 - 40  $\mu$ M) to prevent lipid accumulation.

These results indicated the therapeutic effects of HZ derive from the complex synergistic interactions between the multiple bioactive components within the herb.

Moreover, HZ alleviates steatosis not NASH, indicates it can prevent early liver disease and prevent the severe condition caused by liver steatosis.

## **4.7 Conclusion**

In conclusion, our studies have shown that HZ could reduce the lipid accumulation in *vitro* and in *vivo* mainly by regulating the imbalance between lipid acquisition and removal, especially through lipophagy and bile acids synthesis to remove lipid from body. In addition, we demonstrated that the lipid reduction effects of HZ were achieved by regulating multiple targets, including the suppression of oxidative stress, activation of lipophagy and the enhancement of bile acid synthesis (Fig. 4.7.1). Further, the synergistic action of HZ may be more plausible for beneficial effects exerted exhibiting

anti-NAFLD activity. Taken together, these findings may offer useful insight into the prevention and treatment of NAFLD by HZ.

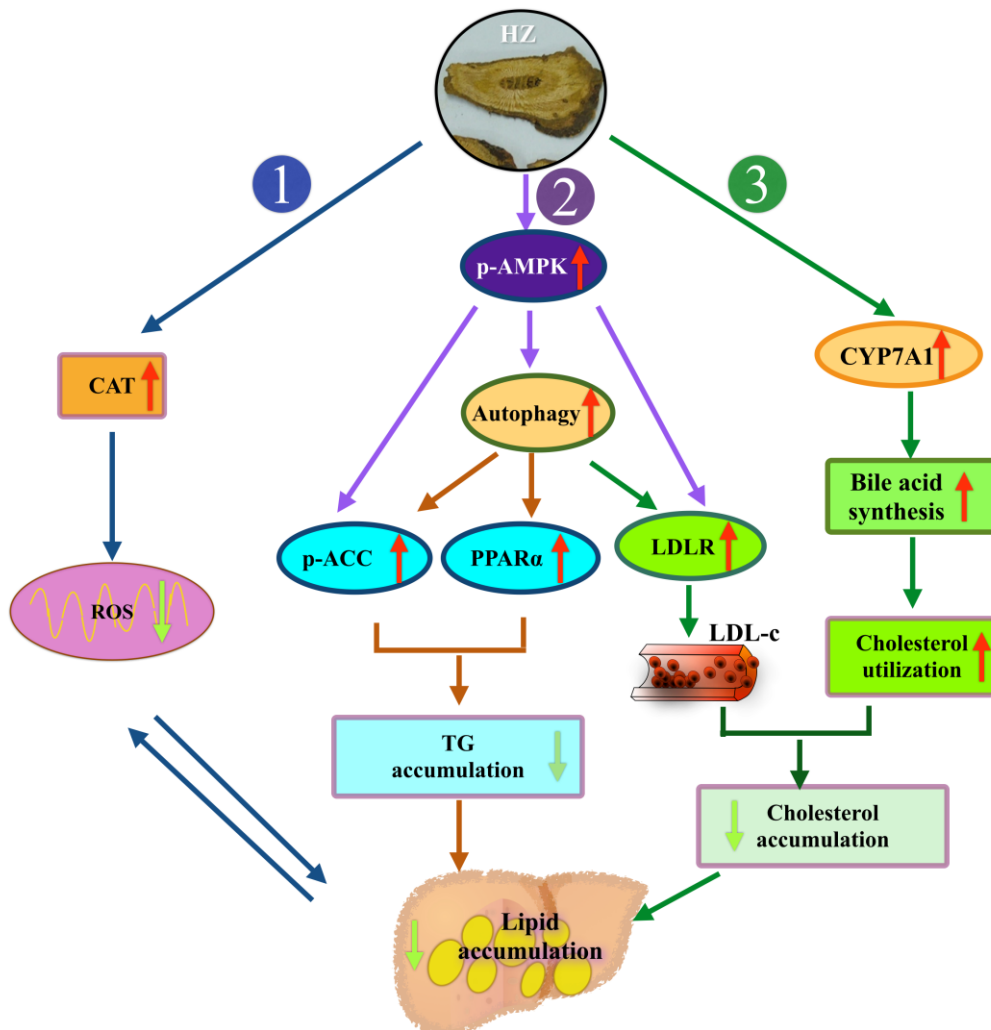


Fig. 4.7.1 The potential mechanisms of anti-NAFLD of HZ

## 4.8 Future studies

In order to confirm autophagy regulate lipid metabolism, co-localization of lipid droplets and autophagosome proteins will be needed. In this experiment, lipid droplets,

LC3-II (an autophagosomal membrane protein), and also LAMP-1 (a lysosomal membrane protein) are stained. Confocal fluorescence microscopy can be used to study co-localization of lipid droplets and these autophagosome proteins. Co-localization of lipid droplets, LC3-II and LAMP-1 under HZ treatment can provide supporting evidence and confirm the maturation of autophagosomes to autophagolysosomes.

If only the p62 protein level is measured, it will lead to an incorrect interpretation of autophagic flux. Thus, the level of p62 mRNA should be simultaneously determined along with the p62 protein level as an autophagy indicator. Further investigation should measure both protein and mRNA expressions of p62 to fully evaluate the role of autophagy.

Enhanced the excretion of faecal bile acids also lead to lower cholesterol content in blood. Further *in vivo* study should measure the amount of bile acids in faeces, the liver and small intestine to understand the therapeutic action of HZ.

It is well known that primary bile acids secreted into intestinal lumen are metabolized to secondary bile acids by intestinal microflora. HZ supplement also change the some

primary and secondary bile acids, further study is certainly necessary to provide a better picture on the role of gut microbiota in improving the health of the host through the consumption of HZ.

## References

- Aguirre, Leixuri, et al. (2014), 'Effects of resveratrol and other polyphenols in hepatic steatosis', *World journal of gastroenterology: WJG*, 20 (23), 7366.
- Ahmed, Mohamed H and Byrne, Christopher D (2007), 'Modulation of sterol regulatory element binding proteins (SREBPs) as potential treatments for non-alcoholic fatty liver disease (NAFLD)', *Drug discovery today*, 12 (17), 740-47.
- Alisi, Anna, et al. (2012), 'Emodin prevents intrahepatic fat accumulation, inflammation and redox status imbalance during diet-induced hepatosteatosis in rats', *International journal of molecular sciences*, 13 (2), 2276-89.
- Andrade, João Marcus Oliveira, et al. (2014), 'Resveratrol attenuates hepatic steatosis in high-fat fed mice by decreasing lipogenesis and inflammation', *Nutrition*, 30 (7), 915-19.
- Anwer, Mohammed Sawkat (2012), 'Intracellular signaling by bile acids', *Journal of bio-science*, 20, 1-23.
- Armstrong, Matthew J, et al. (2016a), 'Glucagon-like peptide 1 decreases lipotoxicity in non-alcoholic steatohepatitis', *Journal of hepatology*, 64 (2), 399-408.
- Armstrong, Matthew James, et al. (2016b), 'Liraglutide safety and efficacy in patients with non-alcoholic steatohepatitis (LEAN): a multicentre, double-

- blind, randomised, placebo-controlled phase 2 study', *The Lancet*, 387 (10019), 679-90.
- Birkenfeld, Andreas L and Shulman, Gerald I (2014), 'Nonalcoholic fatty liver disease, hepatic insulin resistance, and type 2 diabetes', *Hepatology*, 59 (2), 713-23.
- Caballero, Francisco, et al. (2009), 'Enhanced free cholesterol, SREBP-2 and StAR expression in human NASH', *Journal of hepatology*, 50 (4), 789-96.
- Chatrath, Hemant, Vuppalanchi, Raj, and Chalasani, Naga (2012), 'Dyslipidemia in patients with nonalcoholic fatty liver disease', *Seminars in liver disease* (32: Thieme Medical Publishers), 022-29.
- Chen, Qiong, et al. (2012), 'Dietary resveratrol increases the expression of hepatic 7 $\alpha$ -hydroxylase and ameliorates hypercholesterolemia in high-fat fed C57BL/6J mice', *Lipids in health and disease*, 11 (1), 56.
- Chen, Shao Dong, et al. (2013), 'Decoction vs extracts-mixed solution: effect of yiqihuoxue formula on non-alcoholic fatty liver disease in rats', *Journal of Traditional Chinese Medicine*, 33 (4), 513-17.
- Clarke, Siobhan F, et al. (2012), 'The gut microbiota and its relationship to diet and obesity: new insights', *Gut microbes*, 3 (3), 186-202.
- de Aguiar Vallim, Thomas Q, Tarling, Elizabeth J, and Edwards, Peter A (2013), 'Pleiotropic roles of bile acids in metabolism', *Cell metabolism*, 17 (5), 657-69.
- Dong, Hui, et al. (2005), 'Effects of emodin on treating murine nonalcoholic fatty liver induced by high caloric laboratory chaw', *World journal of gastroenterology*, 11 (9), 1339-44.
- Dormandy, John A, et al. (2005), 'Secondary prevention of macrovascular events in patients with type 2 diabetes in the PROactive Study (PROspective pioglitAzone Clinical Trial In macroVascular Events): a randomised controlled trial', *The Lancet*, 366 (9493), 1279-89.

- Dowman, Joanna K, Tomlinson, JW, and Newsome, PN (2010), 'Pathogenesis of non-alcoholic fatty liver disease', *QJM: An International Journal of Medicine*, 103 (2), 71-83.
- Drenick, Ernst J, Fisler, Janis, and Johnson, Daisie (1982), 'Hepatic steatosis after intestinal bypass-prevention and reversal by metronidazole, irrespective of protein-calorie malnutrition', *Gastroenterology*, 82 (3), 535-48.
- Drexler, Helmut (1999), 'Nitric oxide and coronary endothelial dysfunction in humans', *Cardiovascular research*, 43 (3), 572-79.
- Dunn, Warwick B., et al. (2011), 'Procedures for large-scale metabolic profiling of serum and plasma using gas chromatography and liquid chromatography coupled to mass spectrometry', *Nature Protocols*, 6 (7), 1060-83.
- Fan, Jian Gao (2004), 'Evaluating the efficacy and safety of Danning Pian in the short-term treatment of patients with non-alcoholic fatty liver disease: a multicenter clinical trial', *Hepatobiliary Pancreat Dis Int*, 3 (3), 375-80.
- Farrell, Geoffrey C and Larter, Claire Z (2006), 'Nonalcoholic fatty liver disease: from steatosis to cirrhosis', *Hepatology*, 43 (S1), S99-S112.
- Farrell, Geoffrey C, Wong, Vincent Wai-Sun, and Chitturi, Shiv (2013), 'NAFLD in Asia-as common and important as in the West', *Nature Reviews Gastroenterology and Hepatology*, 10 (5), 307-18.
- Feng, Qin, et al. (2013), 'Qushi huayu decoction inhibits hepatic lipid accumulation by activating AMP-activated protein kinase in vivo and in vitro', *Evidence-Based Complementary and Alternative Medicine*, 2013.
- Feng, Qin, et al. (2017), 'Multi-targeting therapeutic mechanisms of the Chinese herbal medicine QHD in the treatment of non-alcoholic fatty liver disease', *Oncotarget*, 8 (17), 27820.
- Finucane, Mariel M, et al. (2011), 'National, regional, and global trends in body-mass index since 1980: systematic analysis of health examination surveys and epidemiological studies with 960 country-years and 9· 1 million participants', *The Lancet*, 377 (9765), 557-67.

- Fujimoto, Makoto, et al. (2010), 'The traditional Japanese formula keishibukuryogan reduces liver injury and inflammation in patients with nonalcoholic fatty liver disease', *Annals of the NEW YORK Academy of Sciences*, 1190 (1), 151-58.
- Fujimoto, Makoto, et al. (2008), 'Evidence-based efficacy of Kampo formulas in a model of non alcoholic fatty liver', *Experimental Biology and Medicine*, 233 (3), 328-37.
- Gambino, Roberto, et al. (2016), 'Different serum free fatty acid profiles in NAFLD subjects and healthy controls after oral fat load', *International journal of molecular sciences*, 17 (4), 479.
- Gao, Nannan, et al. (2016), 'Dyslipidemia in rural areas of North China: prevalence, characteristics, and predictive value', *Lipids in Health and Disease*, 15 (1), 154.
- Gitto, S, et al. (2015), 'Treatment of nonalcoholic steatohepatitis in adults: present and future', *Gastroenterology research and practice*, 2015.
- Gómez-Lechón, María José, et al. (2007), 'A human hepatocellular in vitro model to investigate steatosis', *Chemico-biological interactions*, 165 (2), 106-16.
- Gong, Zi Zhen, et al. (2016), 'Chenodeoxycholic acid activates NLRP3 inflammasome and contributes to cholestatic liver fibrosis', *Oncotarget*, 7 (51), 83951.
- Gonnella, Roberta, et al. (2015), 'PKC theta and p38 MAPK activate the EBV lytic cycle through autophagy induction', *Biochimica et Biophysica Acta (BBA)-Molecular Cell Research*, 1853 (7), 1586-95.
- Guo, De Jian, et al. (2008), 'Antioxidative activities and the total phenolic contents of tonic Chinese medicinal herbs', *Inflammopharmacology*, 16 (5), 201-07.
- Guo, Jiao, et al. (2011), 'A new TCM formula FTZ lowers serum cholesterol by regulating HMG-CoA reductase and CYP7A1 in hyperlipidemic rats', *Journal of ethnopharmacology*, 135 (2), 299-307.
- Henao-Mejia, Jorge, et al. (2012), 'Inflammasome-mediated dysbiosis regulates progression of NAFLD and obesity', *Nature*, 482 (7384), 179-85.

- Hsu, Wei Fan, et al. (2016), 'A review of western and traditional chinese medical approaches to managing nonalcoholic fatty liver disease', *Evidence-Based Complementary and Alternative Medicine*, 2016.
- Huang, Dejian, Ou, Boxin, and Prior, Ronald L (2005), 'The chemistry behind antioxidant capacity assays', *Journal of agricultural and food chemistry*, 53 (6), 1841-56.
- Ikonen, Elina (2008), 'Cellular cholesterol trafficking and compartmentalization', *Nature reviews Molecular cell biology*, 9 (2), 125-38.
- Inami, Yoshihiro, et al. (2011), 'Hepatic steatosis inhibits autophagic proteolysis via impairment of autophagosomal acidification and cathepsin expression', *Biochemical and biophysical research communications*, 412 (4), 618-25.
- Jacobo-Velázquez, DA and Cisneros-Zevallos, L (2009), 'Correlations of antioxidant activity against phenolic content revisited: a new approach in data analysis for food and medicinal plants', *Journal of Food Science*, 74 (9), R107-13.
- Jiang, Qing Lan, et al. (2009), 'Gene Expressions in the Adipose Tissue of NAFLD Rats Intervened with the Extracts of Polygonum Caspidatum', *Journal of Medical Research*, 38 (5), 54-57.
- Jiang Qinglan, et al. (2008), 'Variances of the Gene Expression in Adipose Tissue of NAFLD Rats Intervened with the Compound of Polygonum Caspidatum', *Journal of Medical Research* 37 (11), 63-65.
- Kang, Hyun and Koppula, Sushruta (2014), 'Houttuynia cordata attenuates lipid accumulation via activation of AMP-activated protein kinase signaling pathway in HepG2 cells', *The American journal of Chinese medicine*, 42 (03), 651-64.
- Kang, OH, et al. (2013), 'Curcumin decreases oleic acid-induced lipid accumulation via AMPK phosphorylation in hepatocarcinoma cells', *European Review for Medical and Pharmacological Sciences*, 17 (19), 2578-86.

- Kang, Ok Hwa, et al. (2015), 'Puerarin ameliorates hepatic steatosis by activating the PPAR $\alpha$  and AMPK signaling pathways in hepatocytes', *International journal of molecular medicine*, 35 (3), 803-09.
- Kars, Marleen, et al. (2010), 'Tauroursodeoxycholic acid may improve liver and muscle but not adipose tissue insulin sensitivity in obese men and women', *Diabetes*, 59 (8), 1899-905.
- Kim, Jin Hwan, et al. (2014), 'Raf/MEK/ERK can regulate cellular levels of LC3B and SQSTM1/p62 at expression levels', *Experimental cell research*, 327 (2), 340-52.
- Kirpich, Irina A, Marsano, Luis S, and McClain, Craig J (2015), 'Gut-liver axis, nutrition, and non-alcoholic fatty liver disease', *Clinical biochemistry*, 48 (13), 923-30.
- Klein, Eric A, et al. (2011), 'Vitamin E and the risk of prostate cancer: the Selenium and Vitamin E Cancer Prevention Trial (SELECT)', *Jama*, 306 (14), 1549-56.
- Koga, Hiroshi, Kaushik, Susmita, and Cuervo, Ana Maria (2010), 'Altered lipid content inhibits autophagic vesicular fusion', *The FASEB Journal*, 24 (8), 3052-65.
- Koo, Seung Hoi (2013), 'Nonalcoholic fatty liver disease: molecular mechanisms for the hepatic steatosis', *Clinical and molecular hepatology*, 19 (3), 210.
- Kuipers, Folkert, Bloks, Vincent W, and Groen, Albert K (2014), 'Beyond intestinal soap [mdash] bile acids in metabolic control', *Nature Reviews Endocrinology*, 10 (8), 488-98.
- Kwanten, Wilhelmus J, et al. (2014), 'Role of autophagy in the pathophysiology of nonalcoholic fatty liver disease: a controversial issue', *World Journal of Gastroenterology*, 20 (23), 7325-38.
- L Abner, Erin, et al. (2011), 'Vitamin E and all-cause mortality: a meta-analysis', *Current aging science*, 4 (2), 158-70.

- Lau, Jennie Ka Ching, Zhang, Xiang, and Yu, Jun (2016), 'Animal models of non-alcoholic fatty liver disease: current perspectives and recent advances', *The Journal of pathology*.
- Lee, Tzung Yan, et al. (2010), 'Alleviation of hepatic oxidative stress by Chinese herbal medicine Yin-Chen-Hao-Tang in obese mice with steatosis', *International journal of molecular medicine*, 25 (6), 837.
- Li, Hong Shan, Feng, Qin, and Hu, Yi Yang (2009), 'Effect of qushi huayu decoction on high-fat diet induced hepatic lipid deposition in rat', *Chinese journal of integrated traditional and Western medicine*, 29 (12), 1092-95.
- Li, Jing Jie, et al. (2015a), 'Cortex Fraxini (Qingpi) protects rat pheochromocytoma cells against 6-hydroxydopamine-induced apoptosis', *Parkinson's Disease*, 2015.
- Li, Sha, et al. (2015b), 'The role of oxidative stress and antioxidants in liver diseases', *International journal of molecular sciences*, 16 (11), 26087-124.
- Li, Wang, et al. (2014), 'Crude extracts from *Lycium barbarum* suppress SREBP-1c expression and prevent diet-induced fatty liver through AMPK activation', *BioMed research international*, 2014.
- Li, Yu, et al. (2011), 'AMPK phosphorylates and inhibits SREBP activity to attenuate hepatic steatosis and atherosclerosis in diet-induced insulin-resistant mice', *Cell metabolism*, 13 (4), 376-88.
- Lieber, Charles S, et al. (2004), 'Model of nonalcoholic steatohepatitis', *The American journal of clinical nutrition*, 79 (3), 502-09.
- Liu, K and Czaja, MJ (2013), 'Regulation of lipid stores and metabolism by lipophagy', *Cell death and differentiation*, 20 (1), 3.
- Liu, Tong Yan, et al. (2016), 'FNDC5 Alleviates Hepatosteatois by Restoring AMPK/mTOR-Mediated Autophagy, Fatty Acid Oxidation, and Lipogenesis in Mice', *Diabetes*, 65 (11), 3262-75.
- Liu, Wen Sheng, et al. (2015), 'Antioxidant mechanisms in nonalcoholic fatty liver disease', *Current drug targets*, 16 (12), 1301-14.

- Liu, Zhao Lan, et al. (2013), 'Herbal medicines for fatty liver diseases', *The Cochrane Library*, (8).
- Lonardo, Amedeo, et al. (2015), 'Nonalcoholic fatty liver disease: a precursor of the metabolic syndrome', *Digestive and Liver Disease*, 47 (3), 181-90.
- Longato, Lisa, et al. (2012), 'High fat diet induced hepatic steatosis and insulin resistance: Role of dysregulated ceramide metabolism', *Hepatology Research*, 42 (4), 412-27.
- McMahan, Rachel H, et al. (2013), 'Bile acid receptor activation modulates hepatic monocyte activity and improves nonalcoholic fatty liver disease', *Journal of Biological Chemistry*, 288 (17), 11761-70.
- Miele, Luca, et al. (2009), 'Increased intestinal permeability and tight junction alterations in nonalcoholic fatty liver disease', *Hepatology*, 49 (6), 1877-87.
- Min, Hae Ki, et al. (2012), 'Increased hepatic synthesis and dysregulation of cholesterol metabolism is associated with the severity of nonalcoholic fatty liver disease', *Cell metabolism*, 15 (5), 665-74.
- Musso, Giovanni, Cassader, Maurizio, and Gambino, Roberto (2016), 'Non-alcoholic steatohepatitis: emerging molecular targets and therapeutic strategies', *Nature Reviews Drug Discovery*, 15 (4), 249-74.
- Ngamukote, Sathaporn, et al. (2011), 'Cholesterol-lowering activity of the major polyphenols in grape seed', *Molecules*, 16 (6), 5054-61.
- Nishikawa, Kahoko, et al. (2013), 'Resveratrol ameliorates high fat diet-induced fatty liver with alteration of Kupffer cell subset in mice.(P1106)', *The Journal of Immunology*, 190 (1 Supplement), 185.28-85.28.
- Ogawa, Kazuki, et al. (2015), 'Interaction between tea polyphenols and bile acid inhibits micellar cholesterol solubility', *Journal of agricultural and food chemistry*, 64 (1), 204-09.
- Pan, Chun Hsu, et al. (2012), 'Ethanol extract of *Vitis thunbergii* exhibits lipid lowering properties via modulation of the AMPK-ACC pathway in

- hypercholesterolemic rabbits', *Evidence-based Complementary and Alternative Medicine*, 2012.
- Pérez-Carreras, Mercedes, et al. (2003), 'Defective hepatic mitochondrial respiratory chain in patients with nonalcoholic steatohepatitis', *Hepatology*, 38 (4), 999-1007.
- Pompilio, Giulio, et al. (2001), 'Comparison of endothelium-dependent vasoactivity of internal mammary arteries from hypertensive, hypercholesterolemic, and diabetic patients', *The Annals of thoracic surgery*, 72 (4), 1290-97.
- Puissant, Alexandre, et al. (2010), 'Resveratrol promotes autophagic cell death in chronic myelogenous leukemia cells via JNK-mediated p62/SQSTM1 expression and AMPK activation', *Cancer research*, 70 (3), 1042-52.
- Puri, Puneet, et al. (2007), 'A lipidomic analysis of nonalcoholic fatty liver disease', *Hepatology*, 46 (4), 1081-90.
- Raman, Maitreyi, et al. (2013), 'Fecal microbiome and volatile organic compound metabolome in obese humans with nonalcoholic fatty liver disease', *Clinical Gastroenterology and Hepatology*, 11 (7), 868-75. e3.
- Roma, Marcelo G, et al. (2011), 'Ursodeoxycholic acid in cholestasis: linking action mechanisms to therapeutic applications', *Clinical science*, 121 (12), 523-44.
- Rotman, Yaron and Sanyal, Arun J (2017), 'Current and upcoming pharmacotherapy for non-alcoholic fatty liver disease', *Gut*, 66 (1), 180-90.
- Sahani, Mayurbhai Himatbhai, Itakura, Eisuke, and Mizushima, Noboru (2014), 'Expression of the autophagy substrate SQSTM1/p62 is restored during prolonged starvation depending on transcriptional upregulation and autophagy-derived amino acids', *Autophagy*, 10 (3), 431-41.
- Sanyal, Arun J, et al. (2001), 'Nonalcoholic steatohepatitis: association of insulin resistance and mitochondrial abnormalities', *Gastroenterology*, 120 (5), 1183-92.

- Sayin, Sama I, et al. (2013), 'Gut microbiota regulates bile acid metabolism by reducing the levels of tauro-beta-muricholic acid, a naturally occurring FXR antagonist', *Cell metabolism*, 17 (2), 225-35.
- Schürks, Markus, et al. (2010), 'Effects of vitamin E on stroke subtypes: meta-analysis of randomised controlled trials', *Bmj*, 341, c5702.
- Sham, Tung Ting, et al. (2017), 'Cholesterol-lowering effects of piceatannol, a stilbene from wine, using untargeted metabolomics', *Journal of Functional Foods*, 28, 127-37.
- Shang, Jing, SUN, Hui, and XIAO, Hu (2008), 'Resveratrol improves non-alcoholic fatty liver disease by activating AMP-activated protein kinase', *Acta Pharmacologica Sinica*, 29 (6), 698-706.
- Shaw, Lawrence, et al. (1981), 'Chenodiol (chenodeoxycholic acid) for dissolution of gallstones: The National Cooperative Gallstone Study', *Annals of Internal Medicine*, 95, 257-82.
- Singh, Rajat and Cuervo, Ana Maria (2011), 'Autophagy in the cellular energetic balance', *Cell metabolism*, 13 (5), 495-504.
- Singh, Rajat, et al. (2009), 'Autophagy regulates lipid metabolism', *Nature*, 458 (7242), 1131-35.
- Souza-Mello, Vanessa (2015), 'Peroxisome proliferator-activated receptors as targets to treat non-alcoholic fatty liver disease', *World journal of hepatology*, 7 (8), 1012.
- Souza, Mônica Rodrigues de Araújo, et al. (2012), 'Metabolic syndrome and risk factors for non-alcoholic fatty liver disease', *Arquivos de gastroenterologia*, 49 (1), 89-96.
- Srivastava, Rai Ajit K, et al. (2012), 'AMP-activated protein kinase: an emerging drug target to regulate imbalances in lipid and carbohydrate metabolism to treat cardio-metabolic diseases Thematic Review Series: New Lipid and Lipoprotein Targets for the Treatment of Cardiometabolic Diseases', *Journal of lipid research*, 53 (12), 2490-514.

- Staels, Bart, Handelsman, Yehuda, and Fonseca, Vivian (2010), 'Bile acid sequestrants for lipid and glucose control', *Current diabetes reports*, 10 (1), 70-77.
- Swann, Jonathan R, et al. (2011), 'Systemic gut microbial modulation of bile acid metabolism in host tissue compartments', *Proceedings of the National Academy of Sciences*, 108 (Supplement 1), 4523-30.
- Tang, Hong, et al. (2016), 'Irisin inhibits hepatic cholesterol synthesis via AMPK-SREBP2 signaling', *EBioMedicine*, 6, 139-48.
- Thomas, Charles, et al. (2008), 'Targeting bile-acid signalling for metabolic diseases', *Nature reviews Drug discovery*, 7 (8), 678-93.
- Tiemann, Michaela, et al. (2004), 'Cholesterol feeding of mice expressing cholesterol 7 $\alpha$ -hydroxylase increases bile acid pool size despite decreased enzyme activity', *Proceedings of the National Academy of Sciences*, 101 (7), 1846-51.
- Tiniakos, Dina G, Vos, Miriam B, and Brunt, Elizabeth M (2010), 'Nonalcoholic fatty liver disease: pathology and pathogenesis', *Annual Review of Pathological Mechanical Disease*, 5, 145-71.
- Vacca, Michele, et al. (2015), 'Fatty acid and glucose sensors in hepatic lipid metabolism: implications in NAFLD', *Seminars in liver disease* (35: Thieme Medical Publishers), 250-61.
- Vandewynckel, Yves-Paul, et al. (2015), 'Tauroursodeoxycholic acid dampens oncogenic apoptosis induced by endoplasmic reticulum stress during hepatocarcinogen exposure', *Oncotarget*, 6 (29), 28011.
- Vanni, Ester, et al. (2015), 'Systemic complications of nonalcoholic fatty liver disease: when the liver is not an innocent bystander', *Seminars in liver disease* (35: Thieme Medical Publishers), 236-49.
- VanWagner, Lisa B, et al. (2012), 'Patients transplanted for nonalcoholic steatohepatitis are at increased risk for postoperative cardiovascular events', *Hepatology*, 56 (5), 1741-50.

- Vernon, G, Baranova, A, and Younossi, ZM (2011), 'Systematic review: the epidemiology and natural history of non-alcoholic fatty liver disease and non-alcoholic steatohepatitis in adults', *Alimentary pharmacology & therapeutics*, 34 (3), 274-85.
- Viollet, Benoit, et al. (2006), 'Activation of AMP-activated protein kinase in the liver: a new strategy for the management of metabolic hepatic disorders', *The Journal of physiology*, 574 (1), 41-53.
- Wang, Chun Mei, et al. (2016a), 'Schisandra polysaccharide inhibits hepatic lipid accumulation by downregulating expression of SREBPs in NAFLD mice', *Lipids in Health and Disease*, 15 (1), 195.
- Wang, Guang Li, et al. (2009), 'Resveratrol inhibits the expression of SREBP1 in cell model of steatosis via Sirt1–FOXO1 signaling pathway', *Biochemical and biophysical research communications*, 380 (3), 644-49.
- Wang, Jiaoying, et al. (2016b), 'Hypocholesterolemic effect of emodin by simultaneous determination of in vitro and in vivo bile salts binding', *Fitoterapia*, 110, 116-22.
- Wang, Jie Wei, et al. (2014), 'Lipotoxic effect of p21 on free fatty acid-induced steatosis in L02 cells', *PloS one*, 9 (4), e96124.
- Wang, Lu Wen, et al. (2005), 'Therapeutic effects of Huganning pill on patients with nonalcoholic steatohepatitis', *Chinese Journal of Integrated Traditional and Western Medicine on Digestion*, 6, 373-75.
- Wang, Min Jiang, et al. (2012), 'Lipid regulation effects of Polygoni Multiflori Radix, its processed products and its major substances on steatosis human liver cell line L02', *Journal of Ethnopharmacology*, 139 (1), 287-93.
- Ward, Carl, et al. (2016), 'Autophagy, lipophagy and lysosomal lipid storage disorders', *Biochimica et Biophysica Acta (BBA)-Molecular and Cell Biology of Lipids*, 1861 (4), 269-84.
- Wong, Vincent Wai Sun, et al. (2012), 'Prevalence of non-alcoholic fatty liver disease and advanced fibrosis in Hong Kong Chinese: a population study

- using proton-magnetic resonance spectroscopy and transient elastography', *Gut*, 61 (3), 409-15.
- Wouters, Kristiaan, et al. (2008), 'Dietary cholesterol, rather than liver steatosis, leads to hepatic inflammation in hyperlipidemic mouse models of nonalcoholic steatohepatitis', *Hepatology*, 48 (2), 474-86.
- Wu, Jian Hong, et al. (2012), 'Suppression of diet-induced hypercholesterolemia by turtle jelly, a traditional Chinese functional food, in rats', *Evidence-Based Complementary and Alternative Medicine*, 2012.
- Wu, Jian Hong, et al. (2010), 'Formononetin, an isoflavone, relaxes rat isolated aorta through endothelium-dependent and endothelium-independent pathways', *The Journal of nutritional biochemistry*, 21 (7), 613-20.
- Yang, Ling, et al. (2010), 'Defective hepatic autophagy in obesity promotes ER stress and causes insulin resistance', *Cell metabolism*, 11 (6), 467-78.
- Yang, Wen Ying, et al. (2012), 'Serum lipids and lipoproteins in Chinese men and women', *Circulation*, 2212-21.
- Ye, Jin and DeBose-Boyd, Russell A (2011), 'Regulation of cholesterol and fatty acid synthesis', *Cold Spring Harbor perspectives in biology*, 3 (7), a004754.
- Yiyong, Song (2016), 'Experimental study on effects of Giant knotweed on lipid peroxidation and oxidative stress in nonalcoholic fatty liver disease', *Chinese Journal of Clinicians(Electronic Edition)*, 10 (11), 1580-83.
- Yu, Jin Sheng, et al. (2016), 'The pathogenesis of nonalcoholic fatty liver disease: interplay between diet, gut microbiota, and genetic background', *Gastroenterology research and practice*, 2016.
- Zang, Meng Wei, et al. (2006), 'Polyphenols stimulate AMP-activated protein kinase, lower lipids, and inhibit accelerated atherosclerosis in diabetic LDL receptor-deficient mice', *Diabetes*, 55 (8), 2180-91.
- Zhang, Hong, et al. (2012a), 'Protective effects of polydatin from *Polygonum cuspidatum* against carbon tetrachloride-induced liver injury in mice', *PLoS One*, 7 (9), e46574.

- Zhang, Huan, et al. (2013), 'A review of the pharmacological effects of the dried root of *Polygonum cuspidatum* (Hu Zhang) and its constituents', *Evidence-based complementary and alternative medicine*, 2013.
- Zhang, Hui, et al. (2008a), 'Effects of Qushi Huayu Decoction on cathepsin B and tumor necrosis factor-alpha expression in rats with non-alcoholic steatohepatitis', *Zhong xi yi jie he xue bao= Journal of Chinese integrative medicine*, 6 (9), 928-33.
- Zhang, Jing Ming, et al. (2012b), 'Polydatin alleviates non-alcoholic fatty liver disease in rats by inhibiting the expression of TNF- $\alpha$  and SREBP-1c', *Molecular medicine reports*, 6 (4), 815-20.
- Zhang, Li, et al. (2014), 'Extracts from *Salvia-Nelumbinis naturalis* alleviate hepatosteatosis via improving hepatic insulin sensitivity', *Journal of Translational Medicine*, 12.
- Zhang, Qi, et al. (2015), 'Polydatin supplementation ameliorates diet-induced development of insulin resistance and hepatic steatosis in rats', *Molecular medicine reports*, 11 (1), 603-10.
- Zhang, Qing Qing and Lu, Lun Gen (2015), 'Nonalcoholic fatty liver disease: dyslipidemia, risk for cardiovascular complications, and treatment strategy', *Journal of Clinical and Translational Hepatology*, 3 (1), 78.
- Zhang, Rui Juan, et al. (2016), 'Sesamin ameliorates hepatic steatosis and inflammation in rats on a high-fat diet via LXR $\alpha$  and PPAR $\alpha$ ', *Nutrition Research*, 36 (9), 1022-30.
- Zhang, Shi Jun, et al. (2008b), 'The effect of QuYuHuaTanTongLuo Decoction on the non-alcoholic steatohepatitis', *Complementary therapies in medicine*, 16 (4), 192-98.
- Zhang, Yang, et al. (2017), 'Effectiveness of Hugangning Tablet in the treatment of non-alcoholic steatohepatitis', *Acta Academiae Medicinae Qingdao Universitatis*, 53 (1), 100-02.

Zhu, Lixian, Luo, Xin, and Jin, Zhengyu (2008), 'Effect of resveratrol on serum and liver lipid profile and antioxidant activity in hyperlipidemia rats', *Asian Australasian Journal of Animal Sciences*, 21 (6), 890.